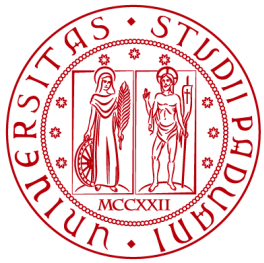

UNIVERSITÀ DEGLI STUDI DI PADOVA

SEDE AMMINISTRATIVA:UNIVERSITÁ DEGLI STUDI DI PADOVA

DIPARTIMENTO DI SCIENZE FARMACEUTICHE

SCUOLA DI DOTTORATO IN SCIENZE MOLECOLARI

INDIRIZZO: SCIENZE FARMACEUTICHE

XXIII CICLO

ANALYSES OF CROSS-LINKING BETWEEN DNA AND ANTHRACYCLINES

Direttore della Scuola: Ch.mo Prof. Maurizio Casarin

Coordinatore d'indirizzo: Ch.mo Prof. Adriana Chilin

Supervisore: Ch.mo Prof. Barbara Gatto

Dottorando: Matteo Scalabrin

31 GENNAIO 2011

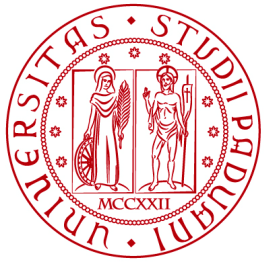

UNIVERSITY OF STUDY OF PADOVA

ADMINISTRATIVE OFFICE: UNIVERSITY OF STUDY OF PADOVA

DEPARTEMENT OF PHARMACEUTICAL SIENCES

PH.D SCHOOL IN MOLECULAR SCIENCES

ORIENTATION: PHARMACEUTICAL SCIENCES

XXIII CYCLE

ANALYSES OF CROSS-LINKING BETWEEN DNA AND ANTHRACYCLINES

School director: Ch.mo Prof. Maurizio Casarin

Orientation assistance director: Ch.mo Prof. Adriana Chilin

Supervisor: Ch.mo Prof. Barbara Gatto

Ph.D student: Matteo Scalabrin

31ST JANUARY 2011

TABLE OF CONTENTS

ABSTRACT

Anthracyclines are a group of chemotherapeutics that include adriamycin (doxorubicin), daunorubicin, idarubicin, and epirubicin. Anthracyclines are active against a wide range of tumours, in particular, adriamycin is used in the treatment of breast cancer, Hodgkin's lymphoma, lung cancer, multiple myeloma and re-occurring ovarian cancer. Despite the broad spectrum of actions, resistance or severe cardio-toxicity limits the use of these important anticancer-drugs. The search for a "better anthracycline" has resulted in more than 2000 analogs, but only a few more anthracyclines have attained clinical approval. Although the exact mechanism by which adriamycin exerts its anti-tumour activity is uncertain, the dominant mechanism appears to involve impairment of topoisomerase IIα activity consistent with observed DNA intercalation and nuclear localization. The search for less toxic and more effective anthracyclines has led to the discovery of nemorubicin, a doxorubicin derivative in which the amino nitrogen of the daunosamine unit is incorporated into a methoxymorpholinyl ring. Preclinical investigations showed that nemorubicin, unlike classic anthracyclines, is not cardiotoxic and retains antitumour activity in various multidrug-resistant tumor models. Encouraging results have been obtained in phase I/II clinical trials in which the drug was administered by the intra-hepatic artery route. Nemorubicin is 80-120 times more potent than doxorubicin in vivo; in contrast, its in-vitro activity is only eight times greater than doxorubicin's toward cultured drug sensitive tumour cells. A recent study established that nemorubicin is converted by enzyme CYP3A in a more cytotoxic metabolite PNU-159682, which was found to be 700-2400 times more potent that its parent drug toward cultured human cancer cells and which exhibits significant efficacy in in vivo tumor models. Ongoing studies aimed at exploring the molecular mechanism of action of PNU-159682 indicate that it has different effects on cell cycle progression and different DNA interacting properties, compared to both MMDX and doxorubicin. Moreover, further recent data suggest that PNU-159682 retains its activity against tumor cell lines with mechanisms of resistance different from those classical anticancer agents including MDR-1 gene overexpression, reduced topoisomerase II activity, and mutations in the topoisomerase I gene, these latter genetic alterations conferring resistance in vitro to the parent drug, MMDX [1]. We used different experimental approaches aimed to rationalizing the high activity of this metabolite. Test in vitro performed in our laboratory with kinetoplast DNA confirmed the inactivity of the metabolite against topoisomerase IIα. The absence of activity toward topoisomerase suggests that the high cytotoxicity of this compound had to be searched elsewhere. Anthracyclines

such as doxorubicin and daunorubicin can bind covalently the DNA when activated with formaldehyde. Moreover, anthracyclines that have intrinsic ability to form cross-links to the DNA, such as cyanomorpholinyl-doxorubicin or barminomycin, were found to exhibit high cytotoxicity comparable with the PNU. Then we considered the possibility that PNU interacts with the DNA as a preactivated anthracycline. Our work evidenced that PNU behaves similarly to the activated doxorubicin (doxorubicin mixed with H_2CO) in DNA melting analyses. PNU quickly reacts with double-strand oligonucleotides to form adducts detectable by DPAGE. These adducts are sufficiently stable to be isolated by HPLC. Mass characterization confirmed that these complexes are formed by duplex DNA bound to the anthracycline. These investigations suggest that the reaction between PNU and DNA does not involve the formation of a classical cross-link, but in relation to the electrophoretic, chromatographic and mass spectrometry results these adducts can be ascribed to the family of "virtual cross-link" (VXL). Anthracyclines-formaldehyde conjugate or anthracyclines in formaldehyde buffer have the specific ability to intercalate into DNA, forming covalent bonding; a methylene bridge links the amino group of the anthracycline to the 2-amino group of a G-base in the minor groove, while the other strand of DNA is stabilized by hydrogen bonds. Such unusual combination of intercalation, covalent bonding and hydrogen bonding is referred to as the *virtual cross-linkink* [2], that leads to the formation of more stable complexes between the anthracyclines and the DNA, improving the drugs' cell killing ability. Among the different mechanisms of anticancer activity of anthracyclines, anthracycline-DNA adducts formation elicited interest related to the possibility to find safer and more efficacious anticancer drugs. Anthracycline-formaldehyde conjugates and cross-linking anthracyclines exhibit high cytotoxicity comparable to classical cross-linking drugs. We used different anthracyclines aimed to rationalize the structure activity relationship for the formation of VXL. We confirmed by electrophoretic and chromatographic analyses that aminosugar and its amino nitrogen is absolutely necessary for the formation of "VXL" and we discussed the role of the 4' position of the daunosamine in modulation of this activity. The presence of methylene bridge and its relationship with guanine was confirmed by mass spectrometry.

RIASSUNTO

Le antracicline sono un'importante famiglia di chemioterapici, tra queste sono usate prevalentemente l'adriamicina (doxorubicina), la daunorubicina, l'idarubicina e l'epirubicina. Sono farmaci con un ampio spettro d'azione, in particolare l'adriamicina è usata nel trattamento del cancro al seno, del linfoma di Hodgkin, del cancro al polmone, del mieloma multiplo e del cancro ovarico recidivo. Nonostante l'ampio spettro d'azione la resistenza e la severa cardiotossicità limitano l'uso di questi importanti farmaci anticancro. La ricerca di migliori derivati ha dato luogo a più di 2000 analoghi dei quali solamente pochi di essi hanno raggiunto l'approvazione clinica. Anche se il meccanismo esatto con il quale l'adriamicina esercita l'attività anticancro è incerta, il meccanismo principale coinvolge un danno nei confronti dell'enzima topoisomerasi II, un meccanismo supportato dall'intercalazione nel DNA e dalla localizzazione nucleare. La ricerca di antracicline meno tossiche e più efficaci ha portato alla scoperta della nemorubicina, un derivato della doxorubicina in cui l'azoto amminico della daunosamina è incorporato in un anello metossimorfolinico. Le indagini precliniche hanno mostrato che la nemorubicina, diversamente dalle antracicline classiche non è cardiotossica e l'attività antitumorale è mantenuta nei vari modelli di tumore resistenti alla terapia. Risultati incoraggianti sono stati ottenuti in fase I/II dove il composto è stato somministrato attraverso l'arteria intraepatica. La nemorubicina è 80-120 più potente della doxorubicina in vivo, diversamente la sua attività in vitro è solamente otto volte rispetto alla doxorubicina verso culture cellulari tumorali sensibili alle antracicline. Un recente studio ha stabilito che la nemorubicina è convertita dall'enzima CYP3A in un metabolita estremamente più citotossico, il PNU-159682. Questo metabolita è risultato dalle 700 alle 2400 volte più potente rispetto al progenitore nemorubicina verso cellule cancerose umane in coltura e ha mostrato un'efficacia significativa in diversi modelli di tumore in vivo. Studi in corso finalizzati a definire il meccanismo molecolare di azione di PNU-159682 indicano differenti effetti sul ciclo cellulare e una differente interazione col DNA rispetto al progenitore nemorubicina e alla doxorubicina. Inoltre, dati recenti indicano che PNU-159682 mantiene la sua attività anche verso cellule aventi diversi meccanismi di resistenza rispetto a diversi agenti anticancro classici, inclusa la sovraespressione del gene MDR-1, la riduzione dell'attività di topoisomerasi II e mutazioni nel gene codificante per la topoisomerasi I: quest'ultima modifica genetica conferisce resistenza in vitro alla nemorubicina [1]. Noi abbiamo usato diversi approcci sperimentali per razionalizzare l'elevata attività di questo metabolita. Test condotti in vitro nel nostro laboratorio con kinetoplast DNA hanno confermato l'inattività del

metabolita nei confronti della topoisomerasi II. L'assenza dell'attività verso la topoisomerasi ci suggerisce che l'alta citotossicità di questo metabolita è da ricercarsi altrove. Antracicline come doxorubicina e daunorubicina possono legare covalentemente il DNA quando attivate con formaldeide. Inoltre è stato trovato che antracicline che hanno un'intrinseca attività a formare cross-link col DNA come la cianomorfolino-doxorubicina o la barminomicina posseggono un'alta citotossicità comparabile col PNU. Quindi abbiamo considerato la possibilità che il PNU interagisca col DNA come una antraciclina preattivata. Il nostro lavoro ha evidenziato che il PNU si comporta in modo analogo alla doxorubicina attivata (doxorubicina con formaldeide) nelle analisi di melting del DNA. PNU reagisce velocemente con oligonucleotidi a doppio filamento per formare addotti visualizzati in DPAGE. Questi addotti sono sufficientemente stabili per essere isolati tramite HPLC. La caratterizzazione ottenuta tramite spettrometria di massa ha confermato che questi complessi sono formati da DNA a doppio filamento legato all'antraciclina. Questi studi suggeriscono che la reazione tra PNU e DNA non coinvolge la formazione di un classico cross-link, ma in relazione ai risultati elettroforetici, cromatografici e di spettrometria di massa questi addotti possono essere annoverati nella famiglia dei "virtual cross-link" (VXL). I coniugati antracicline-formaldeide o le antracicline in tampone contenente formaldeide hanno la specifica abilità di intercalarsi nel DNA formando legami covalenti; un ponte etilenico lega l'ammino gruppo dell'antraciclina col 2-amino gruppo della base guaninica nel solco minore, mentre l' altra catena del DNA è stabilizzata tramite legami idrogeno. Questa particolare combinazione di intercalazione, legame covalente e legame ad idrogeno è chiamata *virtual cross-link* (VXL) [2], che porta alla formazione di complessi più stabili tra le antracicline e il DNA aumentando la tossicità cellulare delle antracicline. Tra i diversi meccanismi anticancro delle antracicline, la formazione di addotti DNA-antracicline ha suscitato notevole interesse riferito alla possibilità di trovare nuovi farmaci anticancro più sicuri e più efficaci. I coniugati antraciclina-formaldeide e le antracicline cross-linkanti esibiscono un'elevata citotossicità comparabile con i classici agenti cross-linkanti. Abbiamo usato differenti antracicline con lo scopo di razionalizzare il rapporto struttura attività nella formazione del VXL. Abbiamo confermato attraverso l'analisi elettroforetica e cromatografica che l'amminozucchero e l'azoto amminico sono assolutamente necessari per la formazione del "VXL" e abbiamo discusso il ruolo della posizione 4' nella daunosamina nella modulazione di questa attività. La presenza del ponte metilenico e la sua relazione con la guanina è stata confermata mediante spettrometria di massa.

1. INTRODUCTION: anthracyclines in cancer therapy

1.1 Cancer

Cancer is a class of diseases in which a group of cells loses control of their growth. Some characteristics peculiar to cancer include:

-Uncontrolled growth.

-Invasion and destruction of adjacent tissue.

-Sometimes metastasis allowing cancer cells to reach other parts of the body via lymphatic tissue or blood.

These malignant properties differentiate cancer from benign tumors, which are self-limited without invasion and metastasis. Some cancers, such as leukaemia, do not form tumours. Most tumours take the names from the organ or the type of cell in which they start.

Cancer may be divided into several categories, based on their characteristics:

- Carcinoma originates in the skin or in tissue that covers internal organs.
- Sarcoma originates in bone, cartilage, adipose tissue, blood vessels or other connective tissue.
- Leukemia originates in blood-forming tissue, such as bone marrow, causing a large number of abnormal blood cells.
- Lymphoma and myeloma set on in the cells of the immune system.
- Central nervous system cancers begin in the tissue of the brain and spinal cord.

Cancer affects people at all ages, but the risk increases with age [3]. Cancer cause approximately 13% (7.9 million) of human deaths in 2007 [4]. Cancer can be considered an environmental disease, with 90-95% of cases due to lifestyle and environmental factors and 5-10% due to genetic factors. The principal causes of cancer are factors that cause damage to the cell's genetic material: i.e., tobacco, diet, obesity, infections, radiation, stress, and environmental pollutants [5].

The branch of medicine related to the study, diagnosis, treatment, and prevention of cancer is called oncology. An ultimate diagnosis of cancer requires the histological examination of a biopsy specimen, even if the initial indication of the cancer can be symptomatic or an abnormal radiographic image. Most cancers can be treated and cured, but this depends on the specific type, location, and stage of the disease. When diagnosed, cancer is usually treated with a combination of surgery, chemotherapy, and radiotherapy. Cancer is fundamentally a disease related to the regulation of tissue growth: when a normal cell transforms into a cancer

cell, the genes that regulate cell growth and differentiation are changed [6]. Genetic changes may occur at different levels, from the gain or loss of entire chromosomes to a mutation affecting a single DNA nucleotide [7].

Genetic abnormalities found in cancer typically affect two groups of genes: oncogenes and tumor suppressor genes. Oncogenes may be normal genes that are overexpressed, or altered genes with novel properties. In both cases, oncogenes are typically activated in cancer cells, promote cancer, and cause in cells the malignant phenotype endowed with hyperactive growth and division, protection against apoptosis, loss of respect for adjacent tissue, and the ability to proliferate in different tissue and environment.

Tumor suppressor genes are genes that limit cell growth, inhibit cell division and survival, and are inactivated in cancer cells with a consequential loss of the cells' normal functions, e.g., accurate DNA replication, control of the cell-cycle, orientation and adhesion within tissues, and interaction with the cells of the immune system. Generally, changes in many genes are required to transform a normal cell into a cancer cell. Different classifications exist for the various genomic changes that may contribute to generating cancer cells. Most of these changes, though not all, are mutations or changes in the nucleotide sequence of genomic DNA.

Aneuploidy, for example, i. e. the presence of an abnormal number of chromosomes, is a genomic change but not a mutation, and may involve either the gain or loss of one or more chromosomes through errors in mitosis. Large–scale mutations involve the deletion or gain of a portion of chromosome. Genomic amplification occurs when a cell gains many copies of a small chromosomal locus, usually containing one or more oncogenes and adjacent genetic material; translocation, instead, is the fusion of two separate chromosomal regions.

Small–scale mutations include point mutations, deletions, and insertions that may occur in the promoter of a gene and affect its expression, or may occur in the gene's coding sequence and alter the function or stability of its protein product. The disruption of a single gene may also result from integration of genomic material from the DNA of a virus or retrovirus, possibly resulting in the expression of viral oncogenes that affect the cell and its genealogy. Living cells that replicate suffer from errors, and unless error correction and prevention is sufficient, errors will survive and might be passed on to daughter cells. Normally the body safeguards against cancer via numerous methods such as apoptosis, helper molecules (some DNA polymerase), or possibly senescence but these error-correction methods often fail, particularly in environments that make errors more likely to form and propagate, as, for example, in the presence of substances called carcinogens or from periodic injury. Cancer is a progressive

disease and so progressive errors slowly accumulate until cells lose control; the errors that cause cancer are often self-amplifying (Fig. 1).

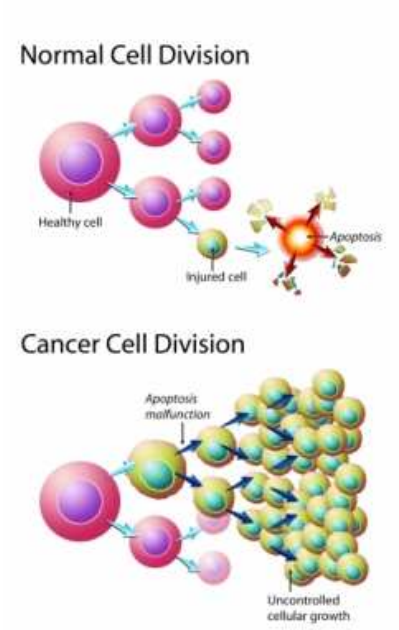

Fig. 1 - Loss of cancer division control. *© 2008 Nucleus Medical Art, Inc*.

Sometimes cancer explodes in a way similar to a chain reaction caused by a few errors that produce more errors. This is effectively the source of cancer and the reason that cancer is so hard to treat: even if the cancer treatment kills almost all cancerous cells, some surviving cells can replicate or send error-causing signal, starting the process all over again. This is an undesirable example of "survival of the fittest" that permits cancer to progress toward more invasive stages; this process is called clonal evolution [8].

1.2 Benefit of Anthracyclines

Anthracyclines are a group of chemotherapeutics that include adriamycin (doxorubicin), daunorubicin, idarubicin, and epirubicin [9]. The first anthracyclines, doxorubicin and daunorubicin, were isolated from the pigment produced by *Streptomyces peucentius* early in the 1960s. Adriamycin (Fig. 2) is active against a broad range of tumors and is now commonly used in treatment of breast cancer, Hodgkin's lymphoma, lung cancer, multiple myeloma, and re-occurring ovarian cancer [10]. Adriamycin represents the anti-cancer agent with the widest spectrum of anti-tumour activity; however, resistance and side effects are major limitations to the success of adriamycin therapy [11]. As with many other anticancer agents clinical use of both doxorubicin and daunorubicin is soon hampered by such serious

problems as the development of resistance in tumor cells, chronic cardiomyopathy, and congestive heart failure.

1.3 The Problem of Cardiotoxicity

Cardiac problems are the principal side effects that affect the therapy with anthracyclines. Dilated cardiomyopathy and congestive heart failure (CHF) develop after completion of cumulative anthracycline regimens. This usually occurs within a year, but delayed forms of cardiac dysfunction have been described. The ultrastructural modifications of anthracycline-induced cardiomyopathy include loss of myofibrils, dilation of the sarcoplasmic reticulum, cytoplasmatic vacuolization, swelling of the mitochondria, and an increased number of lysosomes. Valvular coronary or myocardial heart disease and a long-standing history of hypertension were recognized as independent risk factors of developing cardiomyopathy at cumulative doses of doxorubicin below 500 to 550 mg/m^2.

The quick increment of the incidence of cardiomyopathy at cumulative doses above 550 to 600 mg/m^2 of doxorubicin formed the basis for fixing an empirical dose limit of 500 mg/m^2 as a strategy to minimize the risk of cardiomyopathy. However, ultrastructural changes in endomyocardial biopsies and/or a damage of contractility after provocative tests have been documented in patients treated with reportedly safe cumulative doses. It is no completely certain whether nonsymptomatic cardiac dysfunction eventually would progress to late cardiac events, diminishing or even eliminating the benefit of cumulative doses below 500 mg/m^2 [12].

Even if the risk of cardiac morbidity is possible with low dose treatment, the balance between risks and benefit can still be considered in favour of the use of the anthracyclines, at appropriate dose, in adult patient that can be cured from their neoplastic disease [13].

One of the reasons why cardiomyocytes would be more susceptible than other tissues to apoptosis induced by doxorubicin is that cardiomyocytes exhibit low levels of catalase and readily undergo inactivation of selenium-dependent GSH-peroxidase-1 after exposure to doxorubicin [14]. Lack of this enzyme associated at one increment of superoxide radicals ($O_2^{\cdot -}$) represents the first mechanism of cardiotoxycity.

1.4 Anthracyclines: Anticancer Molecular Mechanisms

Despite extensive clinical use, the mechanisms of action of anthracyclines in cancer cells remain a matter of controversy. The principal mechanisms are the following:

1) intercalation into DNA that inhibits the synthesis of macromolecules,
2) generation of free radicals, leading to DNA damage or lipid peroxidation,
3) DNA cross-linking,
4) interference with DNA unwinding or DNA strand separation and helicase activity,
5) direct membrane effects,
6) initiation of DNA damage via inhibition of topoisomerase II, and
7) induction of apoptosis in response to topoisomerase II inhibition [15].

1.5 Anthracyclines as Topoisomerase II poison

Topoisomerases are a family of enzymes that modify the topology of DNA without altering deoxynucleotide structure and sequence. They can cause transient single-strand (topoisomerase I) or double-strand (topoisomerase II) DNA breaks that result in a change of the twisting status of the double helix. This activity confers topoisomerases an important role as the supercoiling of the DNA double helix is modulated according to the cell cycle phase and transcriptional activity. Anthracyclines act by stabilizing a reaction-intermediate in which DNA strands are cut and covalently linked to tyrosine residues of topoisomerase II, eventually impeding DNA resealing. The formation and stability of an anthracycline-DNA-topoisomerase II ternary complex depend on defined structural characteristics. The planar ring system of anthracyclines is important for intercalation into DNA, as rings B and C overlap with adjacent base pairs and ring D passes through the intercalation site (Fig. 2).

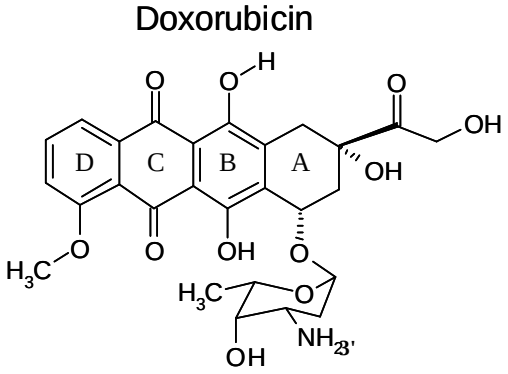

Fig. 2 – Structure of doxorubicin.

The external (non-intercalating) moieties of the anthracycline molecule (i.e., the sugar residue and the cyclohexane ring A) seem to play an important role in the formation and stabilization of the ternary complex. In particular, the sugar moiety, located in the minor groove, is a critical determinant of the activity of anthracyclines as topoisomerase II poisons. Topoisomerase II inhibition increases after removal of amino-substituent at C-3' in the sugar or of the methoxy-group at C-4 in ring D; moreover, the nature of 3'-substituents greatly influences the sequence selectivity of anthracycline-stimulated DNA cleavage [16].

1.6 Role of Free Radicals

The addition of an electron to the quinone moiety in ring C of DOX and other anthracyclines has long been known to result in the formation of a semiquinone that quickly regenerates its parent quinine by reducing oxygen to reactive oxygen species (ROS) such as superoxide anion ($O_2^{\cdot -}$) and hydrogen peroxide (H_2O_2). This futile cycle is supported by a number of NAD(P)H-oxidoreductases [cytochrome P450 or b5 reductases, mitochondrial NADH dehydrogenase, xanthine dehydrogenase, endothelial nitric oxide synthase (reductase domain)]. During this cycle, the semiquinone can also oxidize with the bond between ring A and daunosamine, resulting in reductive deglycosidation and the formation of 7-deoxyaglycone (Fig. 3).

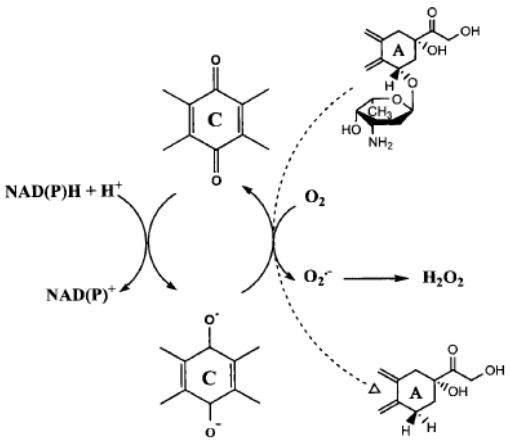

Fig. 3 - One-electron redox cycling of anthracyclines [2].

The aglycones formed have more lipid solubility and intercalate into biologic membranes forming ROS (reactive oxygen species) in the closest proximity to sensitive targets. This one-electron redox cycling of doxorubicin is also accompanied by a release of iron from intracellular stores after interaction with doxorubicin. The release of iron then results in the

formation of 3:1 drug-iron complexes that convert $O_2^{\cdot -}$ and H_2O_2 into more potent hydroxyl radicals ($^{\cdot}OH$). Oxidative damage has therefore been considered an important mechanism of anthracycline activity in tumor cells. Moreover, the iron-mediated formation of ROS and promotion of myocardial oxidative stress remain by far the most frequently proposed mechanism of cardiotoxicity [2], [12].

1.7 Virtual Cross-linking

Although adriamycin exerts its anti-tumor activity with various mechanisms, the dominant mechanism of action appears to involve the impairment of topoisomerase IIα activity [17], [15], [18], consistent with observed DNA intercalation and nuclear localization of adriamycin [19], [20], [21]. Many potential alternative mechanisms of action have been cited and comprehensively reviewed [2], [15]. It is likely that adriamycin acts by many different mechanisms to kill tumor cells, which would be consistent with its broad spectrum of activity. One of these possible mechanisms, Adriamycin–DNA adducts formation, was first reported in 1979 by Sinha and Chignell [22], but the adducts were difficult to isolate and characterize. A further factor in the chemistry of DNA adducts formation is the participation of formaldehyde (H_2CO) in vivo, which activates the anthracyclines to a more reactive electrophile capable of forming covalent adducts with DNA [23].

Doxorubicin and daunorubicin catalyze the formation of formaldehyde under oxidative stress conditions in controlled buffer systems. Koch and colleagues investigated whether the same effect could be observed in tumor cells treated with anthracyclines. In fact, many groups have reported that doxorubicin treatment leads to oxidative stress in tumor cells, and this may contribute to the formation of formaldehyde in vivo [24]. Elevated levels of H_2CO have been detected in doxorubicin-sensitive cancer cells, but not in doxorubicin-resistant cancer cells equipped with higher levels of ROS-detoxifying enzymes [25], [26].

Iron-mediated free radical reactions enable anthracyclines to produce formaldehyde (H_2CO) from carbon cellular sources like spermine and lipids.

Topoisomerase II inhibitors and alkylating agents form two distinct classes of clinical antitumor agents and the presence of both mechanisms of action of the anthracyclines may be an interesting characteristic of these drugs.

In addition to doxorubicin, daunomycin and epirubicin react with formaldehyde to produce conjugates in which two anthracycline molecules become linked through three methylene groups [27] (Fig. 4).

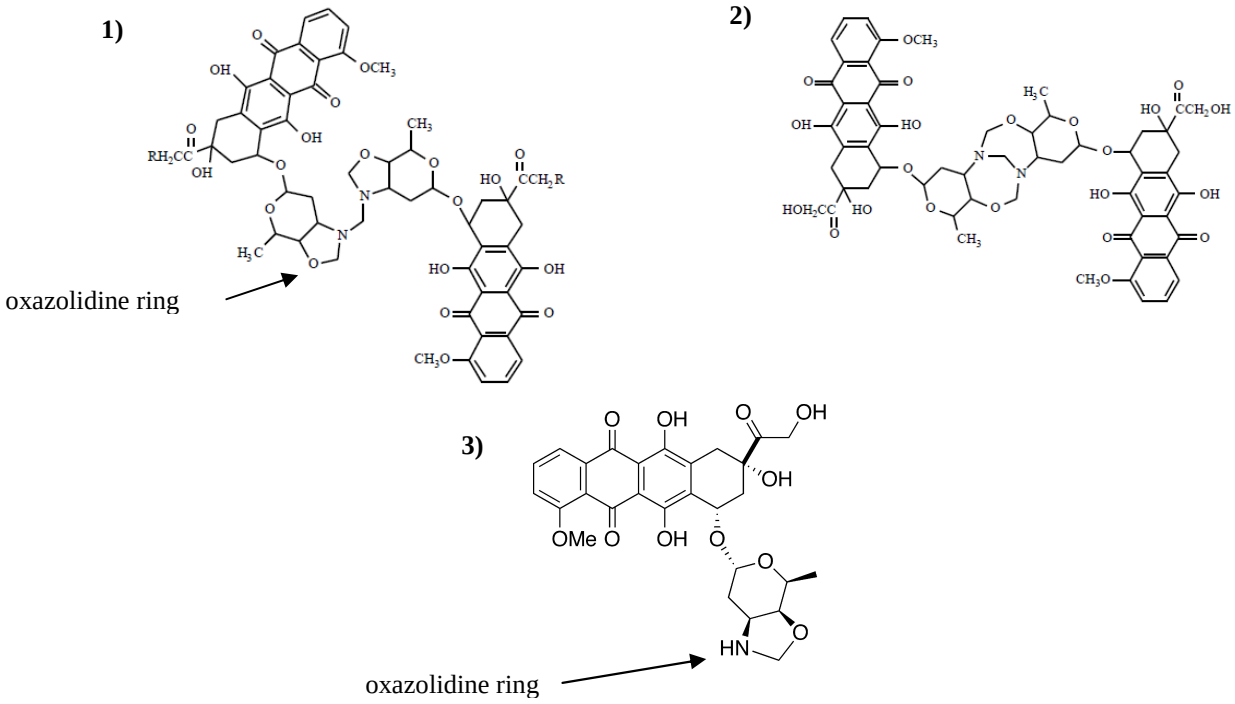

Fig. 4 - Structure of formaldehyde-conjugates anthracyclines. 1) doxoform (R=OH) and daunoform (R=H); 2) epidoxoform; 3) doxazolidine.

These conjugates were synthesized by the reaction of the anthracyclines with a methanolic solution of formaldehyde in an acetate buffer at pH 6 and the conjugates extracted in chloroform as they formed. A presumed intermediate, doxazolidine, was not observed in these conditions[28]. In contrast, the reaction of a doxorubicin free base in chloroform-*d* solvent with paraformaldehyde (the polymer of formaldehyde) monitored by ^{1}H NMR, showed the formation of doxazolidine followed by the formation of doxoform [29]. Doxazolidine induces apoptosis by a topoisomerase II independent mechanism forming adducts to DNA [30]. Anthracycline-formaldehyde conjugates exhibit enhanced toxicity to anthracyclines-sensitive and resistant tumor cells. These conjugates have attracted interest because of their ability to intercalate into DNA, forming covalent bonding between the daunosamine amino-group and the 2-amino group of a G-base in the minor groove of the DNA, linked by a methylene bridge. Some authors observed the formation of more than one adduct anthracycline-DNA using short oligonucleotides at different times of incubation [31]. Each adduct had a different structure and stability. In all cases, such an unusual combination of intercalation, covalent bonding, and hydrogen bonding is referred to as the *virtual cross-linking* of DNA by anthracyclines [32].

Recently, Phillips demonstrated that the anthracyclines in clinical use (doxorubicin, daunorubicin, idarubicin, and epirubicin) cross-link the DNA in the presence of formaldehyde even if epirubicin is less active[33].

Adducts were also detected in MCF-7 breast cancer cells treated with doxorubicin at subclinical doxorubicin concentrations without the addition of exogenous formaldehyde [34].
The requirements for formation of formaldehyde-mediated Adriamycin–DNA adducts, like the presence of the amino group of the daunosamine and the 2'-aminogroup of the guanine, have now been well characterized and reviewed by Cutts and colleagues [23], [35] and their structure proposed [36, 37],[38].

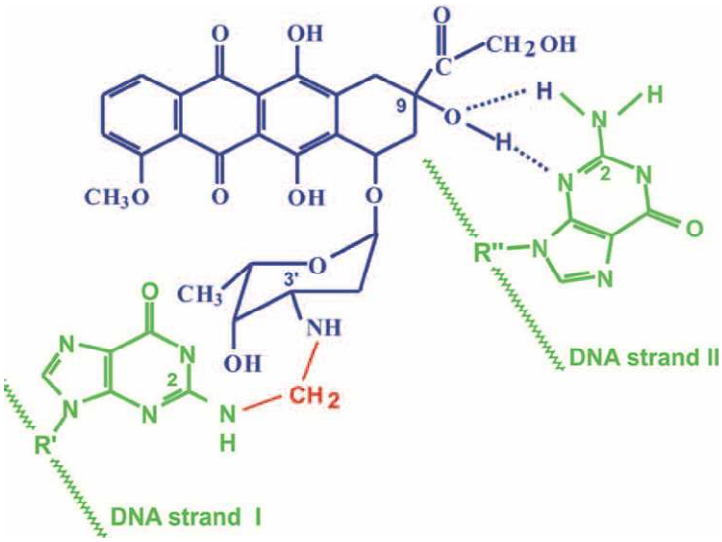

Fig. 5 - Structure proposed for the monoadducts “virtual cross-link” between doxorubicin and DNA [36].

Moreover, some high cytotoxic anthracyclines, such as cyanomorpholinyl-doxorubicin and barminomycin, are able to form covalent adducts with DNA in absence of formaldehyde [39, 40]. These compounds behave as pre-activated anthracyclines.

1.8 Nemorubicin and PNU: A New Perspective for Better Anthracyclines

The search for better performing anthracyclines, with the main goal of limiting cardiotoxicity, has resulted in more than 2000 analogs, a number that should not be surprising considering the number of chemical modifications or substitutions that can be introduced in the tetra-cyclic ring, the side chain, or the aminosugar.
The search for less toxic and more effective anthracyclines has led to the discovery of nemorubicin (3'-deamino-3'-[2"(S)-methoxy-4"-morpholinyl]doxorubicin; MMDX), a doxorubicin derivative in which the amino nitrogen of the daunosamine unit is incorporated into a methoxymorpholinyl ring (Fig. 6) [9], [41].

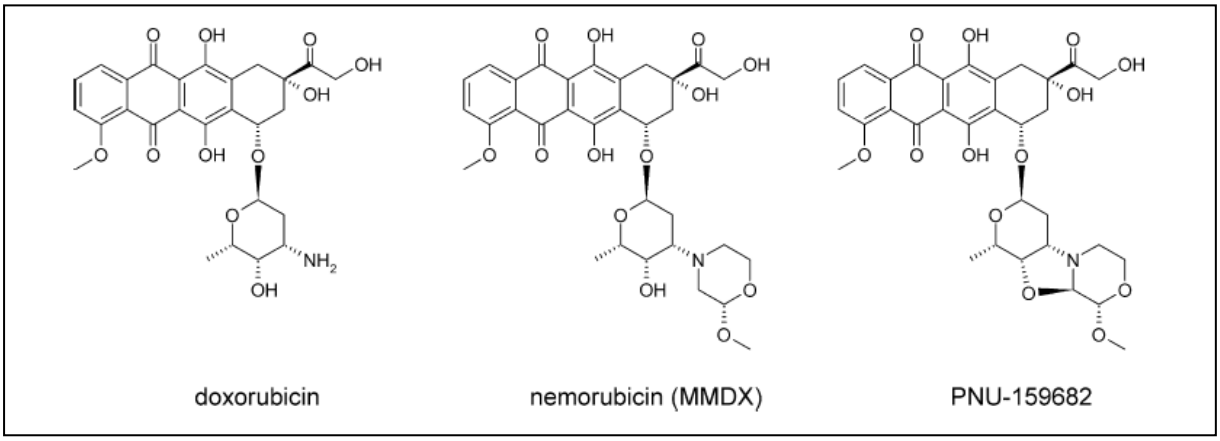

Fig. 6 - Structures of doxorubicin, nemorubicin (MMDX) and PNU-159682 (PNU).

Early preclinical investigations showed that MMDX, unlike classical anthracyclines, is not cardiotoxic at optimal antitumor doses [11] and retains antitumor activity in various multidrug-resistant tumor models [9], [41], [42], [43]. Encouraging results were obtained in Phase I/II clinical trials conducted in Europe and China, where the drug was administered by the intra-hepatic artery route to patients with hepatocellular carcinoma [7]. Based on these clinical data and on preclinical results showing MMDX synergism with cisplatin, the MMDX-cisplatin combination underwent a Phase I/II clinical trial for the loco-regional treatment of hepatocellular carcinoma in Europe.

This compound does not show activity against the enzyme topoisomerase IIα, exhibiting unchanged activity against anthracycline-resistant cells (CEM/VM1) with mutated topo IIα [44].

In vivo, MMDX is 80–120 times more potent than doxorubicin [41]. In contrast, its in-vitro cytotoxicity is only eight and two times greater than that of doxorubicin toward cultured drug sensitive tumor cells and hematopoietic progenitor cells, respectively [11], [45]. Various studies have also shown that incubation of MMDX with NADPH and isolated human, mouse or rat liver microsomes results in marked enhancement of potency toward cultured tumor cells, suggesting that MMDX is converted to a much more cytotoxic metabolite(s) by liver microsomal enzymes. Further in vivo [46] and in vitro result, [47], [48], [49]suggest that enzymes belonging to the CYP3A subfamily are involved in MMDX biotransformation. Moreover a further study [1] established that MMDX is converted by human liver microsomes (HLMs) to a major metabolite, identified as 3'-deamino-3", 4'-anhydro-[2" (S)-methoxy-3" (R)-oxy-4"-morpholinyl]doxorubicin (PNU-159682) (Fig. 6). PNU-159682 was found to be 700–2400 times more potent than nemorubicin toward cultured human tumor cells, and exhibited significant efficacy in in vivo tumor models [1]. These results suggest that

PNU-159682 is the chemical entity responsible for the liver microsome-mediated increase in MMDX cytotoxicity in vitro [46-48], and certainly plays a dominant role in the in vivo antitumor activity of the drug. Ongoing studies aimed at exploring the molecular mechanism of action of PNU-159682 indicate that it has different effects on cell cycle progression and unlike DNA-interacting properties, compared with both MMDX and doxorubicin. Moreover PNU-159682 (PNU) retains its activity against tumor cell lines with different mechanisms of resistance to classical anticancer agents, including MDR-1 gene overexpression, reduced topoisomerase II activity, and mutations in the topoisomerase I gene - these latter genetic alterations conferring resistance in vitro to the parent drug, MMDX [1].

2. AIMS

2.1 PNU Mechanistic Aspects

In our work, we investigated the mechanism by which PNU is remarkably more cytotoxic than its parent compound nemorubicin (MMDX). Tests in vitro performed in our laboratory with kinetoplast DNA confirmed the inactivity of the metabolite against topoisomerase IIα. After incubation of MMDX with liver microsom, Sikic found an increase in cytotoxicity associated with the appearance of alkylating activity based on the alkaline elution even if he did not find the metabolite responsible of this activity [47]. The high cytotoxicity of the major metabolite formed after microsomes incubation, PNU, suggests a possible alkylating activity like cyanomorpholinyl-doxorubicin or barminomycin. We sought after more experimental proof of this hypothesized mechanism using different instrumental methods. The reactivity of this compound toward different synthetic oligonucleotides was studied using gel electrophoresis, fluorescence quenching, chromatographic, and mass spectrometric methods.

2.2 SAR (Structure Activity Relationship) in Virtual Cross-linking

The introduction described the role of virtual cross-linking in the anthracyclines' interaction with DNA. The ability of all therapeutic anthracyclines to form VXLs plays an important role in anticancer activity. Even if topoisomerase II poisoning is the major mechanism of anticancer activity in therapy, the formation of VXL creates new opportunities to individuate more active and less toxic anthracyclines.

We first focused our attention on a study of the structure activity relationships (SAR) of several anthracyclines to clarify their ability to form DNA adducts and cross-links (Fig. 7). We used daunomycin, doxorubicin, idarubicin and epirubicin (anthracyclines in current clinical use) as positive controls and compounds without daunosamine groups (aglycon) as negative controls to validate our methods of analysis.

We evaluate the ability to cross-link DNA by anthracyclines with different modifications at position 4': the –OH group in 4' is crucial in the formation of the reactive oxazoline in doxazolidine and in anthracyclines-formaldehyde conjugates, see (Fig. 4). In epirubicin (4'-epimer), the different configuration of 4'-OH prevents the formation of an oxazoline ring. Consequently epirubicin is less active in forming a cross-link than the other anthracyclines in

clinical use [33]. Therefore, we focused our experiments on deoxydoxorubicin lacking 4'-OH and iododoxorubicin having a 4' iodine substitution.

We used denaturing gel electrophoresis (DPAGE) supported by IP RP HPLC (Ion-Pair Reverse-Phase High Pressure Liquid Chromatography) to investigate the formation of covalent adducts between anthracyclines and DNA.

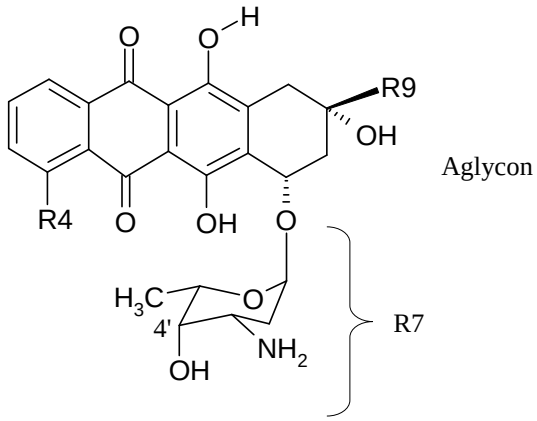

Anthracyclines	R4	R9	R7	ε (M^{-1}*cm^{-1}) #
Doxorubicin (adriamycin) (dx) *	$-OCH_3$	$C(=O)CH_2OH$	Daunosamine	13735±369
Daunorubicin (daunomycin) (dn) *	$-OCH_3$	$C(=O)CH_3$	Daunosamine	9535±201
Epirubicin (4'-epidoxorubicin) (epi) *	$-OCH_3$	$C(=O)CH_2OH$	Daunosamine 4'-epimer	7403±244
Idarubicin (4'-demetoxidaunomycin) (ida) *	-H	$C(=O)CH_3$	Daunosamine	7034±222
Iododoxorubicin (4'-deossi,4'iododoxorubicin) (iodo)	$-OCH_3$	$C(=O)CH_2OH$	Daunosamine with I in 4'	6043±334
Deoxydoxorubicin (deox)	$-OCH_3$	$C(=O)CH_2OH$	Daunosamine without –OH in 4'	9429±299
Doxorubycin aglycon (adriamycinon) (dxru)	$-OCH_3$	$C(=O)CH_2OH$	-OH	9104±285
Daunorubycin aglycon (daunomycinon) (dau)	$-OCH_3$	$C(=O)CH_3$	-OH	7773±443

Fig. 7 - Structure of anthracyclines tested. *Anthracyclines in current clinical use. # Molar extinction coefficient (ε) at 485 nm in Tris 10 mM pH 7.5.

2.3 New Insight into doxorubicin Virtual Cross-Linking

We finally focused our attention on the better-known formaldehyde-mediated doxorubicin-DNA adduct to evaluate the structural characteristics of the methylene bridge using high-resolution mass spectrometry. Our purpose was to investigate the chemical nature of the cross-link between doxorubicin and different synthetic duplex and single stranded oligonucleotides. In this connection, unprecedented high-resolution tandem mass

spectrometry experiments on the above adducts were performed. Formation of the VXL can involve also the formation of adducts between PNU and DNA and a better knowledge of the covalent bond between doxorubicin and DNA can help us to better understand PNU-DNA interactions.

3. MATERIALS

3.1 Compounds

PNU-159682 (ε_{488}= 6310 $M^{-1}cm^{-1}$ in Tris buffer 10 mM pH 7.5), Cyanomorpholinyl-doxorubicin (cma) (ε_{496}= 8685 $M^{-1}cm^{-1}$ in CH_3OH), and MMDX (ε_{495}= 9039 $M^{-1}cm^{-1}$ in Tris buffer 10 mM pH 7.5) were supplied by Nerviano Medical Sciences Srl (Nerviano, Italy).
Doxorubicin (ε_{485}= 13735 $M^{-1}cm^{-1}$ in Tris buffer 10 mM pH 7.5), was supplied by Sigma-Aldrich.
The other anthracyclines tested (Fig. 7 page 18) were supplied by Menarini Industrie Farmaceutiche Riunite, Via Sette Santi, 350131 Firenze.
Compounds were dissolved in DMSO to a 50 mM stock solution and the concentrations were calculated using the molar extinction coefficient (ε).

3.2 Oligos

In the FQA assay (chapter 5.2) we used the follow complementary oligos:
fluorescein labeled oligo z1 forward (z1f): FAM-5'-ACT-ATT-CCC-GGG-TAA-TGA-3' and dabcyl labeled oligo z1 reverse (z1r): 5'-TCA-TTA-CCC-GGG-AAT-AGT-3'-DAB.
In the cross-link assa (chapter 5.3) we used the complementary oligos:
- (z1f): FAM-5'-ACT-ATT-CCC-GGG-TAA-TGA-3' and
oligo zag1 reverse (zag1r): 5'-TCA-TTA-CCC-GGG-AAT-AGT-3'.
- Fluorescein labeled oligo z2 forward (z2f): FAM-5'-ACT-ATT-GGC-GCC -TAA-TGA-3' and oligo zag2 reverse (zag2r): 5'-TCA-TTA-GGC-GCC-AAT-AGT-3'.
In these tests, double stranded-fluorescein labeled z1f-zag1r and z2f-zag2r were visualized by the fluorescence of fluorescein (Excitation λ_{max} = 490 nm, Emission λ_{max} =520 nm).
For the HPLC analysis (chapter 5.4, 5.5, 5.6 and 6.2), we used complementary oligos z1f and zag1r and non fluorescent complementary oligos zag1 forward (zag1f: 5'-ACT-ATT-CCC-GGG-TAA-TGA-3') and zag1r.
For mass spectrometry (chapter 5.7 and 5.8), we use complementary oligos z1f (MW: 6036.2) and zag1r (MW: 5498.6) and self-complementary oligo CG (CG oligo: 5'-CCC-GGG-3' (MW: 1793.2).

All of these oligos were supplied by S.A. Liège Science Park, Rue Bois Saint-Jean 5, 4102 Seraing, Belgium, except oligo CG, which was supplied by Metabion International AG, Lena-Christ-Street 44, 82152 Planegg/Martinsried, Germany.

Structural analyses of the VXL (chapter 6.3) were performed using the following complementary oligos:

- zag1r : 5'-TCA-TTACCC-GGG-AAT-AGT-3' MW: 5498.6
- zag1f: 5'-ACT-ATT-CCC-GGG-TAA-TGA-3' MW: 5498.6
- kt1: 5'-TCT-CGC-TCT-T-3' MW: 2944.97
- kt2: 5'-AAG-AGC-GAG-A-3' MW: 3110.11
- kt3: 5'-TCT-CTC-GCT-CTT-CT-3' MW: 4131.73
- kt4: 5'-AGA-AGA-GCG-AGA-GA-3' MW: 4394.95
- zemen 1 (zm1): 5'-AAT-TAT-GCT-TAA-AA-3' MW: 4269.89
- zemen 2 (zm2): 5'-TTT-TAA-GCA-TAA-TT-3 MW: 4251.86

These oligos were supplied by IDT Integrated DNA Technologies (Coralville, IA, USA).

3.3 Solution buffers

- TE 1X (Tris 10 mM, EDTA 1 mM to pH 7.5)
- TBE 1X (Tris 89 mM, Boric Acid 89 mM, EDTA 2 mM to pH 8.0)
- TEAA (Triethylammonium acetate 100 mM to pH 7.0)
-HFIP/TEA (hexafluoro-2-propanol 100 mM/TEA to pH 8.2)

3.4 Gel electrophoresis

Polyacrylamide and the N,N-bisacrylamide for gel electrophoresis were supplied by Fluka and by National Diagnostic, while the ammonium persulfate and TEMED, used for acceleration of the polymerization of the acrylamide, were respectively supplied by Sigma and by Fluka.

The gel loading buffer used as tracing in the electrophoretic run in the cross-linking assay (chapter 5.3) was composed by Ficoll 400 (Pharmacia Biotech) 18%, EDTA 6 mM, 0.2% of bromophenol blue (Amersham) and 0.2% of xylene cyanol (Amersham).

Images of the DNA in the polyacrylamide gels were obtained using the apparatus Perkin-Elmer Geliance 600; the oligonucleotide z1 forward is functionalized with fluorescein

(Excitation λ_{max} = 490 nm, Emission λ_{max} =520 nm) and therefore could directly be visualized without the addition of ethidium bromide.

The gel loading buffer used in the gels stained with Sigma Stains-All (chapter 6.3) consisted of 50% glycerol (native gel) or 50% glycerol 8M urea (denaturing gel).

The images of these gels were obtained with an HP 7400 scanner.

3.5 General reactants

- Acetic acid supplied by Fluka
- Acetonitrile supplied by Carlo Erba
- Ammonium acetate supplied by Fluka
- APS (ammonium persulfate) supplied by Sigma
- ATP (adenosine-5'-triphosphate) supplied by Sigma
- Boric acid supplied by Sigma
- Bromophenol blue supplied by Amersham
- BSA (bovine serum albumin) supplied by Sigma
- DMSO (dimethyl sulfoxide) supplied by Riedel-de Haën
- DTT (dithiothreitol) supplied by Sigma
- EDTA (disodium ethylenediaminetetraacetate) supplied by Fluka
- Ethidium bromide supplied by Sigma
- Glycerol supplied by Fluka
- HFIP (hexafluoro-2-propanol), supplied by Fluka
- Hydrochloric acid supplied by Carlo Erba
- Isopropanol supplied by Fluka
- KCl (potassium chloride) supplied by Prolabo
- Methanol supplied by Fluka
- $MgCl_2$ x $6H_2O$ (magnesium chloride hexahydrate) supplied by Fluka
- Stains-All supplied by Sigma
- TEA (triethylamine) supplied by Fluka
- TEMED (N,N,N',N' tetramethylethylenediamine)supplied by Fluka
- Tris (tris(hydroxymethyl)aminomethane) supplied by Sigma
- Xylene cyanol supplied by Amersham

4. METHODS

4.1 Topoisomerase II inhibition

Topoisomerases are enzymes that modify the topology of DNA without altering its structure and sequence. They can cause transient single-strand (topoisomerase I) or double-strand (topoisomerase II) DNA breaks; the DNA strands are rejoined after the changing of twisting status of the double helix. This activity confers an important role on topoisomerases, as the supercoiling of the DNA double helix is modulated according to the cell cycle phase and transcriptional activity [16]. Anthracyclines act by stabilizing an intermediate reaction in which DNA strands are cut and covalently linked to tyrosine residues of topoisomerase II, eventually hindering DNA resealing. The formation and stability of an anthracycline-DNA-topoisomerase II ternary complex depend on defined structural properties. The planar ring system is important for intercalation into DNA, as rings B and C overlap with adjacent base pairs, and ring D passes through the intercalation site. The external (nonintercalating) moieties of the anthracycline molecule (i.e., the sugar residue and the cyclohexane ring A) seem to play an important role in the formation and stabilization of the ternary complex. In particular, the sugar moiety, located in the minor groove, is a critical determinant of the activity of anthracyclines such as topoisomerase II poisons. Adriamycin is widely known as a topoisomerase II poison, and therefore in our experiments we have verified whether the structurally correlated PNU is also able to inhibit the human enzyme. To investigate the inhibitory effects of doxorubicin and PNU on the enzymatic activity of topoisomerase II, we used a decatenation assay as in Fig. 8.

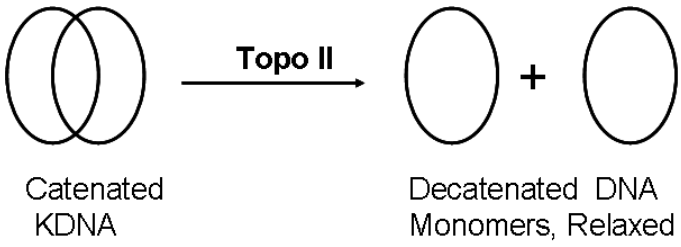

Fig. 8 – Different decatenation products with human topoisomerase II and kDNA

The DNA used in this test is the kinetoplast DNA (kDNA), the mitochondrial DNA of *Crithidia fasciculata*, a catenated network of DNA rings, most of which are 2.5 KB monomers. Type II topoisomerase (although not type I) has the ability to decatenate KDNA and generate the monomer DNA; therefore, decatenation is a highly specific assay for topo II

(Fig. 8). The KDNA networks are large relative to the monomers and do not migrate in the gel remaining in the well while the minicircles can be easily resolved in agarose gel. Both gel and the running buffer are contained the intercalator ethidium bromide, which permits monitoring of the appearance of monomers with a UV light source and to resolve various DNA forms (linear, nicked circular DNA, and relaxed DNA monomers). The presence of ethidium bromide simplifies the gel. In fact different topoisomeres of relaxed minicircles supercoil in the presence of ethidium bromide, forming only bands with the same electrophoretic mobility. This permits to distinguish clearly the linear DNA from the nicked circular DNA that are not affected by supercoiling as intact minicircles (Fig. 9).

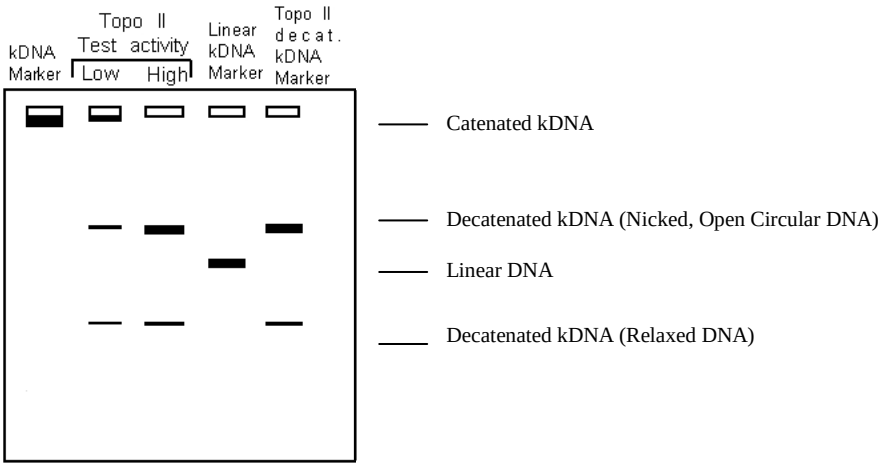

Fig. 9 - Idealized view of kDNA reactivity with eukaryotic topoisomerase II

This test is specific for both isoforms of topoisomerase II (α and β) because it relies on the conversion of catenated DNA to its decatenated form, which requires double strand cut and ligation uniquely done by topoisomerase II.

In this experiment, 200 ng of KDNAs were incubated with adriamycin at concentration 10, 1 and 0.1 μM and with PNU 100, 10 and 1μM, respectively, in the presence of 0.025 U of human topoisomerase IIα in a topoisomerase II reaction buffer (Tris-HCl pH 7.9 40 mM, KCl 80 mM, DTT 5 mM, BSA 15 μg/ml, ATP 1 mM and $MgCl_2$ 10 mM) at 37 °C for one hour. After incubation, we added to each sample 3μl of GLB and analyzed the samples by agarose gel electrophoresis. We performed electrophoretic run in agarose gel 1% in TBE 1X (Tris 89 mM, boric Acid 89 mM, EDTA 2 mM, pH 8.0) in the presence of ethidium bromide 0.5μg/ml. Samples were run overnight at 1 V/cm.

4.2 DNA melting by FQA (Fluorescence-Quenching Assay)

The fluorescence-quenching assay derives from FRET (Fluorescence Resonance Energy Transfer). Fluorescence resonance energy transfer (FRET) has become widely used in all applications of fluorescence, including medical diagnostics. FRET is an electrodynamic phenomenon that can be explained using classical physics. FRET occurs between a donor molecule in the exited state and an acceptor molecule in the ground state. The donor molecules typically emit at shorter wavelength that overlap with the acceptor's absorption spectrum. The term "resonance energy transfer" (RET) is preferred because the process does not involve the appearance of a photon and is the result of a long-range dipole-dipole interaction. The rate of energy transfer depends on the range of spectral overlap of the emission spectrum of the donor with the absorption spectrum of the acceptor, the quantum yield of the donor, the relative orientation of the donor and acceptor transition dipoles, and the distance between the donor and acceptor molecules.

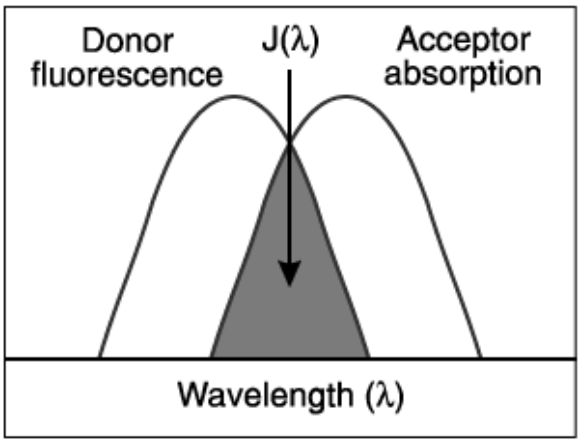

Fig. 10 – Overlapping of spectrum of donor and acceptor to obtain a phenomenon of energy transfer (RET).

The distance at which RET is 50% efficient is called the Förster distance (R_0), which is typically in the range of 20 to 60 Å. The rate of energy transfer from a donor to an acceptor $kT_{(r)}$ is given by

$$kT_{(r)} = (1/\tau_D)*(R_0/r)^6$$

where τ_D is the decay time of the donor in the absence of acceptor, R_0 is the Förster distance [50], and r is the donor-to-acceptor distance. Hence, the rate of transfer is equal to the decay rate of the donor ($1/\tau_D$) when the donor-to-acceptor distance (r) is equal to the Förster distance and the transfer efficiency is 50%. At this distance ($r = R_0$) the donor emission would

be decreased to half its intensity in the absence of acceptors. The rate of RET depends strongly on distance, and is proportional to r^{-6}. Förster distances ranging from 20 to 90 Å are convenient for studies of biological macromolecules, as this distance is comparable to the size of biomolecules and the distance between sites on multi-subunit proteins. Any condition that affects the donor-acceptor distance will affect the transfer rate, allowing the change in distance to be quantified [51]. Fluorescence quenching concerns any process that decreases the fluorescence intensity of a sample, including energy transfer. But if the donor and the acceptor are closer than Förster distance, the intensity of the fluorescence of both is reduced. At these intimate distances, most of the absorbed energy is dissipated as heat and only a small amount of energy is emitted as light. This phenomenon is sometimes called static or contact quenching. Both mechanisms are used in molecular biology. In adjacent probes and in randomly coiled probes, the donor and the acceptor moieties remain at such a distance from each other that FRET is the predominant mechanism of quenching. In contrast, in competitive hybridization probes and in molecular beacons, when they are not hybridized to targets, the two moieties are very close to each other and contact quenching is the predominant quenching mechanism. A useful characteristic of contact quenching is that all fluorophores are quenched equally well, regardless of whether the emission spectrum of the fuorophore overlaps the absorption spectrum of the quencher, one of the key conditions that determines the efficiency of FRET [52].

A further simplification of the tests that use fluorescently-labelled probes is the use of non-fluorescent dyes as acceptor or quencher [53]. Quenching by non-fluorescent dyes enables changes in the intensity of fluorescence to be measured directly, rather than as an alteration in the shape of the emission spectrum, which is more difficult to monitor.

Our model (complementary oligonucleotides 18 base pairs z1f and z1r) contains an oligo duplex where one strand has the 5' extremity labelled with the fluorophore 6-carboxy-fluorescein (FAM) and the other strand with the non-fluorescent quencher Dabcyl (DAB). Dabcyl often behaves as a contact quencher and in our model is sufficiently close to the fluorophore to work as a contact quencher.

Duplex z1f-z1r
- z1 forward (z1f) FAM-5'-ACT-ATT-CCC-GGG-TAA-TGA-3'
- z1 reverse (z1r) DAB-3'-TGA-TAA-GGG-CCC-ATT-ACT-5'

This model allows us to measure the melting temperature of different oligonucleotide duplexes, with information on the interactions with small molecules. The melting temperature

is the temperature at which 50% of the double stranded oligonucleotides are denatured. Compounds that interact with the duplex DNA are able to modify the melting temperature, compounds able to intercalate in the DNA stabilize the double helix and increase the melting temperature of linear double stranded DNA, and molecules that destabilize the helix structure decrease the melting temperature. The oligonucleotide z1 forward (z1f) is labelled with the fluorophore FAM, while z1reverse (z1r) is labelled with the quencher DAB. When the oligos anneal to form the duplex, the fluorophore and the quencher are close and the fluorescence is quenched, but when the duplex denatures FAM and DAB (the quencher) are far and we observe an increment of the fluorescence (Fig. 11).

FQA assays were conducted with a Roche Light Cycler 1.5 instrument, using glass capillaries containing the following reaction mixture: 2 µl of drug examined 10X in water, 2 µl TE 10X (Tris 100 mM, EDTA 10 mM at pH 7.5), duplex z1f-z1r 1 µM (final concentration), and water mQ to 20 µl. The protocol for the assay was: 2 minutes of isotherm at 30 °C, temperature increments to 95 °C in 30 minutes (melting) and finally a step of annealing, cooling the mix in 1 hour to 30 °C. Fluorescence was read during the melting and annealing by the instrument at 530 nm.

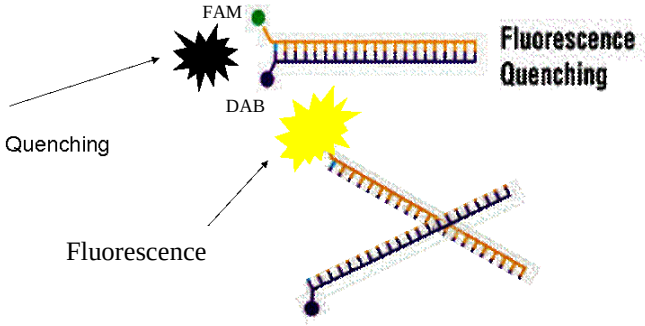

Fig. 11 – Fluorescence quenching of two complementary oligonucleotides functionalized with fluorescein and Dabcyl.

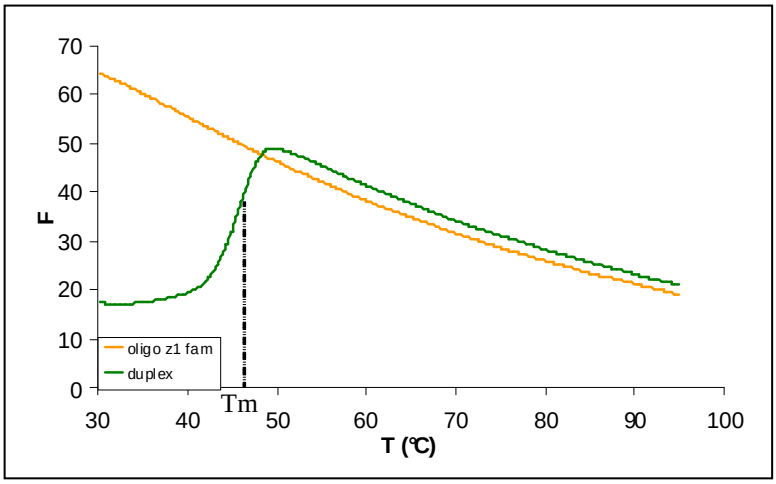

Fig. 12 – Profile of thermal denaturation of oligos z1f single strand (z1fam) and duplex oligo (z1f-z1r) in TE 1X.

In Fig 12 we can observe the thermal denaturation profile of single-stranded oligo z1f and the duplex z1f-z1r, respectively. The flex point of the curve corresponds to the melting temperature where the 50% of the duplex is denatured. The melting point can be determined more easily using the first derivative of the curves (Fig. 13).

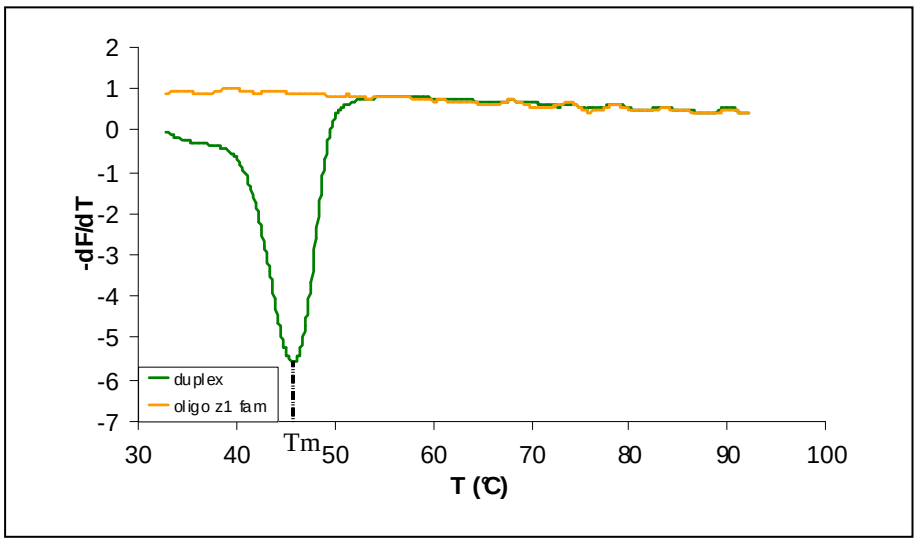

Fig. 13 - First derivative profile of thermal denaturation of oligos z1f single strand (z1fam) and duplex oligo (z1f-z1r) in TE 1X.

The single-stranded oligo z1f decreases its fluorescence intensity with the increment of temperature (generally an increase in temperature decreases the fluorescence). Instead, the duplex oligo has a low fluorescence that increases with the progression of the thermal denaturation. When the duplex is completely denatured, the change in fluorescence with the temperature is the same as that of the single stranded oligo z1f.

4.3 In vitro cross-link assay

The basis of the "in vitro cross-link assay" is that drugs induce stabilization of DNA preventing the complete denaturation of double-stranded DNA (DS) upon exposure to denaturing conditions. Gel electrophoresis technique is a widely used technique for manipulation of different biomolecules, including DNA, RNA and proteins. With the increased availability of relatively short, custom-made oligonucleotides, denaturing polyacrylamide gel electrophoresis (DPAGE) has become a commonly performed assay for manipulating DNA and assessing its interactions with a variety of others compounds. DPAGE is also a useful method for detention of interstrand cross-links. When a double-stranded oligonucleotides is denatured, the single strand moves slowly (compared to the original

duplex) through the gel matrix. If an interstrand cross-link has been formed, however, the strands cannot separate. As a result, they retain their retarded mobility and form a discrete band that does not progress nearly as far through the gel [54]. In the experiments with the PNU (chapter 5.3) and in SAR analysis (chapter 6.1) we used the duplex z1f-zag1r and z2f-zag2r, fluorescein labeled duplexes that permits us to visualize the oligos taking advantage of the fluorescence.

Duplex z1f-zag1r
- z1 forward FAM-5'-ACT-ATT-CCC-GGG-TAA-TGA-3'
- zag1 reverse 3'-TGA-TAA-GGG-CCC-ATT-ACT-5'

Duplex z2f-zag2r
- z2 forward FAM-5'-ACT-ATT-GGC-GCC -TAA-TGA-3'
- zag2 reverse 3'-TGA-TAA-CCG-CGG-ATT-ACT-5'

Operatively oligos were incubated with different amounts of anthracyclines at 37 °C in TE 1X. After incubation the samples were loaded in polyacrylamide (acrylamyde : bisacrylamide ratio 19:1) denaturing gel (DPAGE) 20% containing urea as denaturing agent at the concentration of 6 M. Electrophoretic runs were performed in TBE 1X. The gels were read directly with Perkin-Elmer Geliance 600.
In the part that treats the structure of the cross-link (chapter 6.3, page 94) we used unlabelled oligos kt3, kt4, zm1, zm2, zag1r and zag1f and the gels were stained with Sigma Stains-All.

Duplex kt3-kt4
- kt 3: 5'-TCT-CTC-GCT-CTT-CT-3'
- kt 4: 5'-AGA-AGA-GCG-AGA-GA-3'

Duplex zemen
- zemen1: 5'-AAT-TAT-GCT-TAA-AA-3'
- zemen2: 5'-TTT-TAA-GCA-TAA-TT-3'

Duplex zag
- zag1r: 5'-TCA-TTA-CCC-GGG-AAT-AGT-3'
- zag1f: 5'-ACT-ATT-CCC-GGG-TAA-TGA-3'

Stains-All is suitable to stain both double strand and single strand DNA, and allowed us to use unlabelled oligonucleotides, even if this meant that we had to load the gel with a higher quantity of DNA.
Operatively in the experiments described in chapter 6.3 oligos single and double stranded were incubated with different amounts of anthracyclines at 37 °C (oligo zag), room temperature (oligo zemen) or 4 °C (oligo kt). After incubation the samples were loaded in polyacrylamide (acrylamyde : bisacrylamide ratio 19:1) denaturing gel (DPAGE) 20% containing urea as denaturing agent at the concentration of 7.5 M. Electrophoretic runs were

performed in TBE 1X. Gels were stained with Stains-All and images captured with an HP 7400 scanner. Different conditions will be described in detail during the discussion of the results. The in vitro crosslink study provides direct evidence for the formation of anthracyclines-DNA adducts.

4.4 Ion-pair reversed-phase HPLC

Ion-pair reverse-phase HPLC (IP RP HPLC) is a successful technique used to resolve and purify oligonucleotides. The retention times of solutes such as proteins, peptides, and oligonucleotides can be modified by adding ion pairing agents to the mobile phase. Ion pairing agents bind to the solute by ionic interactions, which results in modification of the solute's hydrophobicity. Both anionic and cationic ion pairing agents are used depending on the ionic character of the solute molecule and the pH of the mobile phase. The ion pairing agent used with oligonucleotides, which contain a negative charge at neutral to high pH, is typically triethylamine. In some cases, the addition of ion pairing agents to the mobile phase is an absolute requirement for binding the solute to the reversed phase medium. For example, retention of deprotected synthetic oligonucleotides (i.e., without the trityl protecting group attached) requires triethylamine in the mobile phase. The concentration of ion pairing agents in the mobile phases is generally in the range 0.1 - 0.3%. Potential problems include possible absorbance of UV light by the ion pairing agent and changes in the extinction coefficient with the concentration of the organic modifier. This can result in either ascending or descending baselines during gradient elution. Temperature plays an important rule in the separation: increasing the temperature, we reach denaturing conditions sufficient to separate the duplex DNA and obtain the two single strands, improving the efficiency of the separation (Fig. 14). If the temperature is too low, we do not have separation of the duplex; and if the temperature is too high, we reduce the life of the column.

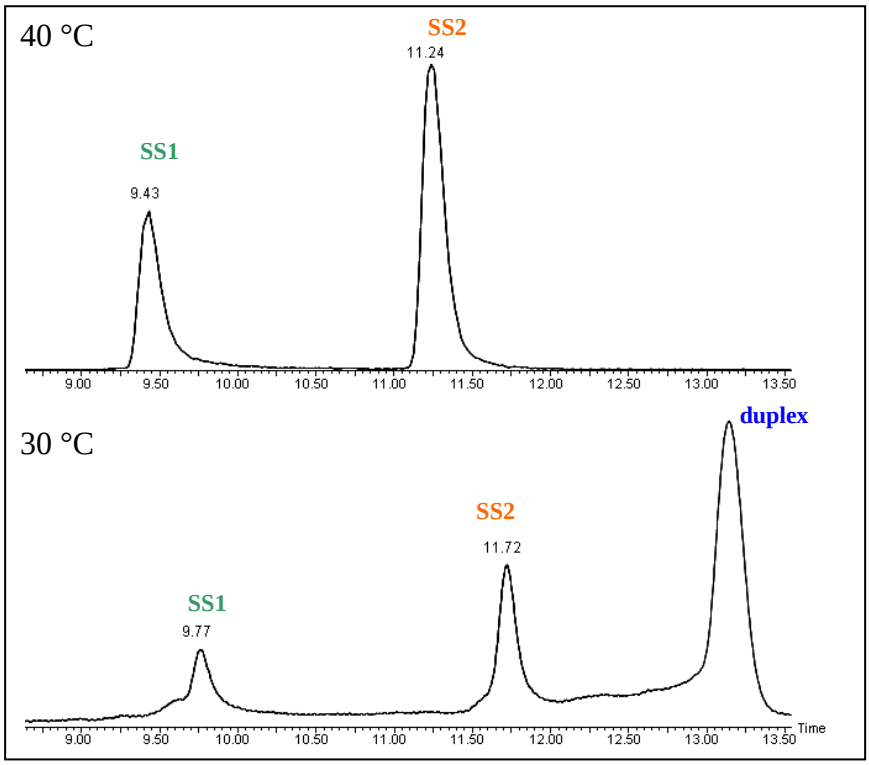

Fig. 14. – Different profile of elution of duplex DNA at 30 °C and 40 °C using IP RP HPLC.

IP RP HPLC allows us to efficiently separate oligonucleotides and drug-DNA adducts. Oligonucleotides are very hydrophilic and interact weakly with reversed-phase C18 column; we improved the interaction using the ion pairing agent triethylammonium acetate, which interacts with the stationary phase of the column and with the oligonucleotide. In particular, the ethyl groups of the salt interact with the stationary phase C18 while the quaternary ammonium charge interacts with the phosphate groups of the DNA, increasing the retention time of the oligonucleotides (Fig. 15).

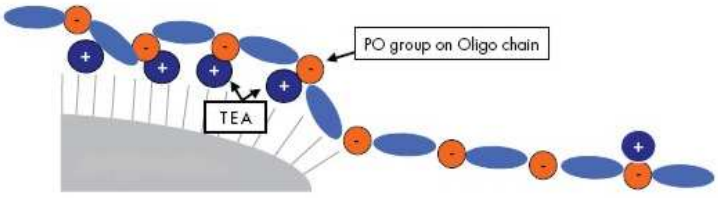

Fig. 15 – Triethylammonium interacts both with the stationary phase of the column and with the DNA, increasing the retention time of oligonucleotides that can be separated according to their size.

We performed and discussed the chromatographic analyses in collaboration with the doctor Luigi Quintieri (Department of Pharmacology and Anesthesiology, University of Padova).

The chromatographic analyses were performed on the instrument Hewlett-Packard series 1100 HPLC system. This instrument is equipped with degasser, quaternary pump, autosampler, and multiple-wavelength detector (Agilent, formerly Hewlett-Packard GMBH, Germany); chromatographic data were collected and integrated by the Hewlett-Packard ChemStation software (version A.06.03) (instrument 1). Some chromatographic analyses were performed in another instrument (instrument 2), a Varian ProStar 210 equipped with a diode array detector (UV-VIS DAD Diod Array ProStar 335). The column used was XTerra (Waters) RP18 (3.0 x 100 mm; 3.5 μm). Chromatographic runs were performed at 40 °C.
The gradient method used two solvents: acetonitrile and TEAA (100 mM pH 7) (Tab. 1).

A)

Time (min)	%CH_3CN	% TEAA 0,1M
0	5%	95%
8	5%	95%
20	40%	60%
25	40%	60%

B)

Time (min)	%CH_3CN	% TEAA 0,1M
0	5%	95%
8	5%	95%
20	40%	60%
25	40%	60%
28	50%	50%

C)

Time (min)	%CH_3CN	% TEAA 0,1M
0	5%	95%
8	5%	95%
15	15%	85%
20	40%	60%
25	40%	60%

Tab. 1 - Methods and gradients used for the chromatographic analyses of DNA-adducts formed by doxorubicin and PNU (A), iododoxorubicin (B) and doxoform (C).

We used method C to analyze doxoform adducts with instrument 1. Instrument 2 gave better results with method A. Method B, used in instruments 2, is method A with an additional 3 minutes with which we reached 50% of CH_3CN, which allowed us to elute iododoxorubicin, more lipophile with respect the other anthracyclines.

4.5 Mass spectrometry analyses

Different methods and techniques are used to investigate oligonucleotides. If the best method available to verify oligonucleotide purity is analytical capillary electrophoresis (CE), the best method available to value compound identity in a high throughput environment is mass

spectrometry (MS). In mass spectrometry analysis, a small quantity of oligonucleotide is ionized and the ions are propelled into a mass detector/analyzer where molecular weight is calculated. In routine use, two methods of mass spectrometry are principally used to investigate nucleic acids: MALDI-TOF (Matrix Assisted Laser Desorption Ionization-Time of Flight) and ESI (ElectroSpray Ionization). Each method has advantages and disadvantages that change with the analytical environment in which they are used.

In MALDI-TOF mass spectrometry, a small amount (1-3 pmol) of a sample is mixed with a matrix solution, usually 3-hydroxypicolinic acid, and the mixture is deposited at a fixed position on a sample grate in the MALDI-TOF instrument. The sample-mixture is then vaporized with a pulse of laser light at a fixed wavelength. This is the desorption phase of the analysis. During desorption, some of the oligonucleotide molecules become ionized through protonation (i.e., the oligonucleotides gain a proton and gain a +1 charge relative to the unprotonated molecules). This instrument works in positive ion mode, then detects the positive ion generated.

ESI Technology was developed around the same time as MALDI. With this technique, a sample in a solvent is introduced into the system via injection of a fine spray from a capillary in the presence of a strong electric field. This electrostatic field causes the break up of the sample solution into small droplets. Typically, solvent is removed from the droplets by passing nitrogen gas into the interface. The molecules are then carried up to a high-vacuum region of the ESI instrument via a low-pressure transport system. In the low-pressure region, which is a heated metal capillary, sample molecules are separated from any remaining solvent in a process called “declustering.” During this process, the molecules become ionized via deprotonation. In the case of oligonucleotides, multiple protons are removed, resulting in a variety of multiply negatively charged species. This is the ionization phase. Generally ESI works in negative ion mode for the analysis of oligonucleotides detecting the negative ions.

In the TOF detection phase, ionized oligonucleotide molecules are then accelerated with an electrostatic field in the instrument to a common kinetic energy.

In the accelerator, ions obey the rule $E = 1/2\ mv^2$, where E is kinetic energy, m is the mass of the ion, and v is the velocity of the moving ion. Under the established condition that E is equal to zA, where z is the charge of the ion and A is the constant accelerating potential applied to all ions, after rearranging we see that $v = (A2z/m)^{½}$. Therefore, in the TOF analyzer, the velocity of an ion is determined completely by its mass and charge state. Remembering that velocity is simply a function of time (t) and distance (d), (v = d/t) the time of flight (TOF) for a fixed distance is completely determined by ion mass and charge state (t =

$d(m/2Az)^{1/2}$). Then, at the same charge state, lighter ions will arrive at the detector faster than heavier ions. In a MALDI-TOF instrument, the entire mass spectrum is recorded in a fraction of a second as ion flux versus time. This spectrum is then compared to the expected mass of the oligonucleotide based on the sequence.

A quadrupole mass analyzer acts as a variable mass filter that separates ionized species using only electrical fields generated by a direct current and superimposed radio-frequency potential. These fields are produced by four rods aligned exactly parallel, with opposite rods linked together (i.e., a quadrupole). Ions are introduced in a path parallel to the quadrupole rod direction and, within a given set of field conditions, only ions of a particular mass and charge state can pass through. All non-conforming ions will have an unstable route and will be filtered out. Thus, if field conditions are varied according to a fixed set of parameters, all ions can be passed and a mass spectrum is acquired. Here again, under the conditions of ESI, variation in the mass spectrum will be completely determined by ionic masses, and these variations can be compared to an expected determination by the known mass of the oligonucleotide sequence.

In general, both MALDI and ESI methods are very sensitive to sample amounts in the range of 100 fmol to 2 pmol for MALDI-TOF and 250 fmol to 10 pmol for ESI. MALDI-TOF is capable of analyzing compounds with a molecular weight greater than 300,000 atomic mass units (amu) while ESI is limited to an effective upper limit of 100,000 amu. MALDI-TOF resolution is limited and analysis of compounds with a molecular weight below 600 Daltons (Da) is difficult due to the presence of matrix signals. ESI also has difficulty analyzing mixtures of compounds, and the presence of salts, buffers, detergents, and other additives reduces sensitivity. MALDI-TOF is reasonably tolerant to the presence of salts, buffers, and other additives.

Mass spectrometry does not measure mass directly, but rather measures a mass/charge ratio (m/z). Ideally, for MALDI-TOF, a single ionized species is present (molecules that gain a single proton, measured as MH^+). Some molecules gain two protons in the desorption phase and represent $M\text{-}2H^+$.

The m/z ratio is calculated by taking the molecular weight of an oligonucleotide, subtracting (or adding if the instrument works in positive mode) out the mass of H^+ removed, and then dividing by the number of H^+ removed ($m/z = m-(z * 1{,}0078))/z$). These raw data are often processed using a deconvolution algorithm that takes all of the peaks present in the trace and performs the reverse computation.

When running through the raw data, the deconvolution program seeks groups of peaks that all add up to the same parent peak. Consequently, the deconvolution analysis removes almost all of the noise because noise does not add up to a consistent figure. Thus, a final deconvoluted ESI trace has a smooth baseline compared to a final MALDI-TOF trace.

During MALDI-TOF analysis, depurination of the oligonucleotides can occur as a result of heating (laser ionization) in the acidic environment (the matrix).

During ESI analysis instead, depurination can occur because of heating in the transport region of the instrument. Depurination can create secondary peaks having 135 (dA) or 151 (dG) mass units less than the major peak.

Noncovalent complexes could be transported intact from solution into the gas phase using electrospray ionization (ESI), and detected using mass spectrometry (MS). Despite the limitations of early instrumentation, various researchers have detected noncovalent complexes between nucleic acids, proteins, and small molecules, and have studied the gas-phase conformations of the ions as a function of both solution and ESI-MS conditions [55], [56].

The utility of ESI-MS for the ionization, detection, and characterization of noncovalent complexes of almost every type of biomolecule has now been described. Mass spectrometry has a key advantage over other biophysical instruments: the identities and abundances of different complexes can be determined from direct observation, since the mass of every molecule serves as the intrinsic detection “label.” ESI-MS has been used to characterize various features of protein-protein, protein-DNA, protein-RNA, and DNA-DNA complexes, including macromolecular and ligand binding stoichiometry, and solution binding affinities. Molecular interactions with dissociation constants ranging from nanomolar to millimolar can be characterized using ESI-MS. Once isolated in the gas phase, noncovalent complexes can be analyzed via dissociation (MS/MS) to determine binding sites or can be probed for structural analyses using ion-molecule reactions. ESI-MS is very powerful for the characterization of noncovalent complexes of nucleic acids. DNA duplexes have long been an attractive model system for ESI-MS studies of noncovalent complexes. Multiply charged duplex ions are stable in the gas phase for extended periods, even with unsolvated charges. Their gas-phase stability is balanced between the number of hydrogen bonds and base stacking among the nucleobases and the total charge present on the strands. Duplex ions with lower charge states are more stable and may retain structures similar to their solvated solution counterparts.

Studies on the gas-phase stability and structure of DNA duplexes are of interest from a physical and biochemical perspective. The solution stability of duplex DNA is attributed to a

variety of factors, including hydrogen bonding between the bases, the screening of backbone charge by solvent, and the stacking of the bases in the hydrophobic interior of the helix. In the gas phase, the latter two stabilizing features may be reduced or unavailable while the strengths of the hydrogen bonds are increased. Although duplex ions have been observed for several years, the nature of the interaction between strands in the gas phase remains an important unanswered question.

Noncovalent interaction of DNA (both single-stranded and duplex) with small molecules provides the basic mechanism of action for a number of therapeutic agents including antitumor, antimicrobial, and antiviral compounds. While a number of analytical schemes have been used to study these interactions, mass spectrometry is emerging as a powerful technique for studying such complexes [57].

We use ESI technology to investigate the complexes anthracyclines.DNA.

We investigated and discussed the complexes PNU-DNA in collaboration with Nerviano Medical Sciences Srl using the instrument Waters Q-TOF Ultima modality ESI.

This instrument had two different associated detectors, a quadrupole (Q) followed by a TOF.

In the direct mass measure, the effective detector is the TOF, but we can perform a tandem mass spectrometry (MS/MS) in which the ions are isolated and activated in the quadrupole, and the fragment formed analyzed by TOF.

The following mass spectrometry investigations were performed and discussed in collaboration with professor Daniele Fabris (The RNA Institute, University at Albany). In the Fabris-laboratory we investigated the interaction between the doxorubicin and formaldehyde by Bruker Daltonics (Billerica, MA) ultrOTOF-Q™, instrument equipped with a quadrupole and TOF analyzer. Then we took advantage of the possibility of using a high-resolution instrument to investigate specifically the VXL. The instrument used was a Bruker Daltonics (Billerica, MA) Apex IV FTICR equipped with a 12T superconductive magnet (Fig. 16). This instrument allowed us to simultaneously use different analytical approaches currently used in mass spectrometry. With this instrument, we used ESI technology to transport intact adducts in the gas phase. The instrument allowed us to successively isolate ions in the quadrupole when necessary. A critical part of this mass spectrometer is the detector. Fourier transform-ion cyclotron resonance-mass spectrometry (FT-ICR-MS), also known as Fourier transform mass spectrometry, is a kind of mass analyzer based on the cyclotron frequency of the ions in a fixed magnetic field. The ions are trapped in a Penning trap (a magnetic field with electric trapping plates) where they are excited to a larger cyclotron radius by an oscillating electric field perpendicular to the magnetic field. The excitation also results in the ions moving in

phase (in a packet). An image signal is produced on the detection plates, which is detected as an image current on a pair of plates. The resulting signal is called free induction decay (FID), a transient or interferogram that consists of a superposition of sine waves. The useful signal is extracted from these data by performing a Fourier transform to give a mass spectrum.

The advantage of this instrument is the very high resolution that allows us to identify unambiguously the species detected.

A) B)

Fig. 16 - Bruker Daltonics (Billerica, MA) Apex IV FTICR. A) Scheme of electrospray. B) ICR cell.

5. PNU-ADDUCTS DISCUSSION AND RESULTS

5.1 PNU and topoisomerase II

Topoisomerase II is an enzyme involved in DNA replication and transcription and is often overexpressed in cancer cells. This enzyme causes a double strand-DNA transient break that allows DNA to untwist during the process of replication and transcription. The principal mechanism by which anthracyclines produce their anticancer activity involves topoisomerase II. Anthracyclines cause stabilization of the ternary complex where DNA is cut and covalently linked to tyrosine residues of topoisomerase II. We then tested if PNU can inhibit the activity of the human topoisomerase IIα. In the methods section (section 4.1 page 25) we described a useful in vitro test to examine the ability of drugs to inhibit this enzymatic activity using kinetoplast DNA and topoisomerase II. Kinetoplast DNA is a network of DNA rings that are released in smaller minicircles by topo II. The network cannot migrate in the gel, but the minicircles released can. When the activity of the enzyme is inhibited, the DNA remains in the well of the gel.

The enzyme was titrated by incubating the KDNA with different amounts of topoisomerase II to determine the correct concentration of the topoisomerase IIα necessary for the test. In fact if the activity is too low we cannot see the inhibition because TopoII is not able to decatenate the DNA; however, if the quantity of enzyme is too high, the activity is present even with inhibition because the drugs are insufficient for all the concentration tested. Titration is necessary to determine the activity and the quantity of enzyme necessary to decatenate the entire DNA used. Generally, we employed a slightly higher quantity of enzyme to balance the enzyme's easy loss of activity. In addition, we used doxorubicin as a positive control.

The test was carried out by incubating 200 ng of KDNA (kinetoplast DNA) and 0.025 U of topoisomerase IIα with different quantities of compounds one hour at 37 °C in topoisomerase II reaction buffer. Samples were resolved in agarose gel 0.5% (Fig. 17).

Doxorubicin, the positive control in this experiment, was able to inhibit decatenation of the DNA at 10 μM concentration. The activity of the topoisomerase was inhibited and the concatenated DNA remained in the well of the gel as the control. PNU did not inhibit enzymatic activity at the lower concentrations while at the higher concentration we observed an irrilevant inhibition. The delay of the highest mobility band with 100 μM in the case of relaxed DNA is apparently connected to a lower degree of supercoiling produced by ethidium bromide in the gel. Hence the interaction involving PNU does not appear to be a classical one.

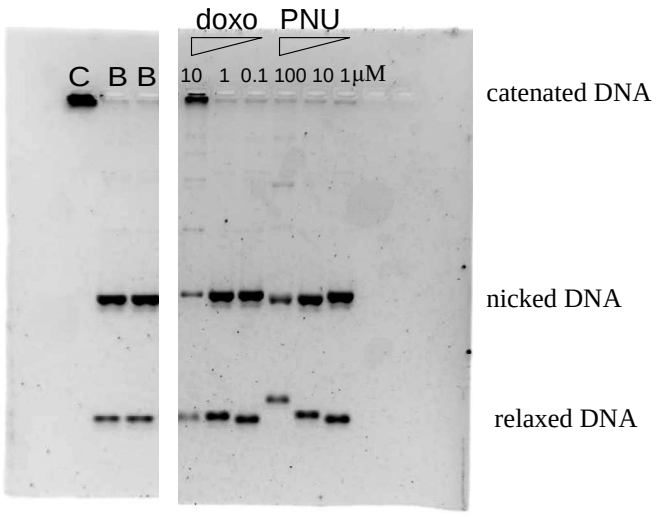

Fig. 17 - Inhibition of topoisomerase II-kDNA decatenation by doxorubicin and PNU. Electrophoretic run was performed in agarose gel 1% with 0.5 μg/ml of ethidium bromide. Electrophoretic buffer was TBE 1X in presence of ethidium bromide 0.5 μg/ml (pre-staining). C = 0.2μg of kDNA; B = 0.2μg of kDNA + 0.025 U of enzyme topoisomerase II; doxo and PNU = 0,2μg of kDNA + 0.025 U of enzyme Topo II + compound at indicated concentration (μM).

Nemorubin (MMDX), the precursor of our metabolite PNU, is a topoisomerase I and II inhibitor when tested in vitro [47], but can overcome atypical (i.e. topoisomerase II-mediated) multidrug resistance [44]. However, PNU does not inhibit the catalytic activity of the enzyme topoisomerase II at the tested concentration. In these experiments of topoisomerase inhibition, we can also see that the anthracycline interacts strongly with relaxed DNA at 100 μM, as indicated by the shift of the relative band. The absence of activity toward this enzyme - so important for activity of the anthracycline - combined with extremely high cytotoxic activity, suggests that the mechanism of action should be sought elsewhere. Previous studies related to the capacity of some highly cytotoxic morpholinyl-anthracyclines (i.e., cyanomorpholinyl-doxorubicin) [40] suggest that DNA cross-link could be the key process related to activity.

5.2 PNU-DNA interactions by melting analysis (FQA)

As previously described (chapter 4.2 page 27), the fluorescence quenching assay (FQA) can be used to determine the melting points of both oligos duplexes and to obtain information regarding the nature of the duplex DNA complexes. Anthracyclines interact with DNA intercalating in the duplex with high affinity. PNU has a lower DNA-binding constant with respect to the DNA than doxorubicin does (Ki_{PNU} =1.1 *10^5 M^{-1} and Ki_{doxo} = 23 *10^5 M^{-1} in ETN, ionic strength 0.5 M).

Before the analysis, the complementary single stranded oligos z1f (FAM-5'-ACT-ATT-CCC-GGG-TAA-TGA-3') and z1r (5'-TCA-TTA-CCC-GGG-AAT-AGT-3'-DAB) were annealed by heating the oligos equimolar solutions in TE 1X (Tris 10 mM, EDTA 1 mM a pH 7.5) for 5 minutes at 95 °C and slowly cooling the mix for 1 hour at room temperature to enable the correct annealing.

Then we incubated the duplex 1 µM final concentration with drugs (doxorubicin or PNU) before the FQA experiment.

The protocol for the assay was: 2 minutes of isotherm at 30 °C, temperature increments to 95 °C in 30 minutes (melting) and finally a step of re-annealing, cooling the mix in 1 hour to 30 °C. Fluorescence was read by the instrument Light Cycler at 530 nm.

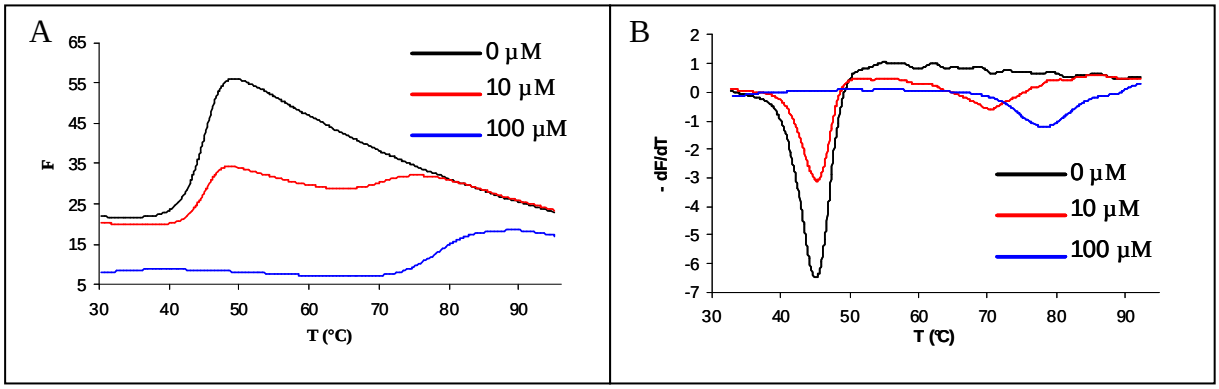

Fig. 18 - Melting profile (A) and relative first derivative of duplex z1f-z1r 1 µM in TE 1X pH 7,5 alone and after incubation for 1 h at 37 °C with different concentration of PNU.

Fig. 18 A represents the thermal denaturation profile of our oligos/PNU mixture. The melting temperature – the temperature at which 50% of the oligos are denatured and corresponds to the flex of the thermal profile - can be easily calculated through the first derivate of the curve (Fig. 18B) and is calculated from the location of the minimum of the curve.

We can easily observe from the melting profile of figure 18A that PNU increased the melting temperature and then stabilized the duplex. The duplex had a melting point of 45.0 °C. When PNU 10 µM was present we observed two melting points, one corresponding to the duplex alone and the second occurring at 70.6 °C. The presence of two melting points is an indication of the presence of two different species in solution. The increment in the melting temperature (ΔTm) was irrelevant for the first melting point (A) but notable for the second (B) (ΔTm = 25.6 °C), an increment consistent with strong stabilization of the duplex. At high PNU concentration (100 µM), only one melting point (ΔTm = 33.1 °C) is found at a higher temperature that indicates further stabilization of the duplex.

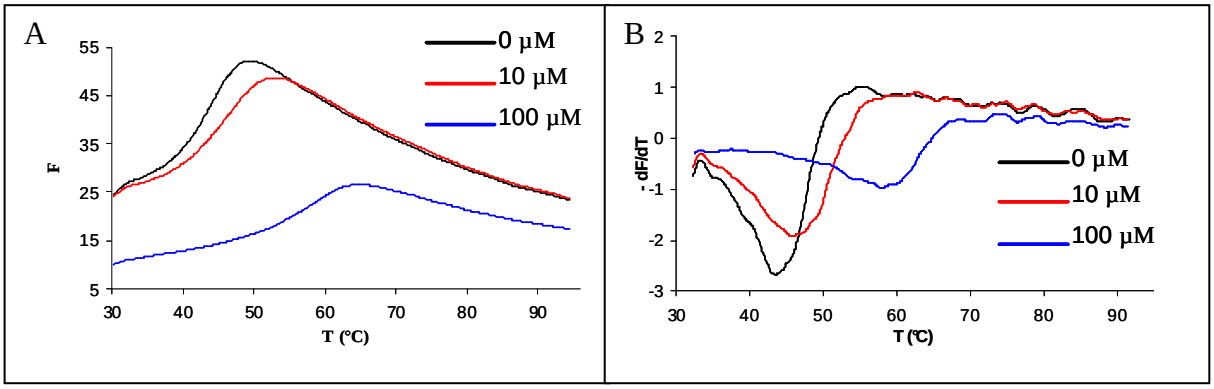

Fig. 19 - Annealing profile (A) and relative first derivative (B) of duplex z1f-z1r 1 µM in TE 1X pH 7.5 alone and after incubation for 1 h at 37 °C with different concentration of PNU.

The annealing profile is the opposite process: the fluorescence readings are recorded upon decreasing the temperature from 95 °C to 30 °C (Fig.19).

The annealing temperature gave us further information, since the duplex annealing temperature is the same (± 2°C correspond at the experimental error). At 10 µM PNU we have only one annealing temperature (46 °C) near the temperature of melting point A (45.4 °C), which suggests that the species corresponding to transition B cannot for form starting from high temperature (Tab. 2). Hence species B is not the result of a reversible binding process.

Mix	**$T_{melting}$ (°C)**	**$T_{annealing}$ (°C)**	**$\Delta T_{melting}$ (°C)**	**$\Delta T_{annealing}$ (°C)**
Duplex	45.0	43.6	0	0
Duplex + PNU 10 µM	45.4 (A) 70.6 (B)	46.0	0.4 (A) 25.6 (B)	2.4
Duplex + PNU 100 µM	78.1	58.2	33.1	14.6

Tab. 2 – Melting and annealing temperature of duplex z1f-z1r 1 µM in TE 1X pH 7.5 alone and after incubation 1 h 37 °C with PNU.

Annealing of the construct with 100 µM PNU gave an annealing temperature significantly lower (58.2 °C, ΔTa = 14.6 °C) than the melting temperature (ΔTm = 33.1) °C. This is consistent with the loss of strong stabilization substituted with weaker stabilization of the duplex.

To rationalize these experimental data, we decided to apply the same experimental protocol comparing the PNU with doxorubicin alone and in the presence of H_2CO. We used the doxorubicin as the control because the interaction with this anthracycline and short oligonucleotides is now well described in literature.

Doxorubicin forms intercalation complexes with duplex DNA, but when we add H_2CO to the system, doxorubicin covalently binds the DNA, forming VXLs. First, we analyzed the duplex (1 µM) incubated with doxorubicin in TE 1 X for 2 hours (Fig. 20, 21).

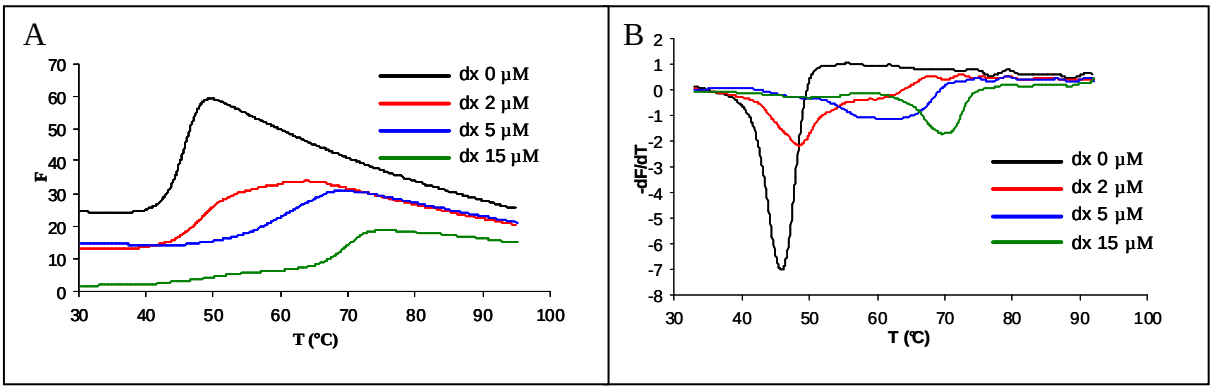

Fig. 20 - Melting profile (A) and relative first derivative (B) of duplex z1f-z1r 1 µM in TE 1X pH 7.5 alone and after 2 h incubation at 37 °C with doxorubicin

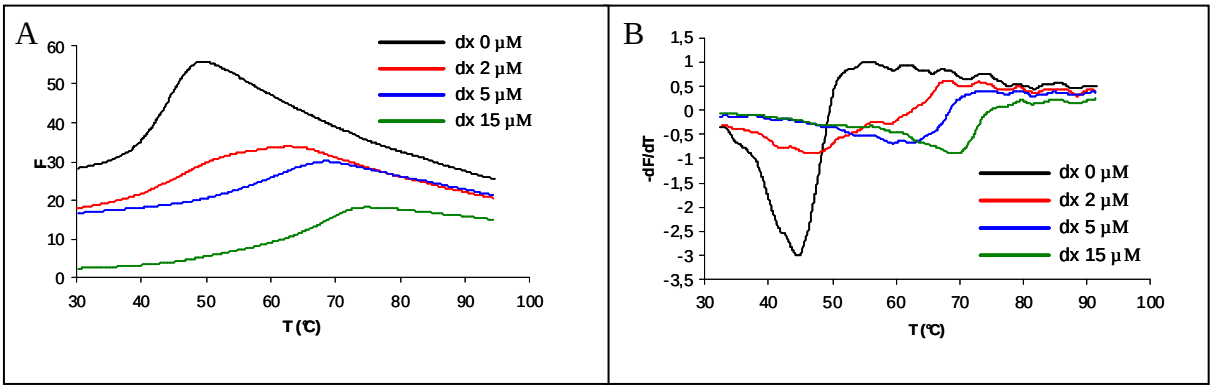

Fig. 21 - Annealing profile (A) and relative first derivative (B) of duplex z1f-z1r 1 µM in TE 1X pH 7.5 alone and after incubation 2 h at 37 °C with doxorubicin.

Mix	**$T_{melting}$**	**$T_{annealing}$**	**$\Delta T_{melting}$ (°C)**	**$\Delta T_{annealing}$ (°C)**
Duplex	45.9	44.3	0	0
Duplex + dx 2 µM	48.5	46.5	2.6	2.2
Duplex + dx 5 µM	62.3	62.1	16.4	17.8
Duplex + dx 15 µM	70.8	69.4	24.9	25.1

Tab. 3 – Melting and annealing temperature of duplex z1f-z1r 1 µM in TE 1X pH 7,5 alone and after incubation 2 h at 37 °C with doxorubicin.

Doxorubicin interacted with the oligos, increasing the melting temperature and stabilizing the duplex. The increments in the melting temperature are reported in (Tab.3). When we add formaldehyde to the drug-DNA complex, the behavior is different (Fig 22, 23).

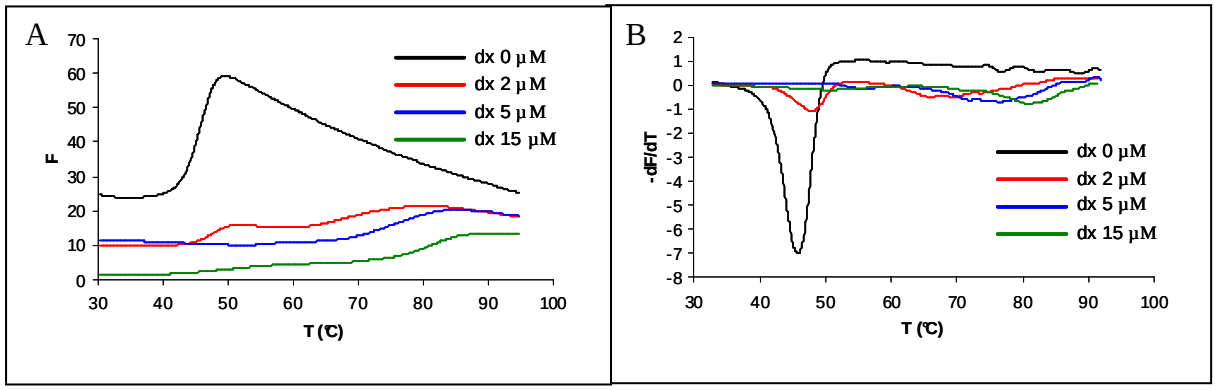

Fig. 22 - Melting profile (A) and relative first derivative (B) of duplex z1f-z1r 1 µM in TE 1X pH 7.5 alone and after incubation 2 h at 37 °C with doxorubicin activated with 2 mM H_2CO.

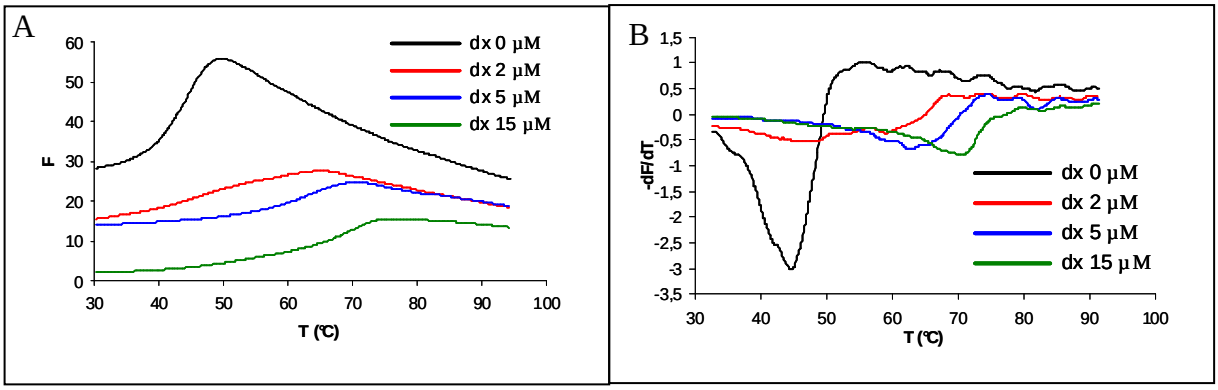

Fig. 23 - Annealing profile (A) and relative first derivative (B) of duplex z1f-z1r 1 µM in TE 1X pH 7.5 alone and after incubation 2 h at 37 °C with doxorubicin activated with H_2CO 2 mM.

Mix	**$T_{melting}$**	**$T_{annealing}$**	**$\Delta T_{melting}$ (°C)**	**$\Delta T_{annealing}$ (°C)**
Duplex	45.9	44.3	0	0
Duplex + dx 2 µM + H_2CO 2 mM	48.0 67.6	45.7	2.1 21.7	1.4
Duplex + dx 5 µM + H_2CO 2 mM	56.0 76.6	63.0	10.1 30.7	18.7
Duplex + dx 15 µM + H_2CO 2 mM	80.8	70.5	10.3	26.2

Tab. 4 – Melting and annealing temperature of duplex z1f-z1r 1 µM in TE 1X pH 7.5 alone and after incubation 2 h at 37 °C with doxorubicin and H_2CO.

Adding H_2CO, the thermal denaturation profile changed, the melting temperature increased with respect to doxorubicin alone, and the difference melting and annealing temperature is more pronounced. Moreover, at the concentration of 2 µM and 5 µM of doxorubicin we had two melting points but one annealing point. Incubating with doxorubicin at 15 µM, we had one melting point at higher temperature (Tab. 4).

We then repeated the experiments with PNU in the same range of concentration (Fig. 24, 25).

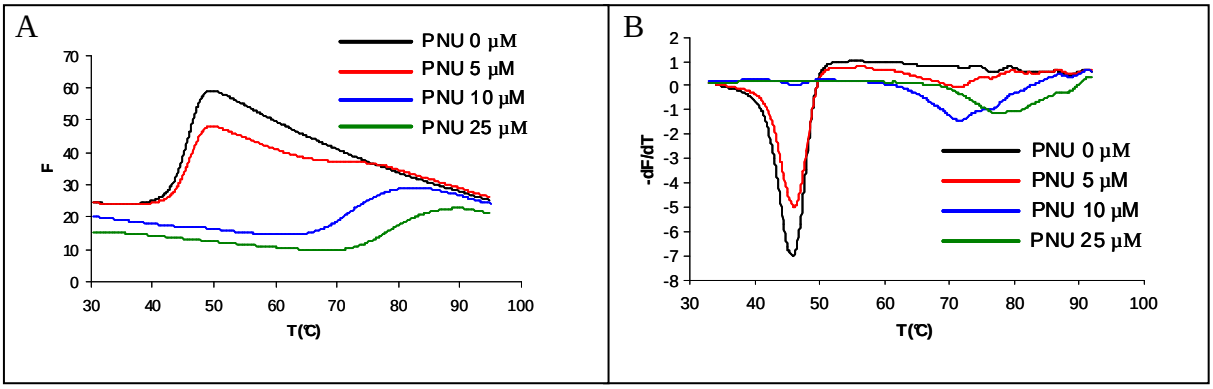

Fig. 24 - Melting profile (A) and relative first derivative (B) of duplex z1f-z1r 1 µM in TE 1X pH 7.5 alone and after incubation 2 h at 37 °C with PNU.

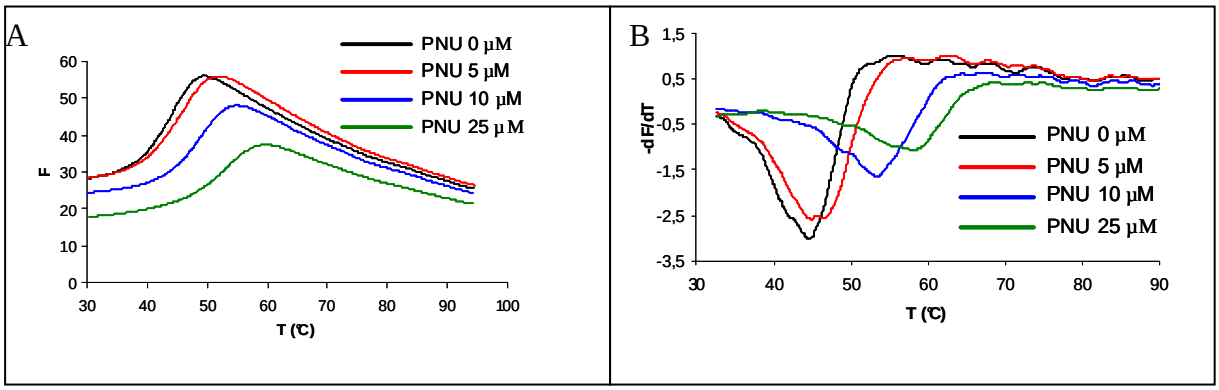

Fig. 25 - Annealing profile (A) and relative first derivative (B) of duplex z1f-z1r 1 µM in TE 1X pH 7.5 alone and after incubation 2 h at 37 °C with PNU.

Mix	**$T_{melting}$**	**$T_{annealing}$**	**$\Delta T_{melting}$ (°C)**	**$\Delta T_{annealing}$ (°C)**
Duplex	45.9	44.3	0	0
Duplex + PNU 5 µM	46.1 71.4	44.8	0.2 25.5	0.5
Duplex + PNU 10 µM	46.7 71.6	48.6	0.8 25.7	4.3
Duplex + PNU 25 µM	77.1	53.7	31.2	9.4

Tab. 5 – Melting and annealing temperature of duplex z1f-z1r 1 µM in TE 1X pH 7.5 alone and after incubation 2 h at 37 °C with PNU.

The behavior of PNU is analogous to the behavior of doxorubicin in the presence of formaldehyde, with strong stabilization of the duplex.

The presence of two melting points and the strong difference between melting and annealing temperature suggest that PNU's reactivity is similar to that of doxorubicin in the presence of formaldehyde (Tab. 5). The PNU-adducts have different behavior with reference to the non-

covalent intercalation-complex between doxorubicin and DNA. The intercalation complex presents a dynamic equilibrium, depending upon the binding constant. The intercalative process is expected not to show significant differences in melting temperature either by starting from the duplex or the single stranded species (see Table 3). When we introduce formaldehyde, instead, the formation of a VXL changes the mechanism of binding and makes Doxorubicin behave similarly to PNU. The difference between melting temperature and melting/annealing ΔT are a direct consequence of the new methylene bridge between the guanine amino group and the doxorubicin amino group. PNU behaves as a formaldehyde-activated anthracycline confirming the original hypothesis of different mechanism of binding between this anthracycline and DNA

5.3 PNU and DNA cross-linking

The basis of the in vitro cross-linking assay is that drug induced stabilization of DNA will prevent complete denaturation of double-stranded DNA (DS) after exposure to denaturing conditions. The gel electrophoresis technique is a widely used technique for manipulation of biomolecules, including DNA, RNA, and proteins. With the increased availability of relatively short oligonucleotides, denaturing polyacrylamide gel electrophoresis (DPAGE) has become a common assay for investigation of DNA and its interactions with a variety of compounds. DPAGE is a useful method for detection of interstrand cross-links. When a double-stranded oligonucleotide is denatured, the single strand moves faster (compared to the original duplex) through the gel matrix. However, in the presence of a cross link, the strands cannot separate. As a result, a cross-linked duplex retains its retarded mobility and forms a discrete bands with lower mobility than the denatured oligos [54].

In the previous section (chapter 5.2 page 42) the thermal denaturation profile of PNU incubated with oligos suggested us that PNU interacts with DNA like the doxorubicin activated by formaldehyde (i.e. forming DNA cross-links).

High toxicity is then consistent with the formation of a cross-link. To evaluate this possibility we tested PNU with the duplex z1f-zag1r, a fluorescein labeled duplex that permits us to visualize the oligos taking advantage of their fluorescence emission.

Duplex z1f-zag1r { z1 forward FAM-5'-ACT-ATT-CCC-GGG-TAA-TGA-3'
zag1 reverse 3'-TGA-TAA-GGG-CCC-ATT-ACT-5'

Operatively, 25 µl of duplex (z1f-zag1r) 1µM (DS) were incubated with different amounts of PNU for 1h, in TE buffer pH 7.5 at 37 °C. After incubation in 12 µl of each sample, we added 8 µl of gel loading buffer (xilene cyanol 0.25%, blu bromophenol 0.25%, Ficoll 400 18%, urea 8M and EDTA 6 mM). Samples were then loaded onto polyacrylamide denaturing gel (6 M urea). Electrophoretic runs were carried out at 3 V/cm for 15 h (overnight) in TBE 0.5 X. Gel was read with Perkin-Elmer Geliance 600 (Fig. 26).

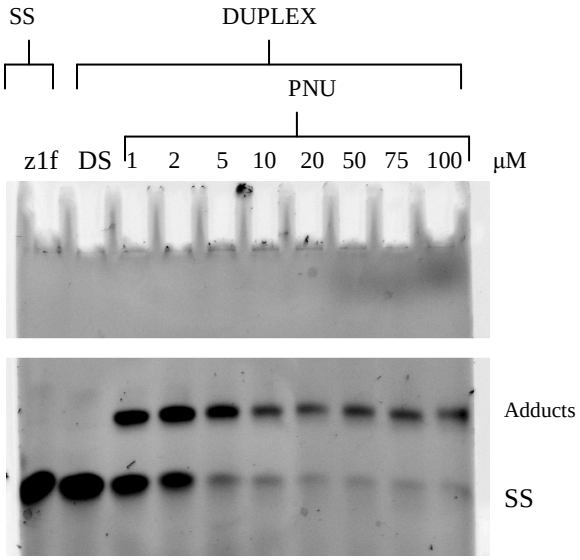

Fig. 26 - Oligonucleotide 1µM DS was incubated with different amounts of PNU for 1h, in TE buffer pH 7.5 at 37 °C. Samples were loaded onto polyacrylamide denaturing gel (6 M urea). Electrophoretic run was conducted at 3 V/cm for 15 h (overnight) in TBE 0.5 X. Z1f is the single strand control, DS a double strand control, and SS corresponds to the mobility of the oligo-FAM not annealed (z1 forward). Gel was read with Perkin-Elmer Geliance 600.

The duplex incubated without drug (DS) has the same electrophoretic mobility as the single strand (z1f); this demonstrates that the duplex is completely denatured and that the denaturing conditions are suitable. PNU stabilized the duplex, forming drug-DNA adducts that can be resolved in DPAGE. This experiment suggests the presence of interstrand cross-link, but we need to consider the limits found by Luce with this analysis technique that gives positive results also for anthracyclines that form the characteristic mono-adducts (VXL) when activated with formaldehyde [54].

We repeated the experiment (Fig. 27) using doxorubicin as a control; doxorubicin intercalates into DNA and stabilizes the duplex form but this stabilization is not sufficient to avoid the denaturation. When we incubate the duplex DNA in the presence of both H_2CO and doxorubicin, we obtain the VXL monoadducts. These complexes are made up of duplexes where only one strand of DNA is bound to the doxorubicin by a methylene bridge. The

stabilization from this VXL is sufficient to delay denaturation of the duplex even if we are not in the presence of a classical cross-link between both strands.

PNU behaves, in this test, as a cross-linker (or virtual cross-linker), which is sufficient to explain the high cytotoxicity of this metabolite (Fig. 26, 27).

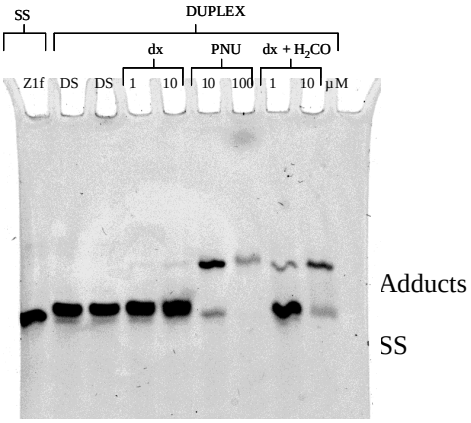

Fig. 27 - Annealed oligonucleotide 1 µM DS was incubated with different amount of PNU, doxorubicin (dx) and doxorubicin in presence of 2 uM of formaldehyde for 2h, in TE buffer pH 7.5 at 37 °C. Samples were loaded onto polyacrylamide denaturing gel (4 M urea). Electrophoretic run was conducted at 6 V/cm for 15 h (overnight) in TBE 0.5 X. Z1f is the single strand control, DS a double strand control, SS corresponds at the mobility of the not annealed oligo-FAM (z1 forward). Gel was read with Perkin-Elmer Geliance 600.

The limit of the present experimental methodology is that we cannot distinguish between classical cross-link involving both strand of the DNA in covalent bonds and the VXL that involves only one strand

5.4 Analyses of PNU-adducts formation

To better investigate the nature of the adducts that form between PNU and DNA and isolate them we used IP RP HPLC (Ion-Pair Reversed-Phase HPLC). (See methods section (chapter 4.4, page 32) for the experimental chromatographic conditions).

If the adducts contain anthracyclines bound to oligonucleotides, the lipophilic anthracyclines will increase the retention time (t_R) of oligo-adducts.

When we analysed ds-oligonucleotides (z1f-zag1r) (1µM in TE 1X) by ion-pair reversed-phase HPLC, we found two signals at the same retention time (t_R) as the authentic single stranded oligonucleotides z1f and zag1r (Fig.28). Our method enables us to denature double stranded DNA (ds-DNA) into the two respective single stranded oligos z1f (t_R: 13.5 min) and zag1r (t_R:12.6 min).

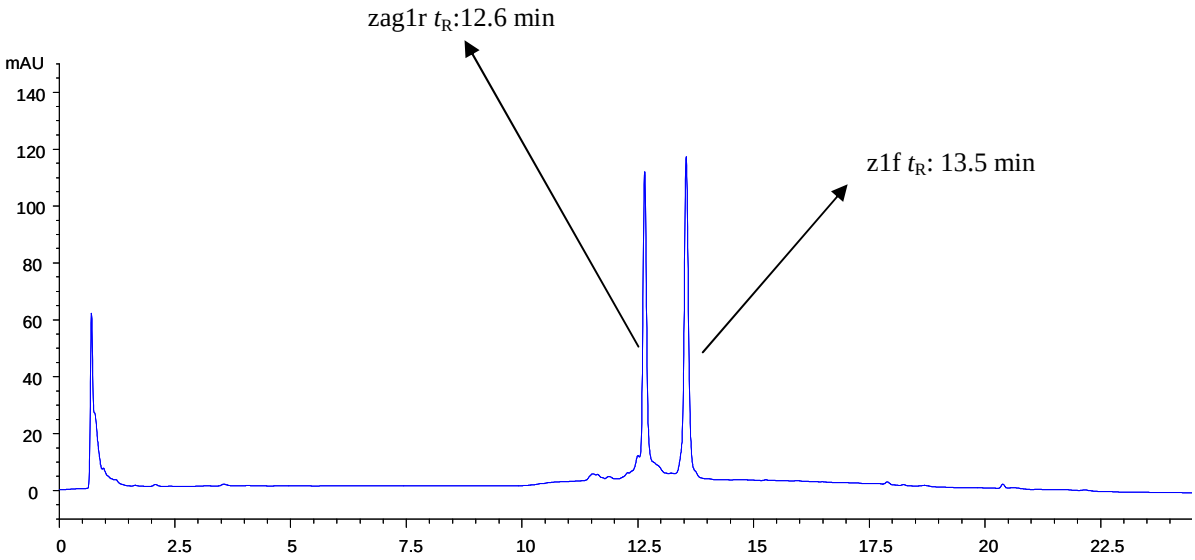

Fig. 28 - Chromatogram of the oligonucleotide ds z1f-zag1r 1 µM (FAM-5'-ACT-ATT-CCC-GGG-TAA-TGA-3' annealed with 5'-TCA-TTA-CCC-GGG-AAT-AGT-3') in TE 1X. Spectrophotometric detector λ=260 nm. Instrument 1, method A.

PNU in this condition has a higher retention time due to its higher hidrophilicity with t_R of 22 min (Fig. 29)

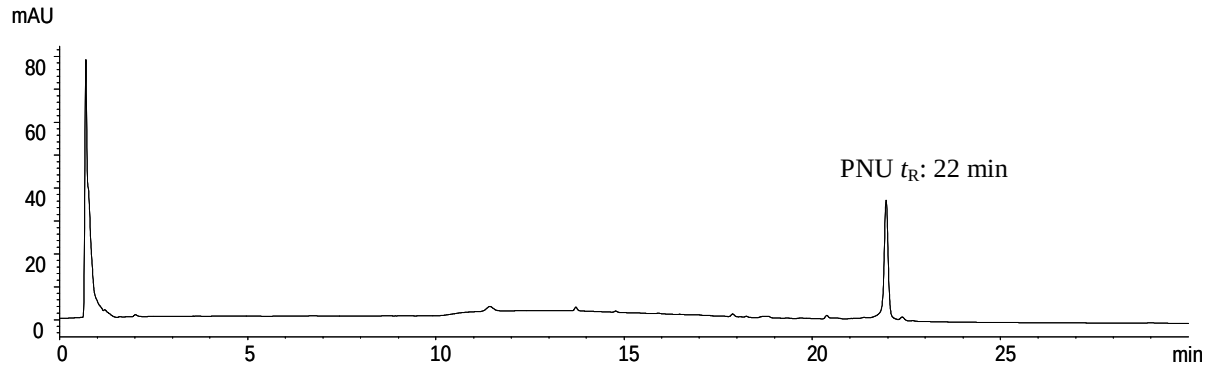

Fig. 29 - Chromatogram of PNU 10 µM in TE 1X. Spectrophotometric detector λ=260 nm. Instrument 1, method A.

We then incubated the annealed z1f-zag1r (1 µM) with the anthracycline PNU (1 µM) 1 hour in TE 1X pH 7.5 at 37 °C. Samples were then analyzed by HPLC with instrument 1 method A.

We observed the signals of the oligonucleotides zag1r (t_R:12.6 min), z1f (t_R: 13.5 min) and the formation of a new peak (adduct A, t_R:13.9 min) that has a different retention time than the two single stranded DNAs or than the anthracycline (Fig. 30).

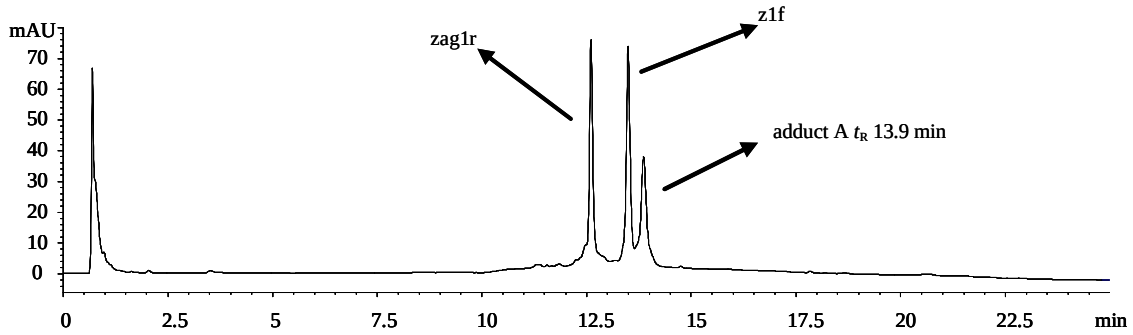

Fig. 30 - Chromatogram of the oligonucleotide ds z1f-zag1r 1 μM (FAM-5'-ACT-ATT-CCC-GGG-TAA-TGA-3' annealed with 5'-TCA-TTA-CCC-GGG-AAT-AGT-3') incubated 1 h at 37 °C in TE 1X with PNU 1 μM. Spectrophotometric detector λ=260 nm. Instrument 1, method A.

Incubating the double stranded z1f-zag1r (1 μM) with highest anthracycline PNU concentration (10 μM) 1 hour in TE 1X pH 7.5 at 37 °C and analyzing the samples with ion-pair reversed-phase HPLC with the anthracycline PNU (10 μM), we observed the formation of another new peak (adduct B, t_R: 14.1 min) in greater quantity than adduct A and having a different retention time than adduct A. (Fig. 31).

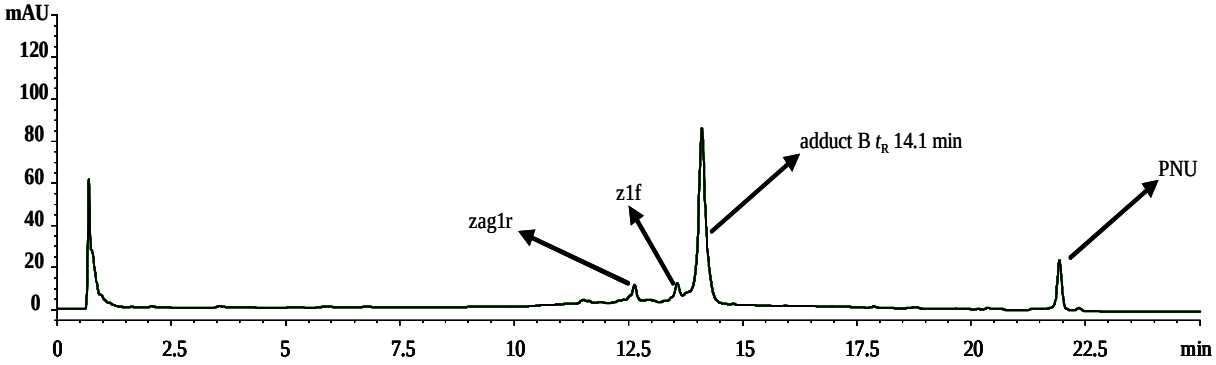

Fig. 31 - Chromatogram of the oligonucleotide ds z1f-zag1r 1 μM (FAM-5'-ACT-ATT-CCC-GGG-TAA-TGA-3' annealed with 5'-TCA-TTA-CCC-GGG-AAT-AGT-3') incubated 1 h at 37 °C in TE 1X with PNU 10 μM. Spectrophotometric detector. λ=260 nm. Instrument 1, method A.

We also tested an intermediate concentration of PNU. Incubating oligos duplex with PNU at duplex/PNU ratio 1:2, we obtain the copresence of both adducts A and B (Fig. 32).

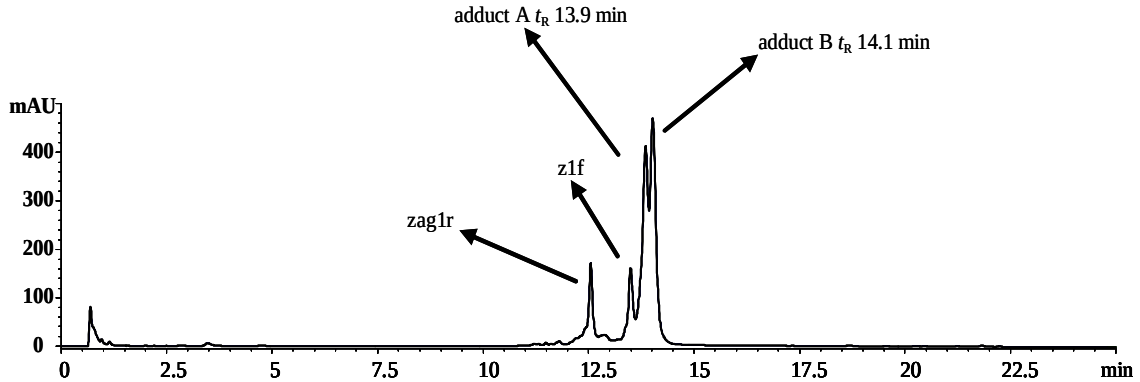

Fig. 32 - Chromatogram of the oligonucleotide ds z1f-zag1r 10 μM (FAM-5'-ACT-ATT-CCC-GGG-TAA-TGA-3' annealed with 5'-TCA-TTA-CCC-GGG-AAT-AGT-3') incubated 1 h at 37 °C in TE 1X with PNU 20 μM. Spectrophotometric detector. λ=260 nm. Instrument 1, method A.

In both cases, the formation of adducts proceeds with a concomitant decrease of oligos z1f, zag1r, and PNU. This finding is consistent with stabilization of ds DNA stably bound to the anthracyclines and is in agreement with gel electrophoresis data. PNU reacts with oligos, forming adducts detected and isolated by HPLC. The formation of the two adducts A and B depends on the ratio PNU/DNA. With a low quantity of PNU (duplex:PNU ratio 1:1), only adduct A is formed; with an excess of PNU, adduct B is formed (duplex:PNU ratio 1:10) and with a PNU: duplex ratio 1:2, both adducts are detected.

To verify the reliability of our method of analysis we tested doxorubicin, the precursor of PNU (MMDX) that has lower cytotoxicity, and the high cytotoxic anthracycline cyanomorpholyno-doxorubicin (cma). The precursor MMDX and the doxorubicin do not react with duplex DNA, but cyanomorpholinyl-doxorubicin, known as an alkylating anthracycline, reacts to form new adducts (fig. 33).

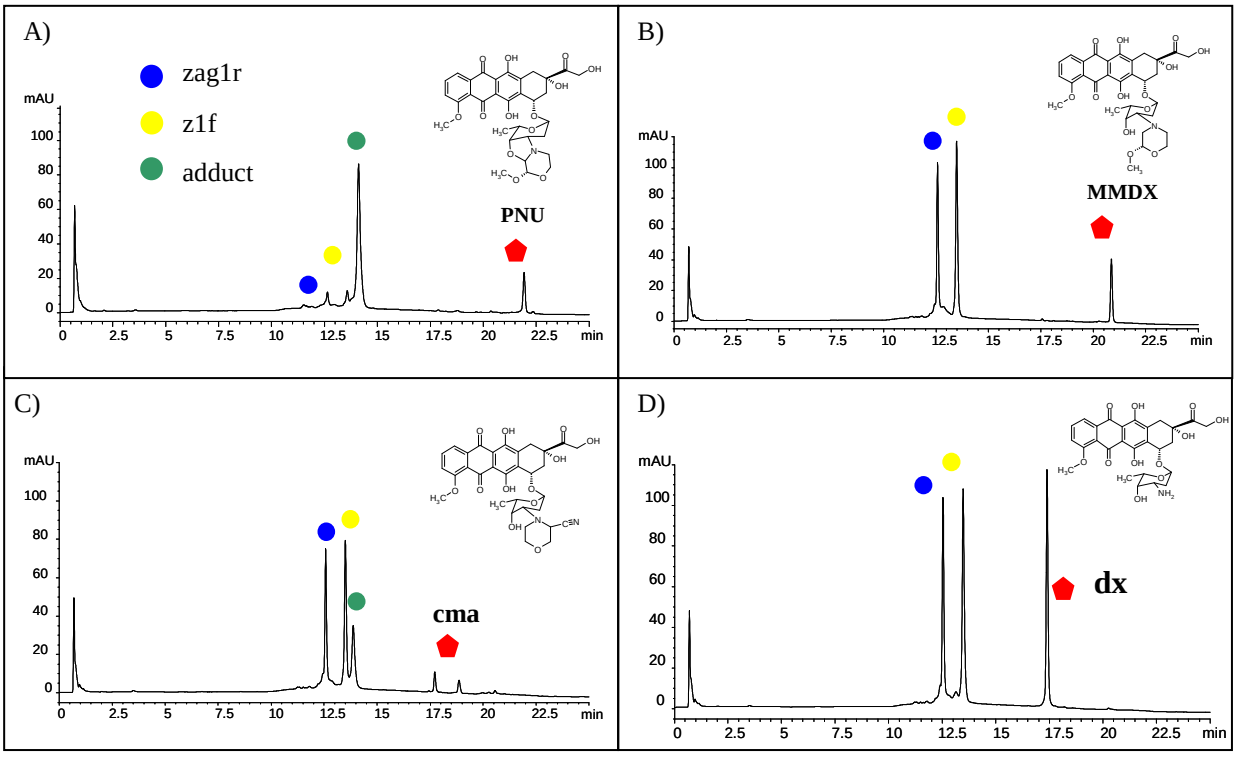

Fig. 33 – Chromatogram of the oligonucleotide ds z1f-zag1r 1 µM (FAM-5'-ACT-ATT-CCC-GGG-TAA-TGA-3' annealed with 5'-TCA-TTA-CCC-GGG-AAT-AGT-3' incubated 1 h at 37 °C in TE 1X with 10 µM anthracyclines: PNU (A), cma (B), MMDX (C) and dx (D). Column temperature 40 °C. Spectrophotometric detector λ=260 nm. Instrument 1, method A.

Despite the fact that doxorubicin intercalates into DNA with greater affinity than PNU (Ki_{PNU} =1.1 *10^5 M^{-1} and Ki_{doxo} = 23 *10^5 M^{-1} in ETN, ionic strength 0.5 M), no adducts were isolated when the duplex was incubated with this anthracycline. The stronger interaction of PNU with DNA due to the cross-linking adducts formation is confirmed. The

cyanomorpholinyl-doxorubicin (cma) is a compound tested that was known to form cross-linking adducts with the DNA, and can be used in this context as a positive control.

We checked if single strand oligos was able to react with PNU; single stranded oligonucleotides zag1r and z1f were incubated separately for 1h in TE 1X at 37 °C with PNU 10 μM.

Single stranded oligonucleotides did not react with PNU and we did not observe the formation of new peaks when this anthracycline was incubated with the single stranded oligos (Fig. 34 and Fig. 35).

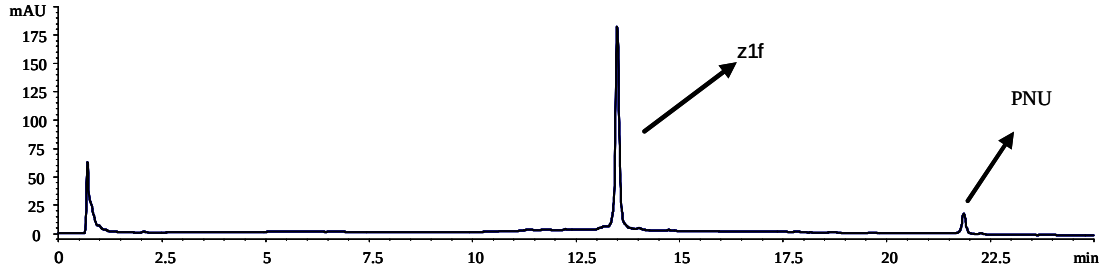

Fig. 34 - Chromatogram of the oligonucleotide ss z1f 1 μM (FAM-5'-ACT-ATT-CCC-GGG-TAA-TGA-3') incubated 1 h at 37 °C in TE 1X with PNU 10 μM. Spectrophotometric detector. λ=260 nm. Instrument 1, method A.

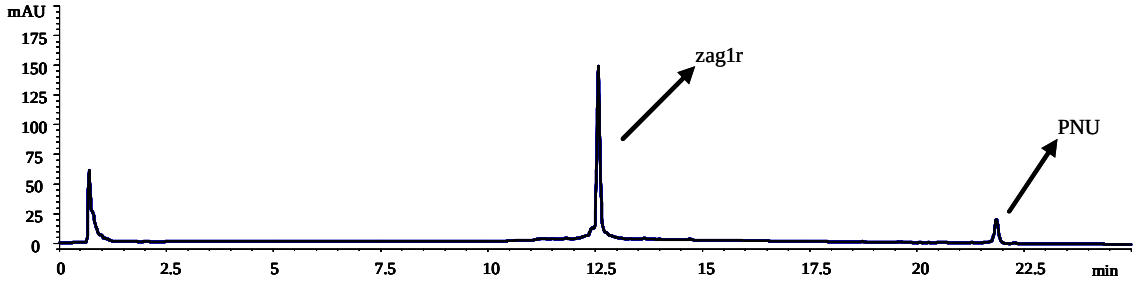

Fig. 35 - Chromatogram of the oligonucleotide ss zag1r 1 μM (5'-TCA-TTA-CCC-GGG-AAT-AGT-3') incubated 1 h at 37 °C in TE 1 X with PNU 10 μM. Spectrophotometric detector. λ=260 nm. Instrument 1, method A.

We can therefore conclude that the double stranded form of DNA is necessary to promote the formation of adducts. This is strongly consistent with a mechanism that considers the intercalation as a first step in the formation of a DNA-anthracycline covalent bond.

5.5 Kinetics of formation of the PNU-adducts

To evaluate the kinetics of the formation of adducts PNU-DNA we incubated ds oligo z1f-zag1r 1 μM in TE 1X in the presence of PNU (1 μM and 10 μM) at 37 °C at different incubation times.

PNU 1 μM and ds z1f-zag1r 1 μM were incubated at T_0 and at 5, 15, 30 min

T_0 was ds oligo z1f-zag1r, analyzed by HPLC immediately after we added the PNU without incubation. Remaining samples were incubated for the time, as indicated in Fig. 36 and analyzed by HPLC.

We observed the formation of adduct A (t_R: 13.9 min) at T_0; adduct A increased with increasing incubation time. The initial quantity of adduct A formed is very low at T_0, but rapidly increases, reaching the greatest amount after 15 minutes of incubation. The progression of the reaction implicated a decrease of initial reagents z1f, zag1r and PNU (Fig. 36).

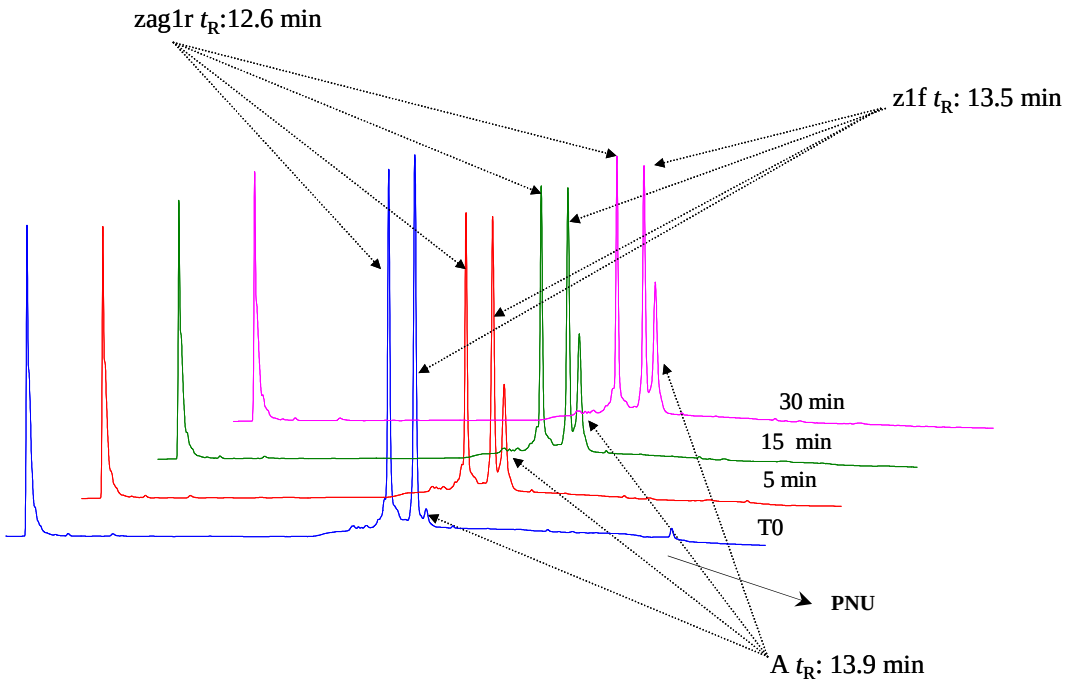

Fig. 36 - Kinetics of the formation of adducts PNU/DNA . Chromatograms of the oligonucleotide ds z1f-zag1r 1 μM (FAM-5'-ACT-ATT-CCC-GGG-TAA-TGA-3' annealed with 5'-TCA-TTA-CCC-GGG-AAT-AGT-3') incubated at 37 °C in TE 1X with PNU 1 μM are reported at different incubation times (0, 5, 15and 30 min). Spectrophotometric detector λ=260 nm. Instrument 1, method A.

When we incubated oligonucleotide double stranded z1f-zag1r (1 μM) with PNU (10 μM) in TE 1X pH 7.5 at 37 °C at different incubation time we had a different behavior. We observed a high amount of adduct (adduct A, t_R: 13.9 min), in the sample not incubated (T_0).

However after 5 minutes of incubation, we observed the copresence of two adducts: adduct A and adduct B (t_R: 14.1 min). After 15 minutes of incubation, adduct A disappeared and the amount of adduct B increased, but when we incubated for 30 minutes we saw only adduct B at maximum concentration (Fig. 37). The progression of the reaction caused a substantial decrease of the quantity of free oligos z1f and zag1r.

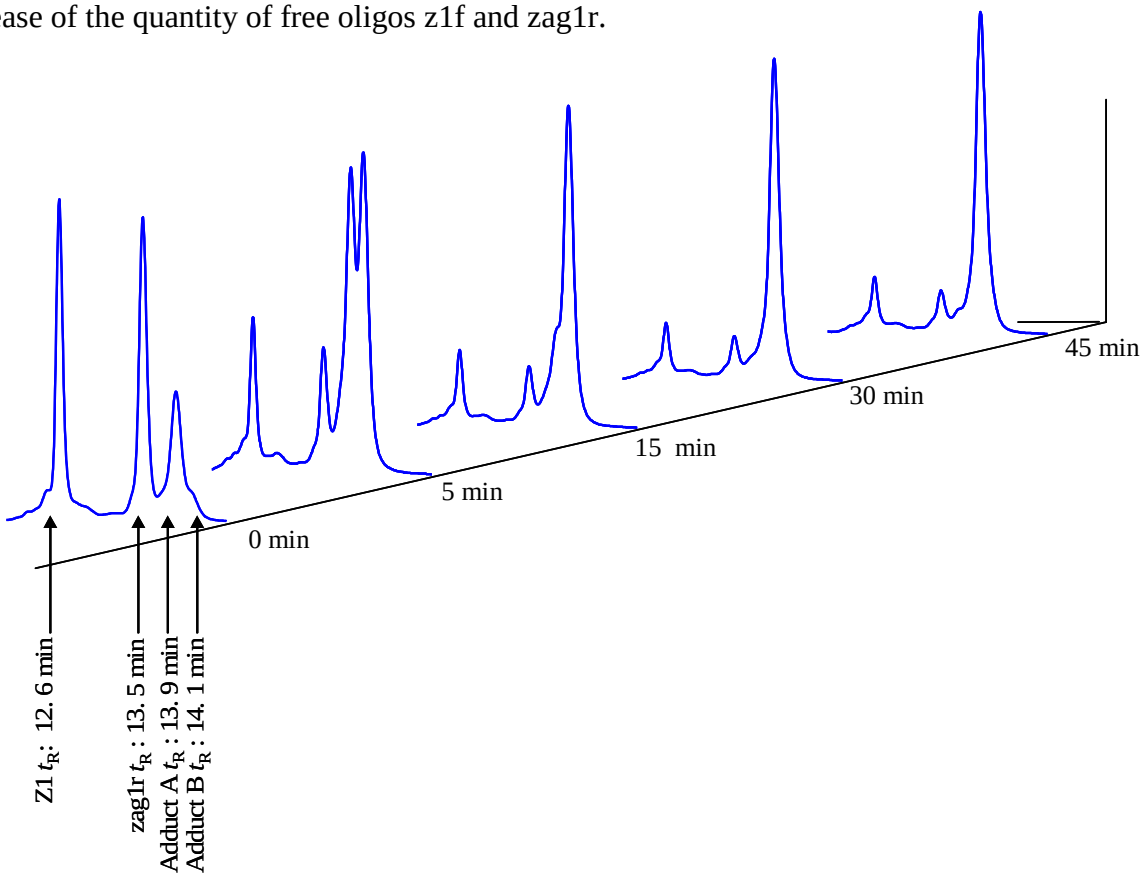

Fig. 37 – Kinetics of the formation of adducts PNU/DNA. Chromatograms of the oligonucleotide ds z1f-zag1r 1 μM (FAM-5'-ACT-ATT-CCC-GGG-TAA-TGA-3' annealed with 5'-TCA-TTA-CCC-GGG-AAT-AGT-3') incubated at 37 °C in TE 1X with PNU 10 μM are reported at different incubation time (0, 5, 15, 30 and 45 min). Spectrophotometric detector λ=260 nm. Instrument 1, method A.

5.6 Stability of the PNU-adducts

We could observe in the previous experiments that formation of the adduct does not involve the complete disappearance of the original oligos, even if we incubated the duplex with an excess of PNU. Moreover, if we perform the chromatographic run at a higher temperature of the column (60 °C), the amount of free oligos and PNU increases (Fig. 38)

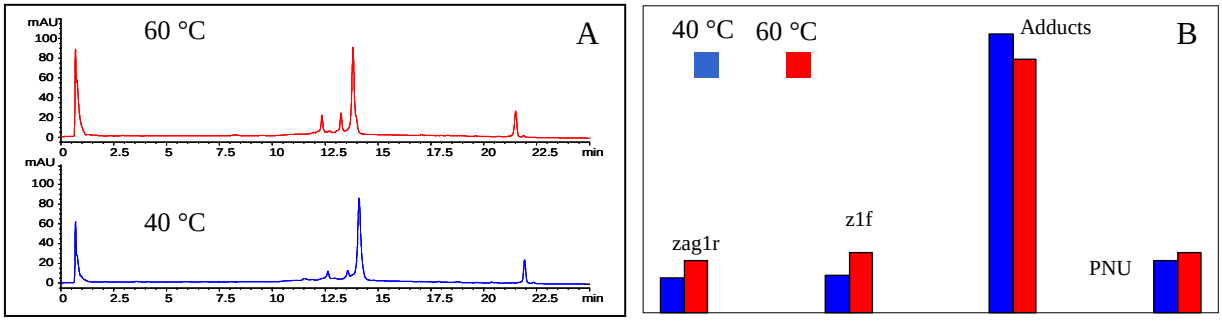

Fig. 38 – A) Chromatogram of the oligonucleotide ds z1f-zag1r 1 µM (FAM-5'-ACT-ATT-CCC-GGG-TAA-TGA-3' annealed with 5'-TCA-TTA-CCC-GGG-AAT-AGT-3') incubated 1 h at 37 °C in TE 1X with PNU 10 µM. Column temperature 40 °C (blue) and 60 °C (red). Spectrophotometric detector. λ=260 nm. Instrument 1, method A. B) Quantifications of the species at the two different temperature of elution.

If we incubate oligo ds z1f-zag1r 10 µM with PNU 20 µM (ds oligo:PNU ratio 1:2) both adduct A (t_R : 13.9) and B (t_R : 14.1) are detected and isolated in these experimental conditions (Fig. 39).

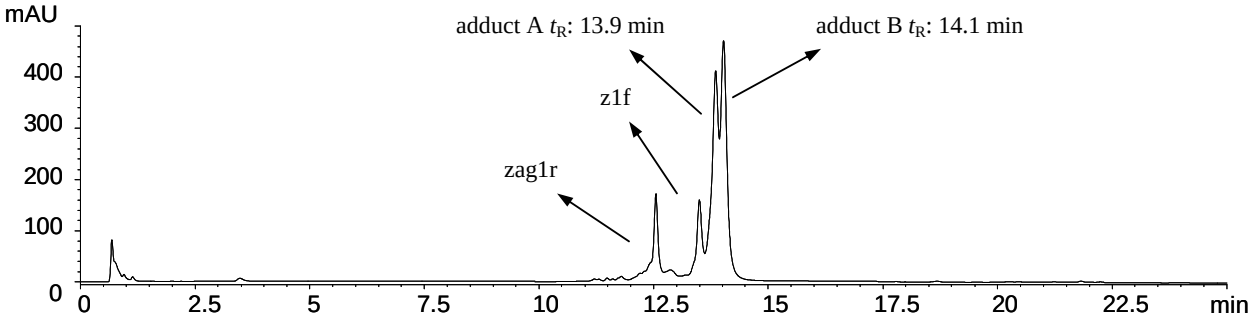

Fig. 39 -Chromatogram of the oligonucleotide ds z1f-zag1r 10 µM (FAM-5'-ACT-ATT-CCC-GGG-TAA-TGA-3' annealed with 5'-TCA-TTA-CCC-GGG-AAT-AGT-3') incubated 1h at 37 °C in TE 1X with PNU 20 µM. Spectrophotometric detector λ=260 nm. Instrument 1, method A.

We then collected the two peaks containing adducts A and B, stored them overnight at 4 °C and reanalyzed the two peaks collected to have information about the stability of these adducts .

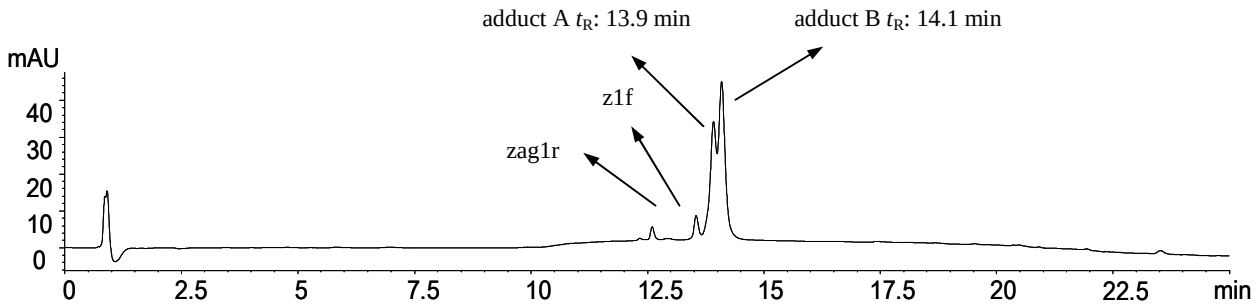

Fig. 40 - Adduct (A+B) analyzed by HPLC after storing overnight at 4°C. Spectrophotometric detector λ=260 nm. Instrument 1, method A.

In these conditions, both adducts were relatively stable, since they are still present, but small quantities of oligos reformed (Fig. 40).

When we heated the same adducts for 5 minutes at 100 °C, they formed greater quantity of the initial oligonucleotides and PNU; interestingly, adduct B disappeared while adduct A did not (Fig. 41).

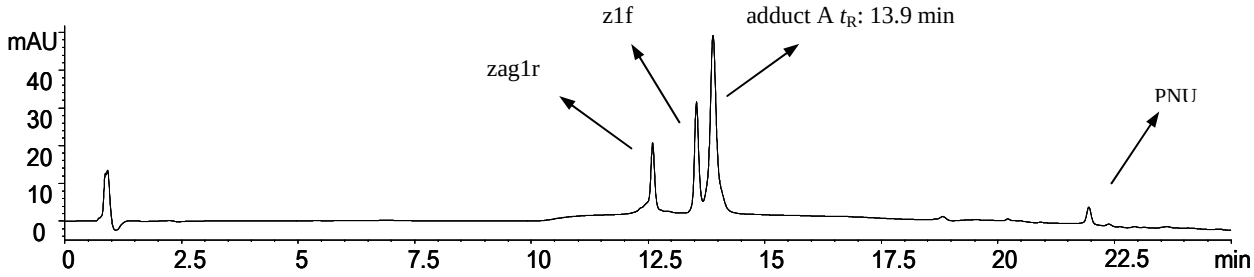

Fig. 41 -Adduct (A+B) analyzed by HPLC after 5 minutes at 100°C. Spectrophotometric detector λ=260 nm. Instrument 1, method A.

Adducts A and B were collected separately from an incubating duplex with quantity of PNU that promotes formation of adduct A or B. We used method C (section 4.4, page 34) to isolate separately the adducts A an B; this method foresees a slow gradient in the range of elution of the adducts that improves the resolution, causing the shift of the chromatographic peaks to higher t_R. Both adduct A and B are relatively stable if stored 20 h at room temperature (~23 °C), even if adduct A begins to release the original oligos when reanalyzed by HPLC (Fig. 42). Part of these adducts were preserved for the following mass spectrometry experiments (chapter 5.7, page 60).

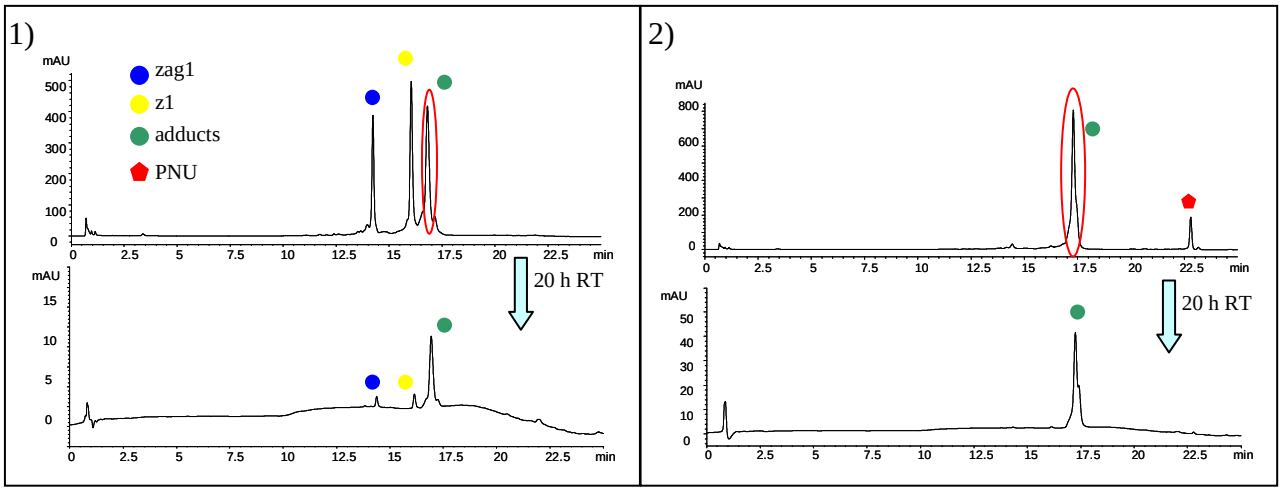

Fig. 42 -1) Adducts A collected, stored 20 h at room temperature (RT) and reanalyzed by HPLC. 2) Adducts B collected, stored 20 h at room temperature (RT) and reanalyzed by HPLC. Spectrophotometric detector λ=260 nm. Instrument 1, method C.

Adduct B exhibits higher stability at room temperature; detectable free oligos are not released.

Ratio oligo:PNU	Adducts formed	Adducts detected		
	Incubation 1h 37 °C	Overnight 4 °C	20 h room temp.	5 min 100 °C
1:1	A	N/A	A*	N/A
1:2	A+B	A + B*	N/A	A*#
1:10	B	N/A	B	N/A

Tab. 6 – Adducts detected after incubation of duplex z1f-zag1r and PNU at different ratio oligos-PNU and adduct detected after storage or thermal treatment. * Free oligos z1f and zag1r released. # PNU released.

In Tab. 6 we resumed the results: adduct A and B are stable at 4 °C and at room temperature, but when we incubated both adducts at high temperatures adduct B decomposes to form the initial reagents oligos z1f, zag1r, PNU and forming adduct A. Moreover, in the presence of adduct A free oligos z1f and zag1r are always released, while adduct B does not release free oligos at room temperature. This suggests that adduct A is less stable. Based on the lower stability of adduct A at room temperature and on the faster kinetics of formation of this adduct, probably part of the adduct A detected after degradation of B at 100 °C forms from the released oligos and PNU.

5.7 Structure of PNU-adducts

To better clarify the nature of the new species observed in DPAGE and isolated by HPLC (High Pressure Liquid Chromatography), we analyzed the complex between PNU and DNA by micro-HPLC-mass spectrometry (μHPLC-MS). Micro-HPLC is an HPLC technique that uses chromatographic column with lower inner diameter (below 2.1 mm) compared to conventional HPLC column (ID 4.6 mm). Miniaturization gives a lot of advantage over the conventional LC in terms of sensitivity and less sample requirement. Furthermore the smaller dimension of the column enables work at a lower flow rate that makes it easier to interface the liquid chromatography to the mass spectrometer.

Generally, HPLC-analysis of oligos was performed with a buffer that permits an ion pairing, but in this case, to improve mass resolution, we used a mobile phase with mass-friendly HFIP/TEA buffer. We cannot use the TEA buffer to perform this analysis because it is not compatible with ESI mass spectrometry. In this instrumental system, we had two detectors: a UV detector followed by mass analyzer (Q-TOF Ultima modality ESI). Mass spectrometry allows determination of the mass of the species resolved by μHPLC (μ-HPLC 1100 Agilent) during the chromatographic run.

With these two coupled detecting systems we obtain two chromatograms (one produced by UV detector and one by mass spectrometer). In this manner we obtain the mass spectrum at every point in the chromatogram acquiring fundamental information on the species detected.

Chromatographic conditions were: column XTerra MS C18 (1.0 x 50 mm, 2.5 μm); mobile phase, HFIP (0.1M)/TEA pH 8.2 (solvent A) and methanol (solvent B), flow rate 40 μL/min Elution program, to 5% from 50% of B in 25 min, column temperature: 40 °C; detection: UV (absorbance at 260 nm) and mass detector.

We first optimized the analysis method using the oligo zag1r-z1f duplex to see if these conditions gave us different results than the previous HPLC experiments. We obtained a chromatogram named TIC (Total Ion Current), elaborated by a mass spectrometer that represents the intensity originated from the entire range of the ions detected (i.e., the current detected) by the instrument. The UV chromatogram, not reported, showed the same peak as the TIC and was used as a control. Even in this chromatographic condition, the duplex was denatured and we obtained two chromatographic peaks corresponding to oligos zag1r (t_R 8.8 min) and z1f (t_R 10.8 min) (Fig. 43). In Fig. 43 the mass spectra obtained at the two different retention time are depicted.

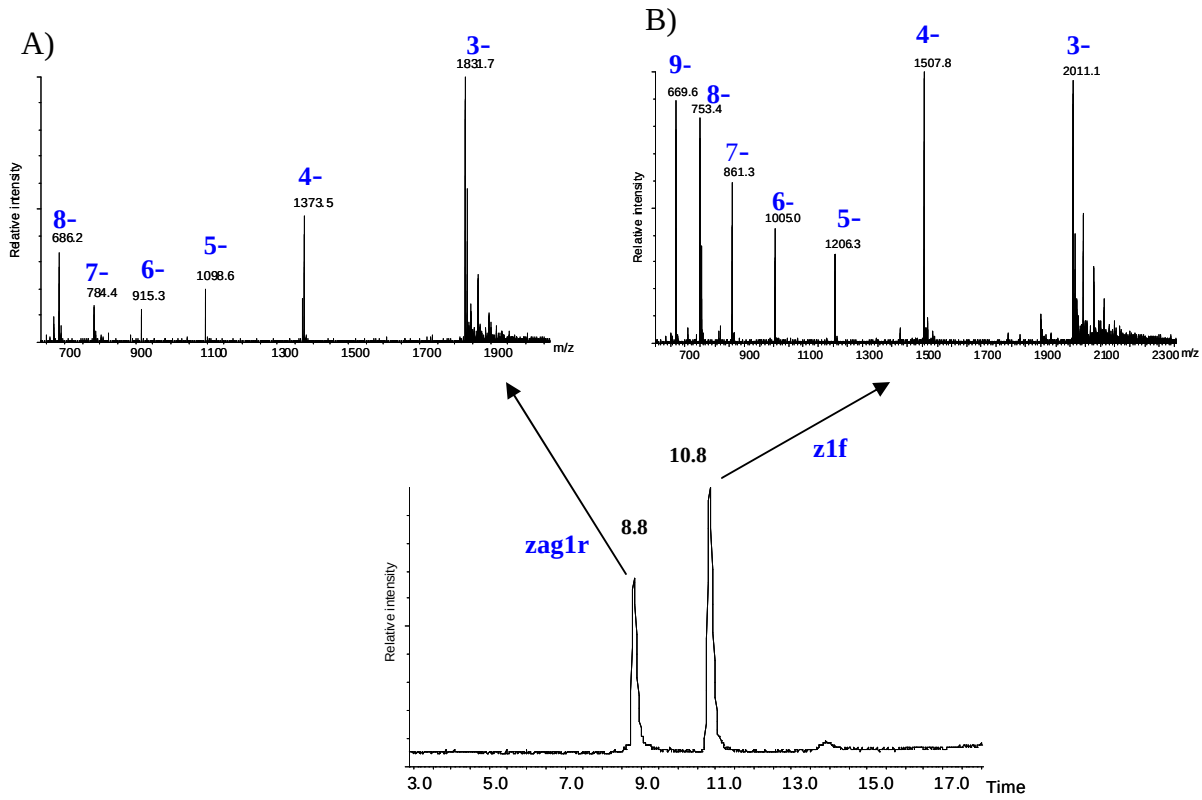

Fig. 43 - Chromatogram of duplex (TIC) z1f-zag1r 1 μM in TE 1X and relative mass spectra acquired online. A) Spectrum obtained on-line of the peak with t_R 8.8 min. B) Spectrum obtained on-line of the peak with t_R 10.8 min. Zag1r: 5'-TCA-TTA-CCC-GGG-AAT-AGT-3'; z1f: FAM-5'-ACT-ATT-CCC-GGG-TAA-TGA-3'.

The ion source used with this mass spectrometer was an Electrospray (ESI), which is relatively soft and gives spectra in which the same compound is detected split up in different ions having same molecular weight but different charge state. This permits the detections of high mass species in a restricted range of masses. Spectrum A (Fig. 43 A), corresponding to the spectrum acquired at 8.8 min of the chromatogram (1st peak), presents a series of ions having different charge state characteristics of the ESI ionization, all of these ions are consistent with the molecular weight of oligo zag1r. We can make the same consideration for spectrum B (z1f), corresponding to the spectrum acquired at 10.8 min (2nd peak) (Fig. 43 B). The theoretical molecular weight and the electrospray series (ion with different charge states) of the two oligos can be calculated with the software Mongo Oligo Mass Calculator v2.06 (http://library.med.utah.edu/masspec/mongo.htm) [58] or with the formula: m/z = (m-z*1.008)/z. Oligos zag1r has the sequence 5'-TCA-TTA-CCC-GGG-AAT-AGT-3' and a mass of 5498.65 Dalton, the oligo z1f has the sequence FAM-5'-ACT-ATT-CCC-GGG-TAA-TGA-3' and mass of 6036.15 Dalton.

In Tab. 7 we report the electrospray series calculated and the signals detected in the MS spectra A and B. Not all of the m/z are detected, in the mass spectra 6 peaks with z from 3 to 8 are present for zag1r and 7 peaks with z from 3 to 9 for z1f.

Z	zag1r m/z calculated*	zag1r m/z measured	z1f m/z calculated*	z1f m/z measured
-1	5497.64		6035.14	
-2	2748.32		3017.07	
-3	1831.88	1831.7	2011.04	2011.1
-4	1373.65	1373.5	1508.03	1507.8
-5	1098.72	1098.6	1206.22	1206.3
-6	915.43	915.3	1005.02	1005.0
-7	784.51	784.4	861.30	861.3
-8	686.32	686.2	753.51	753.4
-9	609.95		669.68	669.6
-10	548.86		602.61	
-11	498.87		547.73	
-12	457.21		502.00	
-13	421.97		463.31	
-14	391.75		430.15	
-15	365.57		401.40	
-16	342.66		376.25	
-17	322.44		354.06	

Tab. 7 – Electrospray series of oligo zag1r and z1f and m/z detected by ESI
* Calculated by Mongo Oligo Mass Calculator v2.06.

First we analyze the adducts A and B isolated in previous HPLC analyses (chapter 5.6, page 58). Our samples were isolated incubating oligo duplex z1f-zag1r in presence of PNU at a duplex-PNU ratio that gives respectively adduct A and B (1:1 and 1:10 respectively). Adducts isolated by IP RP-HPLC were first dialyzed 1 night in purified water and stored at -20 °C. Adducts isolated were then reanalyzed by μHPLC (Fig 44 and 45).

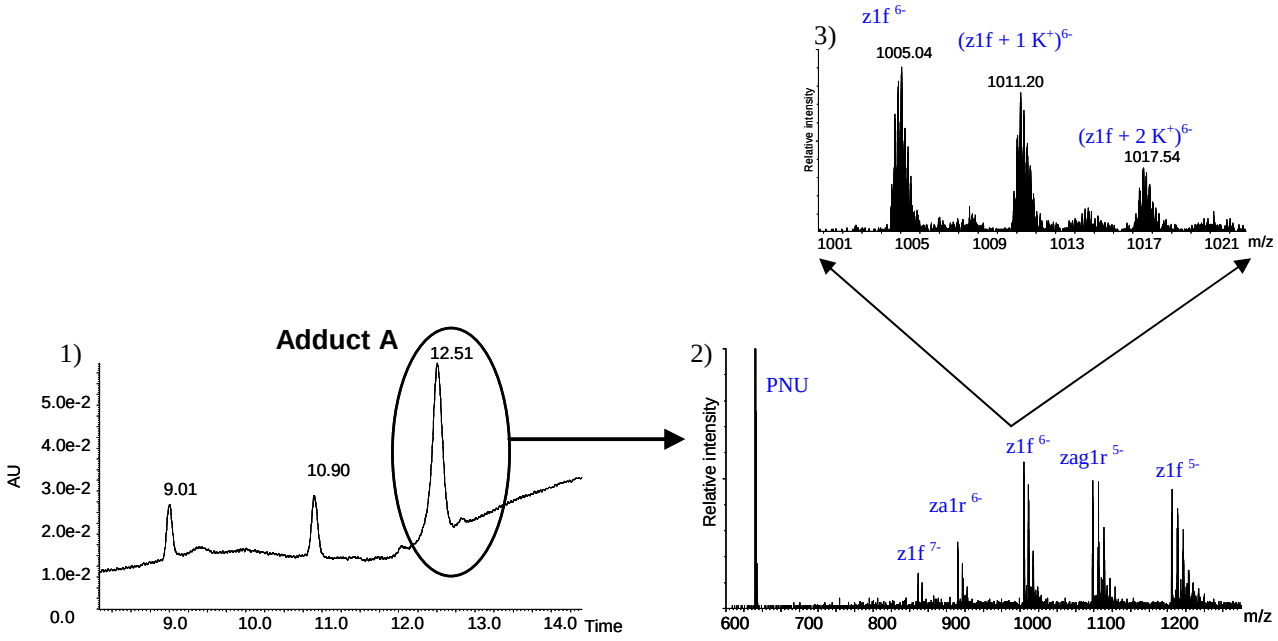

Fig.44 –Adduct A isolated, dialyzed and reanalyzed by μHPLC -MS. 1) Chromatogram (TIC) of adduct A isolated and mass spectra 2) of the correspondent peak acquired online. 3) Zoom around the $z1f^{6-}$ ion.

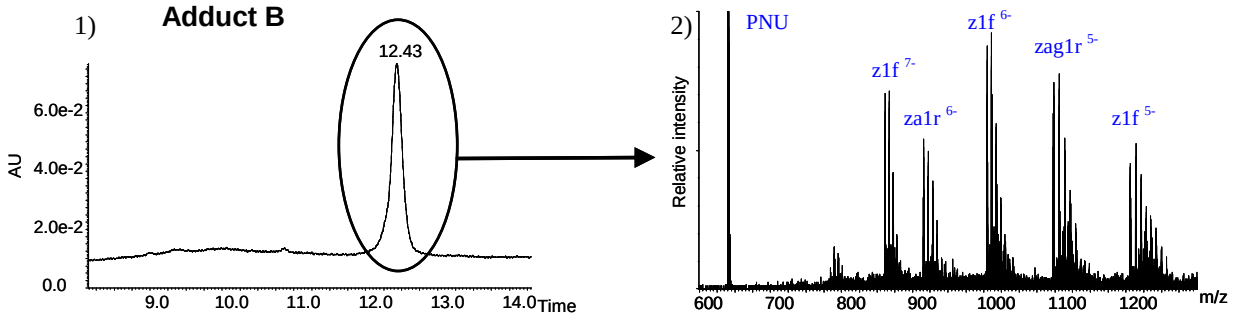

Fig. 45 - Adduct B isolated, dialyzed and reanalyzed by μHPLC -MS. 1) Chromatogram of adduct B and correspondent mass spectra 2) acquired online.

Adduct A exhibits lower stability than adduct B after storage as reported in the preceding section (chapter 5.6, page 57).

The spectrum of the respective adducts A and B revealed their chemical identities: both contain the oligos and PNU to confirm that adducts are composed by duplex and PNU. Despite the high resolution of the μHPLC -MS, our method does not permit us to resolve the two adducts A and B (i.e., they have the same retention time); this probably is due to lower ion-pair ability of the HFIP-TEA buffer compared to the TEAA buffer. Adducts were fragmented completely in this mass spectrometric condition giving single stranded oligos and PNU.

Moreover, probably the chromatographic mobile phase was contaminated with potassium that complicated the interpretation of the data forming many potassium-adducts during the ionization

of the samples (e.g., Fig. 44-3). Aimed to detect the intact complexes we directly analyzed the mixture after incubation without further purification (dialysis) by μHPLC -MS, The duplex 1 μM incubated with PNU 10 μM for 10 min at 37 °C (duplex:PNU ratio 1:10) was analyzed using higher-quality solvent "without potassium" and softer ionization conditions. In this experimental condition, that promotes formation of adduct B, we observed an adduct with t_R of 12.3 min (Fig. 46 A).

The obtained spectrum (Fig. 46 B) showed us that this adduct contained duplex DNA bound to PNU. This fact still evidences the stabilization of the duplex DNA induced by PNU. In detail, we could detect the mass of the species PNU, zag1r, and z1f. We also found the complexes between the single stranded oligos and PNU (z1f + 1PNU, zag1r + 1PNU) and the complexes between the double stranded oligos and PNU (duplex + 2 PNU, and duplex +3 PNU).

PNU, z1f, and zag1r have different μHPLC retention times than DNA-PNU adduct. This indicated that ions detected by TOF analyzer during the elution of the adduct were not present in the chromatographic peak (i.e., in solution), but originated after the fragmentation of the adduct induced by the mass spectrometer. We suppose that the species detected by μHPLC -MS correspond to the duplex with more PNUs bound that is fragmented during the ESI-ionization in the different ions detected. It is reasonable to think that the adduct with more anthracyclines bound would have higher retention time in μHPLC conditions; a possible explanation for the lack of these higher t_R peaks is that when lipophilic drugs are intercalated in the duplex they are "protected" from the interaction with the stationary phase of the column, and that adducts with a different number of drugs bound exhibit the same retention time.

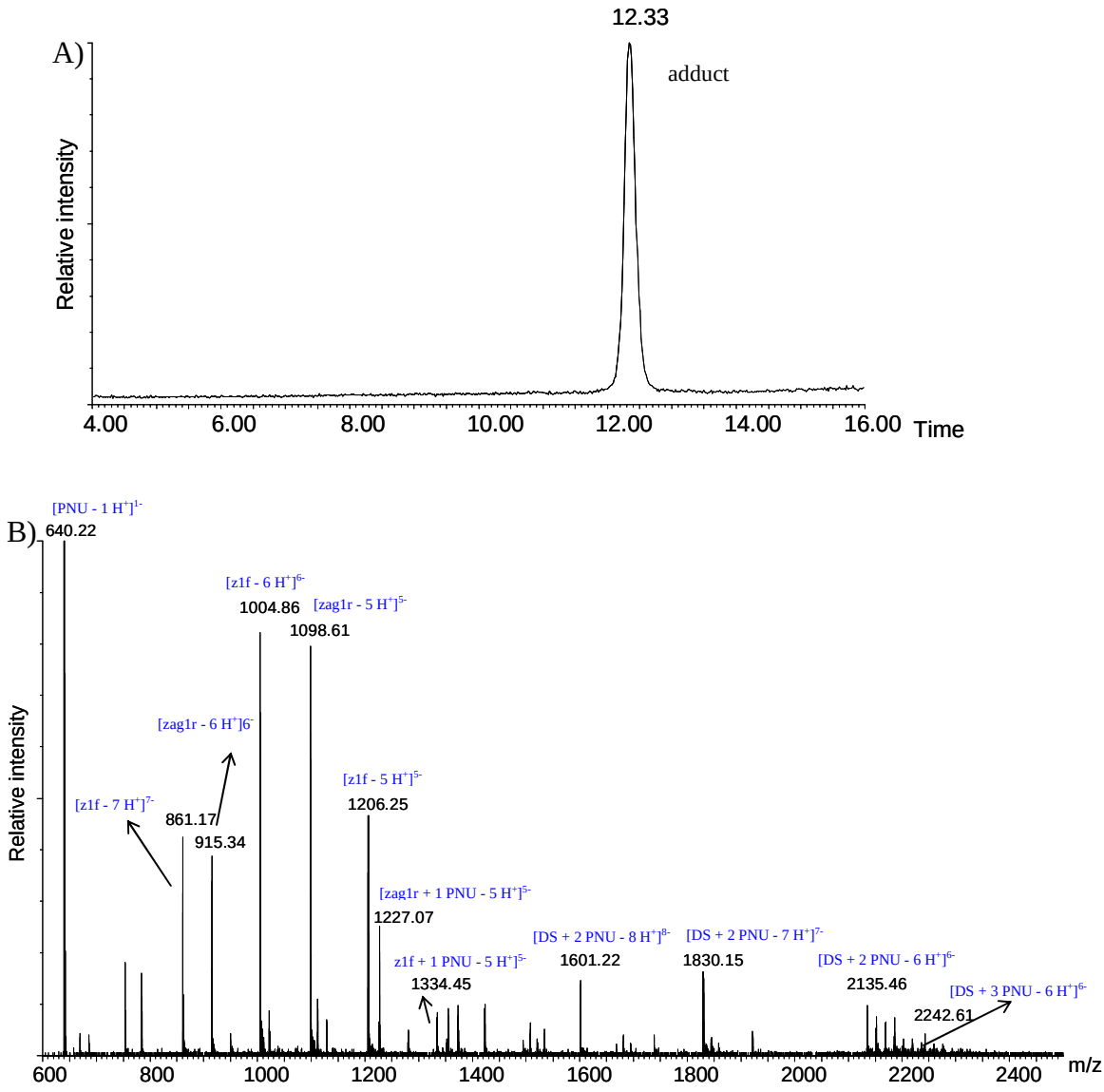

Fig. 46 - A) Chromatogram (TIC) of oligonucleotide z1f-zag1r DS 1 µM incubated 10 min with PNU 10 µM in TE 1X at 37 °C and relative mass spectrum (B).

As we saw before in Fig. 44 and 45, adducts A and B did not have different retention time. Working in conditions that promote the formation of adducts A or B (i.e., ratio PNU-DNA 1:1 or 1:10), they eluted at the same retention time. Further, the fragmentation does not permit us to be certain whether the adducts detected are really the same as those present in solution or whether they are the result of a partial fragmentation (i.e., adducts that lose one or more anthracyclines) (Fig. 46).

To simplify the construct and better rationalize the effects observed, we followed our analysis using self-complementary 5'-CCC-GGG-3', oligo CG, the core of duplex z1f-zag1r to see which adducts it forms.

First, we analyzed by µHPLC -MS the oligo without PNU, maintaining the chromatographic condition previously described and obtaining online chromatographic and mass information.

Chromatographic conditions were: column XTerra MS C18 1.0 x 50 mm, 2.5 µm; mobile phase, HFIP (0.1M)/TEA pH 8.2 (solvent A) and methanol (solvent B), flow rate 40 uL/min, elution program, to 5% from 50% of B in 25 min, column temperature 40 °C; detection UV (absorbance at 260 nm) and mass detector. Only one peak was present in the chromatogram and in the corresponding MS spectrum only ions of the oligo CG in the single stranded form were detected. In agreement to the low melting point of this small oligo, under denaturing chromatographic conditions, no duplex signals were detected (Fig. 47). Tab. 8 reported the ions m/z detected.

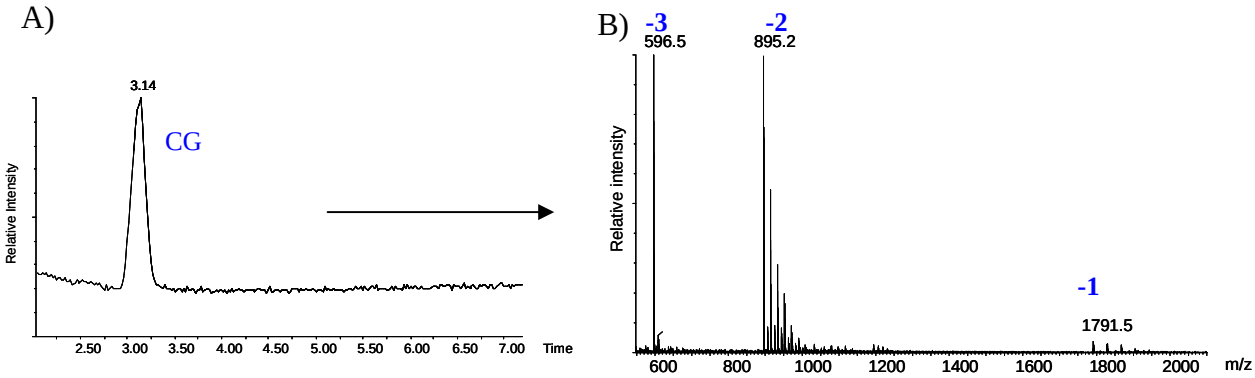

Fig. 47 - A) Chromatogram (TIC) of annealed oligonucleotide CG 2 µM in TE 1X and relative online mass spectrum B).

z	CG oligo m/z calculated*	CG oligo m/z measured
1	1792.21	1791.45
2	895.60	895.2
3	596.73	596.46
4	447.30	
5	457.64	

Tab. 8 –Electrospray series of oligo CG and peak detected by ESI
* Calculated by Mongo Oligo Mass Calculator v2.06

Then we incubated the oligo 2 µM annealed (heating the oligo at 95 °C and slowly cooling to room temperature) with PNU 10 µM in TE 1X overnight at 4 °C. A low temperature is required to be reasonably sure that this short oligo is in duplex form.

Analyzing this construct, we observed the single stranded oligo (t_R 3.0 min) and the formation of two adducts. The major adduct (C1, t_R 7.9 min) analyzed on-line by ESI-MS gave a spectrum containing PNU, SS oligo, SS oligo + 1 PNU, DS +1 PNU (base peak), and DS +2 PNU . The mass spectrum of the second adduct (C2, t_R 9.0 min) contained PNU, SS oligo, SS oligo + 1 PNU, and DS +2 PNU (base peak) (Fig.48).

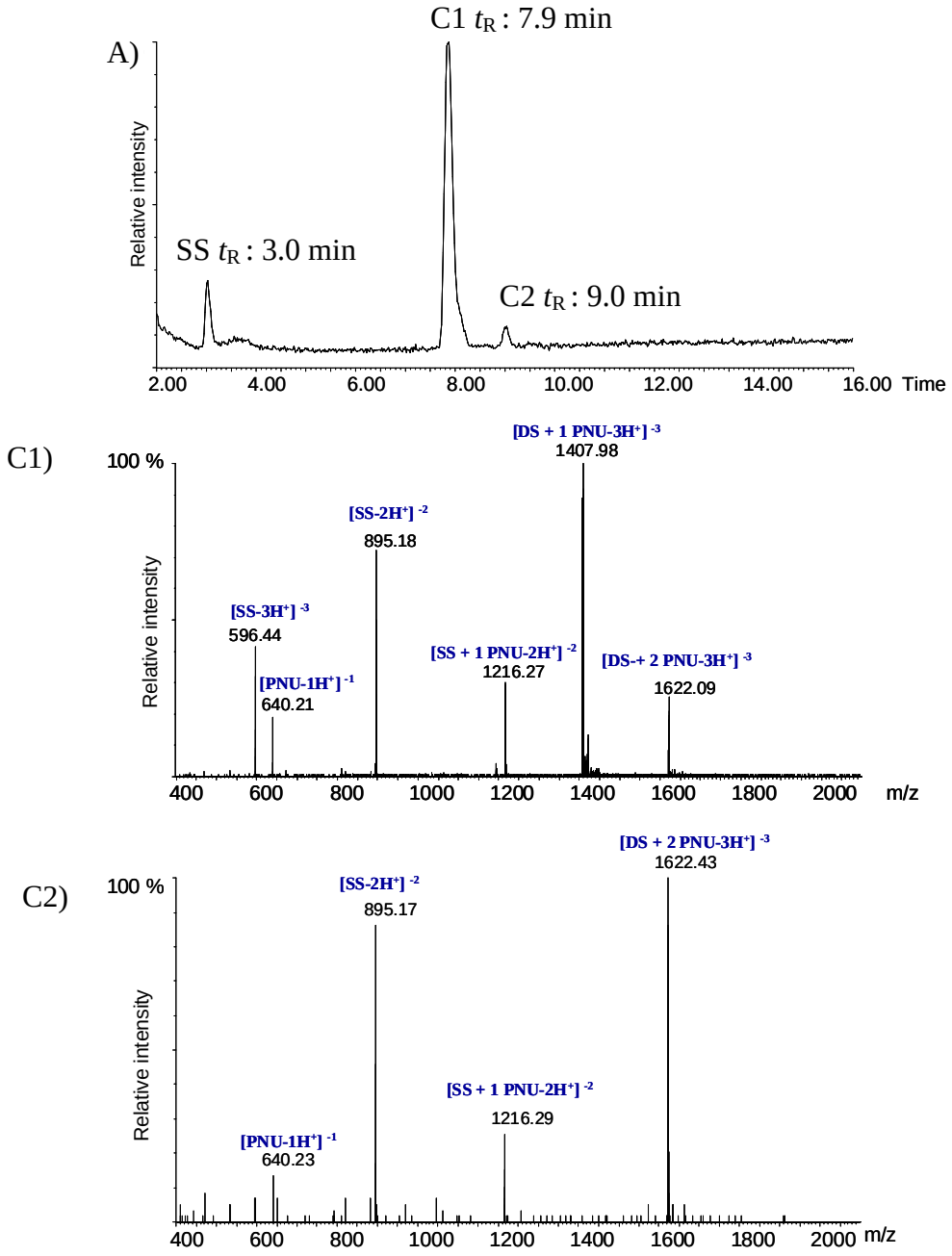

Fig. 48 - A) Chromatogram (TIC) of annealed oligonucleotide CG 2μM incubated with PNU 10 μM overnight at 4 °C in TE 1X and online mass spectra of the adducts C1 and C2.

Duplex CG reacted with PNU forming two isolable different adducts by μHPLC. The hypothesis was that the adduct with major retention time (t_R 9.0 min) contained more PNU bound to the DNA. This hypothesis is supported by evidence that the base peak detected when eluting the second adduct at 9 minutes was a duplex with 2 PNU bound, while when eluting the adduct at 7.9 minutes the base peak was the duplex with 1 PNU bound.

Hence, the shorter CG oligo can bind up to two molecules of PNU, whereas the z1f-zag1r duplex can bind up to 3 molecules of PNU. Evidently, the longer z1f-zag1r provides one more binding site for PNU.

Several adducts containing different numbers of metabolites bound to the duplex z1f-zag1r coeluted, but with oligo GC we detected two different adducts only.

Probably in the shorter oligos the weight of the PNU in the hydrophilic/lipophilic balance is higher, moreover the conformation of the duplex CG could be different and then the bound PNUs exhibits lower protection from the interaction with the column stationary phase. This leads to the possibility of chromatographic separation of the different adducts.

Summarizing adducts A and B isolated by HPLC in the precedent chapters (chapter 5.6, page 58) corresponded to complexes formed between DNA duplex and PNU Optimizing the μHPLC -MS conditions and analyzing the mixture that lead to formation of adduct B we could detect also the complexes between the duplex z1f-zag1r and PNU. These complexes contain up to 3 molecules of PNU bound to DNA, but we cannot exclude that that some drug binding was lost during the ESI ionization. Adducts A and B in HPLC could be constituted by complexes with a different oligo:PNU stoichiometry that are resolved in the efficient elution buffer TEAA/CH_3CN. Unfortunately the μHPLC chromatographic method is not able to separate adducts A and B that had the same t_R in the chromatogram. However, employing shorter oligos (CG sequence) the contribution of the bound species is more relevant and in fact the PNU adducts could be separated chromatographically. These two adducts seem to have different PNU content. However, the complexes detected might also result from partial fragmentation during the ionization, which is supported by the detection of free PNU in the spectra of the adducts.

5.8 Characterization of PNU-adducts

To further characterize adducts between PNU and DNA, we performed MS/MS experiments using the same mass spectrometer. In these experiments, our purpose was to isolate adducts in the first part of the instrument, the quadrupole mass analyzer, and then to fragment them in a collision cell filled with neutral gas (Argon). This permits us to get structural information of the isolated species. Experimental conditions were optimized; we incubated the samples in more mass-friendly ammonium acetate buffer because other buffers (i.e. TE) quench the mass spectrometry resolution. Besides 20 % isopropanol was added before MS/MS experiments to improve sensitivity and stabilize the spray.

Duplex z1f-zag1r 1 μM was incubated for 15 min in ammonium acetate 100 mM in presence of PNU 10 μM at 37 °C and was analyzed with μHPLC -MS to ensure that the different buffer used for incubation did not alter the formation of the adducts .

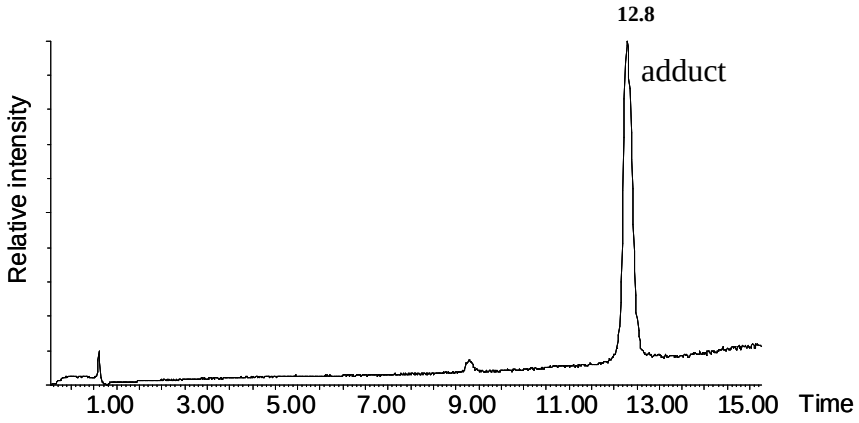

Fig. 49 - Chromatogram (TIC) of oligonucleotide z1f-zag1r DS 1 μM incubated 15 min with PNU 10 μM in ammonium acetate 100 mM at 37 °C.

Incubation in 100 mM ammonium acetate buffer lead to formation of one adduct (Fig. 49) as when we incubated in TE buffer (Fig. 46). Then the same sample was analyzed by direct infusion in the mass spectrometer, adding 20% of isopropanol before the analysis, with the goal to isolate ions corresponding to the complex. Fig. 50 reports the spectrum obtained by infusion.

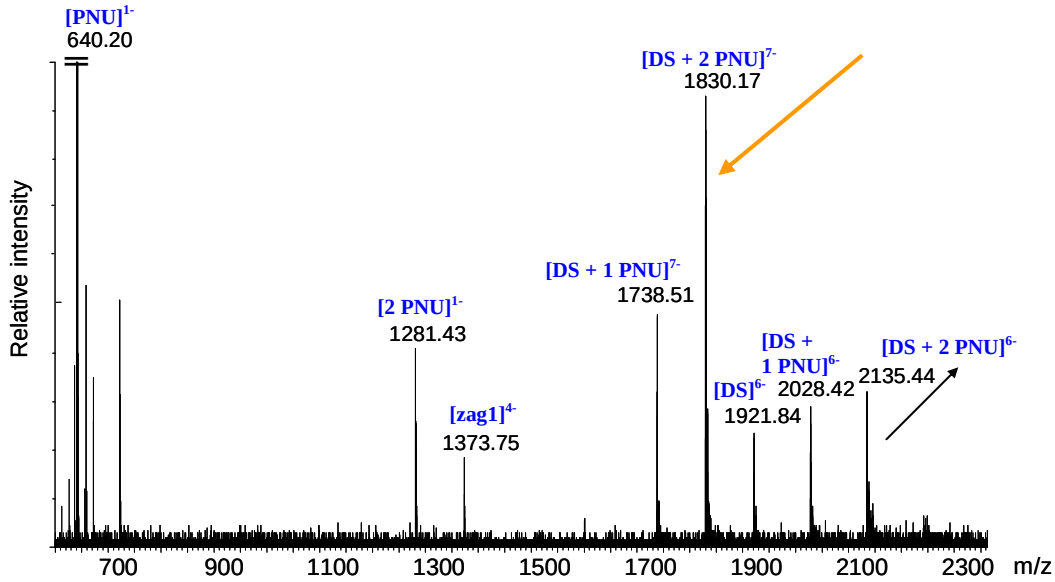

Fig. 50 – Spectrum obtained incubating duplex z1f-zag1r 1 µM with PNU 10 µM 15 min in ammonium acetate 100 mM at 37 °C.

We detected ions corresponding to the duplex linked to 1 PNU or 2 PNUs.

We isolated the ion [duplex + 2 PNU]$^{7-}$ in the quadrupole and we acquired the spectrum in CID (Collision Induced Dissociation) conditions. Following activation, this complex was fragmented and the ions formed detected using TOF mass analyzer.

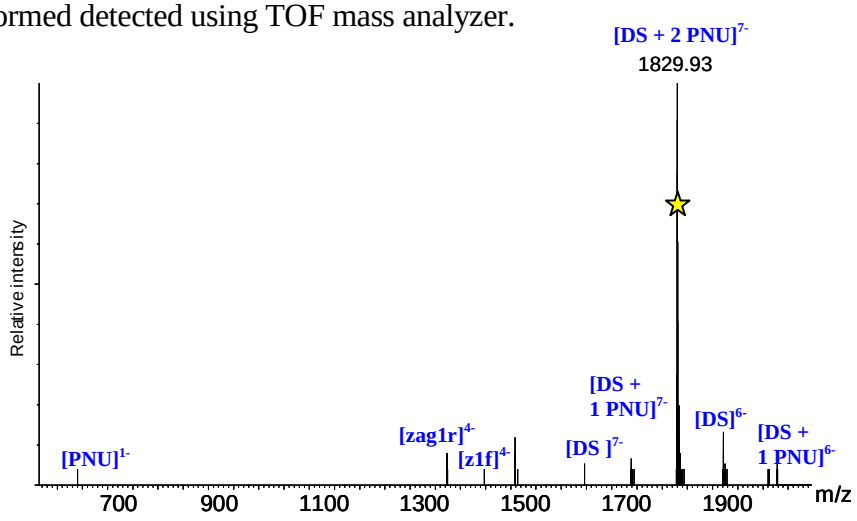

Fig. 51 – MS/MS of adduct [DS + 2 PNU]$^{7-}$ 1829.93 m/z obtained by infusion of annealed oligonucleotides duplex z1f-zag1r 1 µM with PNU 10 µM 15 min in ammonium acetate 100 mM at 37 °C. 20% isopropanol was added before analysis by direct infusion in mass spectrometry.

This ion fragmentation produced loss of the anthracycline and formation of intact oligos single stranded and PNU. In addition it is possible to identify the ions corresponding to the loss of one and two molecules of PNU from the complex [DS + 2 PNU]$^{7-}$ (Fig. 51). Parallel experiments were conducted using the CG oligo.

Duplex CG 2 µM was incubated with PNU 10 µM in ammonium acetate 100 mM overnight at 4 °C. Then we added 20% of isopropanol and performed the analysis by direct infusion in mass spectrometry (Fig. 52).

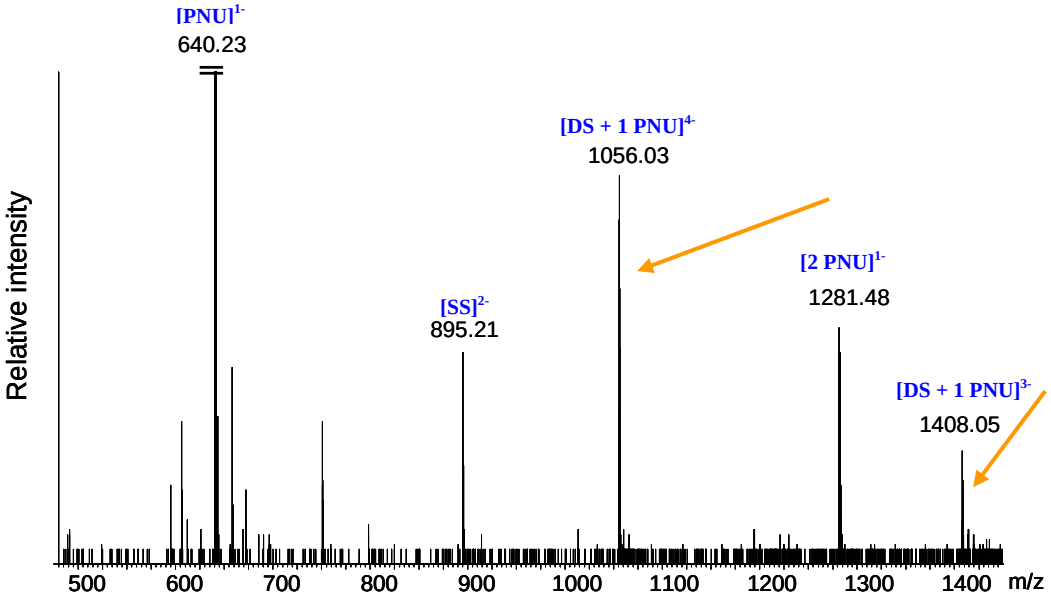

Fig. 52 – Spectrum of annealed oligo CG 2 µM incubated with PNU 10 µM in ammonium acetate 100 mM overnight at 4 °C. 20% isopropanol was added before analysis by direct infusion in mass spectrometry.

In this case we performed CID experiments on the more abundant adducts found in the full scan spectrum.

First we isolated and fragmented the adduct formed by duplex and one PNU, charge state 4- (Fig.53).

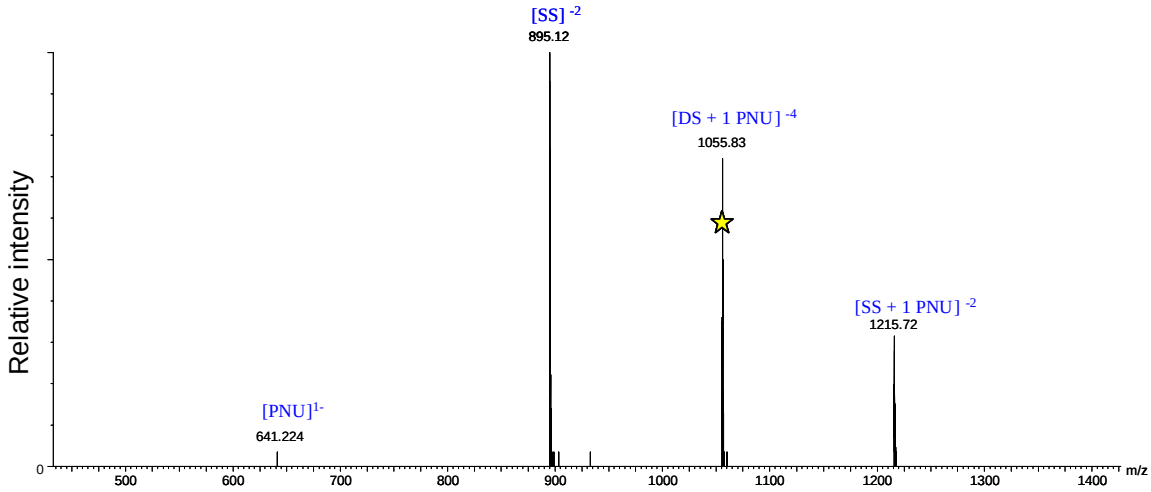

Fig. 53 - MS/MS of adduct [DS + 1 PNU]$^{4-}$ 1055.83 m/z obtained by infusion of annealed oligonucleotide CG 2µM incubated with PNU 10 µM overnight at 4 °C in ammonium acetate 100 mM. 20% isopropanol was added before analyses.

This adduct, corresponding to the duplex bound to one PNU (1055.83 m/z), was fragmented respectively in the single strand and the single strand bound to one PNU. This suggests that PNU strongly binds to the DNA. The signal of the "free" PNU is still present in the spectrum indicating a partial releasing of the drug due to fragmentation condition.

From the same reaction mixture, we selected the ion corresponding to the same species but with lower charge state (m/z = 1407.94 m/z) (Fig. 54).

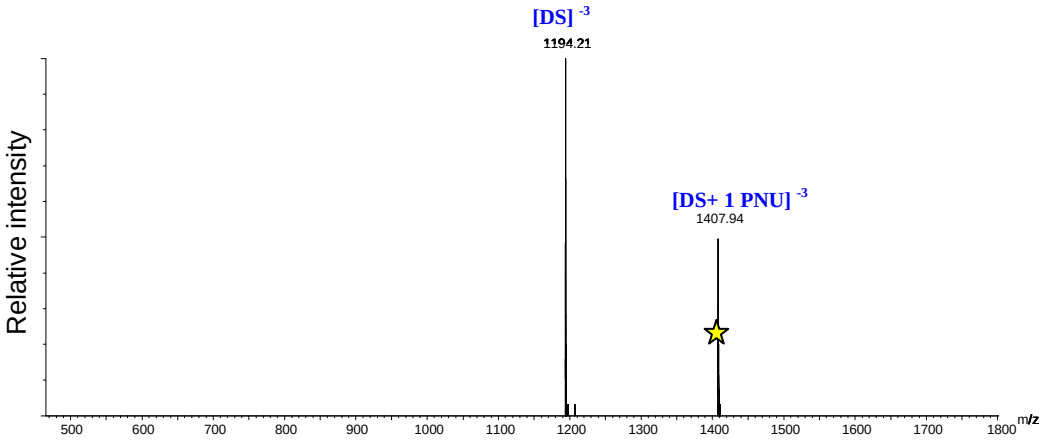

Fig. 54 - MS/MS of adduct [DS + 1 PNU]$^{3-}$ 1407.94 m/z obtained by infusion of annealed oligonucleotide CG 2µM incubated with PNU 10 µM overnight at 4 °C in ammonium acetate 100 mM. 20% isopropanol was added before analyses.

The fragmentation of this adduct formed the original duplex and released PNU as a neutral molecule because we did not detect it and no change in the charge state were highlighted. This fragmentation, instead, suggests a weak binding between PNU and the DNA, in contrast with the previous observation.

We also isolated and fragmented the adduct between PNU and single stranded oligos (Fig. 55).

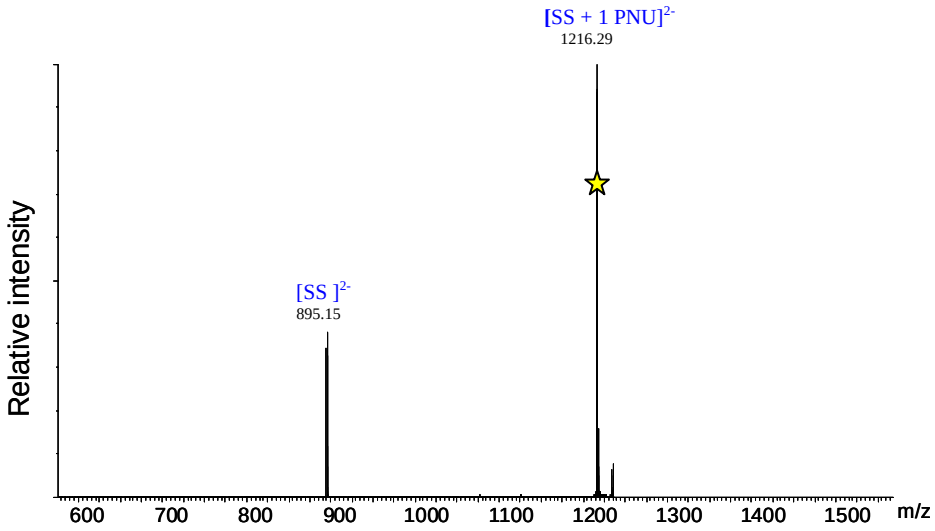

Fig. 55 - MS/MS of adduct [SS + 1 PNU]$^{2-}$ 1216.29 m/z obtained by infusion of annealed oligonucleotide CG 2μM incubated with PNU 10 μM overnight at 4 °C in ammonium acetate 100 mM. 20% isopropanol was added before analyses.

Even this adduct during the fragmentation lost the PNU as a neutral molecule forming single stranded DNA.

Summarizing, the complex between the duplex z1f-zag1r and PNU was dissociated by losing PNU and the same behavior was observed for the adduct formed between duplex CG and PNU (charge state 3-). The same fragmentation pathway was detected for the adduct between single stranded CG and PNU suggesting a non-covalent interaction. On the other side the adduct between the duplex CG and PNU charge state 4- dissociated into two single stranded oligos, one of which carries the PNU, suggesting a covalent monoadduct with one strand of the duplex. In these experiments the behavior of the PNU is ambiguous, sometime it seems covalently bound to one strand of the duplex, sometime not. We observed a similar ambiguous behavior in μHPLC - MS experiments in which the partially fragmented complexes (i.e. the single stranded carrying the PNU) and intact single stranded oligos and PNU were often detected (Fig. 46 and 48). This can be easily explained if we suppose that PNU forms VXL as the doxorubicin in the presence of formaldehyde. This is consistent with a covalent bond at one strand of the DNA in the VXL, accompanied by a weak bond that breaks easily. Finally, in these experiments it was not possible to obtain evidence for the characteristic fragments corresponding to covalent bonds (i.e., PNU bound to DNA-bases) consistent with the presence of a labile cross-link.

6. ANTHRACYCLINES-ADDUCTS AND VIRTUAL CROSS-LINK, DISCUSSION AND RESULTS

6.1 SAR in virtual cross-link

Our experiments revealed that PNU binds strongly DNA preventing its denaturation and forming detectable and isolable adducts with the double helix. These adducts behaved ambiguously, sometimes as covalent cross-links and sometimes as non-covalent complexes. Formation of these characteristic adducts are not a peculiar feature of PNU. The anthracycline doxorubicin has a different reactivity with the DNA, forming intercalative complexes. However, complexes change if formaldehyde is present in the buffer used in experiments (chapter 5.2, 5.3). Formaldehyde promotes formation of DNA-anthracycline adducts that behave similarly to the adducts formed by PNU. Based on this evidence, we decided to clarify and rationalize the nature of these anthracycline-specific interactions. Our goal was to analyse the SAR (structure activity relationship) using different anthracyclines described in table 2 (aims section, chapter 2.2, page 18), in order to reveal which part of the molecules is involved in the link to DNA and to corroborate the results obtained with PNU. Moreover, we aspired to have more structural information about the formation of the VXL. The anthracyclines used can be separated into three groups. The first group includes besides doxorubicin, other anthracyclines in clinical use. These anthracyclines are now well-know for their ability to react with DNA in the presence of formaldehyde [33], and we expected that they would cross-link the short oligos that we used in the experiments. We used these anthracyclines as the positive controls (Fig. 56).

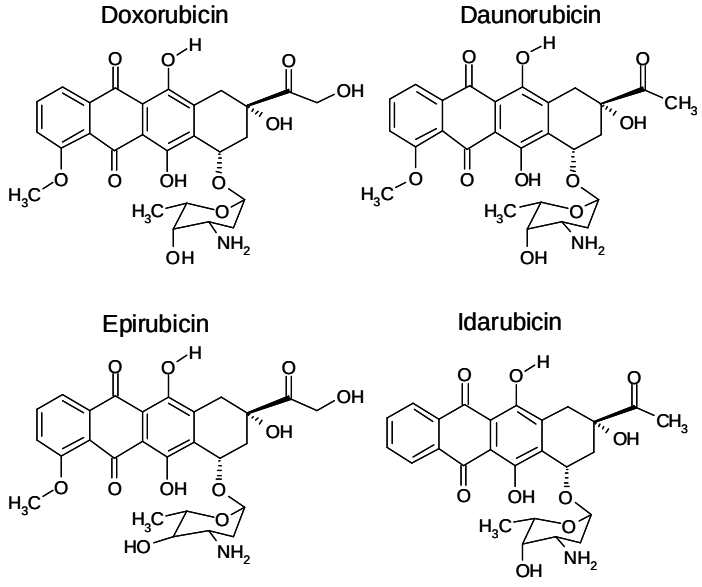

Fig. 56 – Structure of the anthracyclines in clinical use

We tested the ability of the anthracyclines to form cross-links by gel electrophoresis, see chapter 4.3 of the methods section (page 30). All anthracyclines were incubated for 3 hours at 37 °C with oligonucleotides double strand z1f-zag1r in TE 1X pH 7.5 in presence and absence of formaldehyde. Then the samples were loaded into a denaturing DPAGE 6 M urea in the following sequence: we loaded in DPAGE oligo z1f single stranded (C), oligo duplex z1f-zag1r (B), oligo duplex z1f-zag1r incubated with 2 mM of formaldehyde (Bf), oligo duplex z1f-zag1r incubated with anthracyclines daunomycin (dn), doxorubicin (dx) idarubicin (ida) and epirubicin (epi) and then oligo z1f-zag1r incubated with the anthracyclines in the same order in the presence of 2 mM formaldehyde (Dnf, dxf , idaf and epif). For all the anthracyclines we tested 3 concentrations: 1 μM, 10 μM, and 100 μM. As expected, daunorubicin (dn), doxorubicin (dx), idarubicin (ida), and epirubicin did not react with oligos, i.e. they did not prevent the denaturation of the double stranded form of the DNA. However, in presence of formaldehyde, the same anthracyclines daunorubicin (dnf), doxorubicin (dxf), idarubicin (idaf), and epirubicin (epif) promoted a dose-dependent formation of a new electrophoretic band with lower mobility, consistent with the formation of adducts (Fig. 57), while the intensity of the band related at the denatured duplex (SS) decreased. These bands correspond to the monoadducts described as the VXL. In all experiments, we loaded the duplex z1f-zag1r incubated with doxorubicin 10 μM and formaldehyde 2 mM as a positive control.

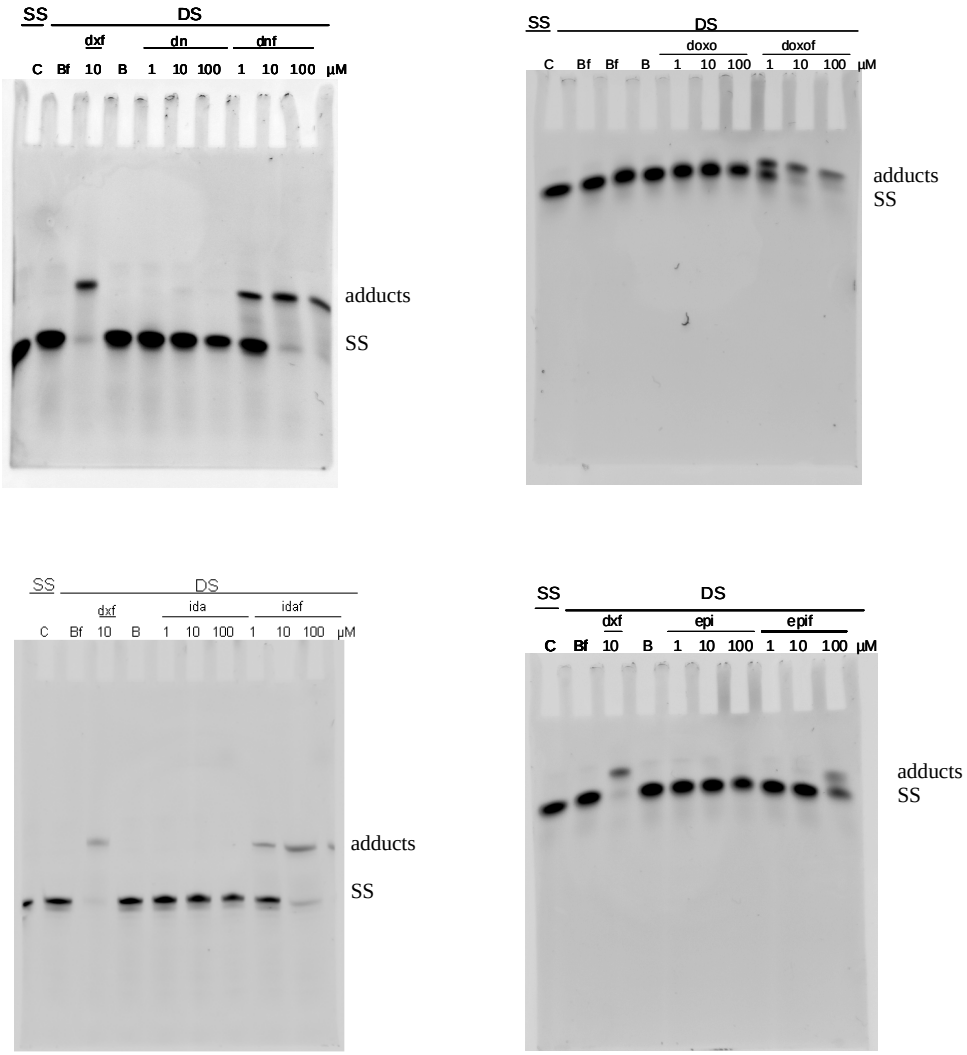

Fig. 57 - Oligonucleotide 1µM z1-zag1r (FAM-5'-ACT-ATT-CCC-GGG-TAA-TGA-3' annealed with 5'-TCA-TTA-CCC-GGG-AAT-AGT-3') double stranded (DS), incubated with daunomycin (dn), doxorubicin (dx), idarubicin (ida), and epirubicin (epi) without formaldehyde or in presence of 2 mM of formaldehyde (dnf), (dxf), (idaf), and (epif). Samples were incubated in TE buffer 1X pH 7.5 for 3 hours at 37 °C. C (control) corresponds to the single stranded (SS) z1, B corresponds to the double stranded z1-zag1r, Bf is z1-zag1r incubated in presence of 2 mM of formaldehyde. The samples were loaded on polyacrylamide denaturing gel (6 M urea). These gels containing fluorescent-labelled DNA were directly photographed with a Perkin-Elmer Geliance 600.

The drugs doxorubicin, daunorubicin, and idarubicin had similar behavior: they prevented denaturation of the DNA even at the lowest concentration (1 µM) in the presence of formaldehyde. Epirubicin incubated in the same conditions, however, had a minor ability to covalently bind the DNA. This anthracycline prevents the denaturation of DNA at higher concentrations (Fig. 57). This behavior is consistent with observations of Cutts and colleagues [33], who explained the lower activity as a result of the different configuration of the 4'-OH group of epirubicin.

The different configuration of the hydroxyl in 4' in epirubicin with reference to the other anthracyclines tested inhibits the formation of a more reactive oxazolidine ring, a hypothetic intermediate that forms after the reactions between anthracyclines and formaldehyde (Fig. 58) [33].

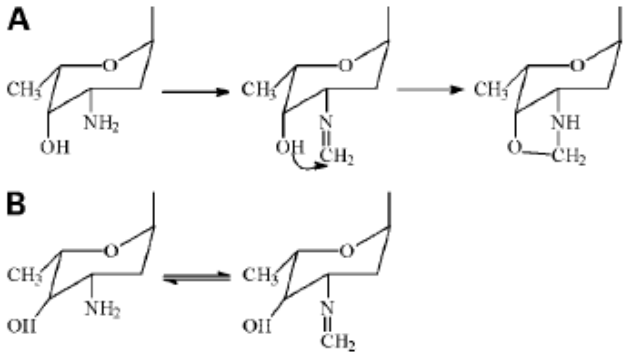

Fig. 58 – A) The axial configuration of the –OH group allows the formation of the oxazolidine ring. B) The equatorial position of this hydroxyl group (as in epirubicin) inhibits the formation of this intermediate [33].

The second group of drugs contains anthracyclines that have a modification in the 4' position, iododoxorubicin and deoxydoxorubicin (Fig. 59), carrying an iodine or no substituents.

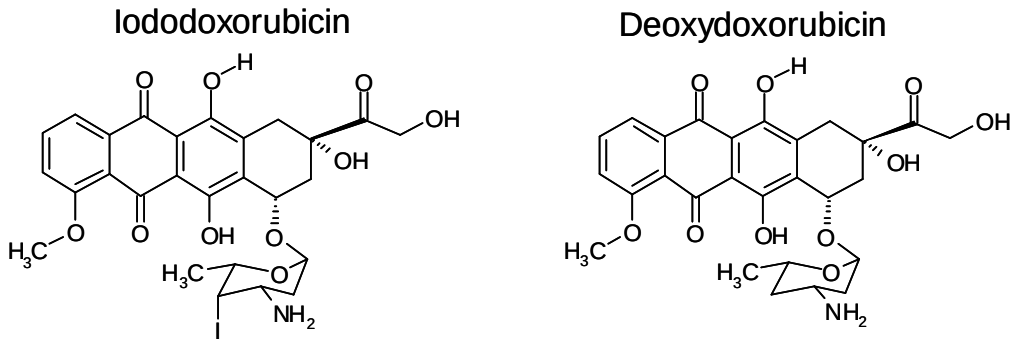

Fig. 59 – Structure of anthracyclines of second group

Anthracyclines were tested as in the preceding experiment. Iododoxorubicin and deoxydoxorubicin were incubated for 3 hours at 37 °C with oligonucleotides double strand z1f-zag1r in TE 1X pH 7.5 in presence and absence of formaldehyde. Then the samples were loaded into a denaturing DPAGE 6 M urea in the following sequence: we loaded in DPAGE oligo z1f single stranded (C), oligo duplex z1f-zag1r (B), oligo duplex z1f-zag1r incubated with 2 mM of formaldehyde (Bf), oligo duplex z1f-zag1r incubated with the anthracyclines iododoxorubicin (iodo) and deoxydoxorubicin (deox) and oligo z1f-zag1r incubated with the preceding anthracyclines in the presence of 2 mM formaldehyde (iodof and deoxf). For both anthracyclines we tested 3 concentrations, 1 μM, 10 μM, and 100 μM (Fig. 60).

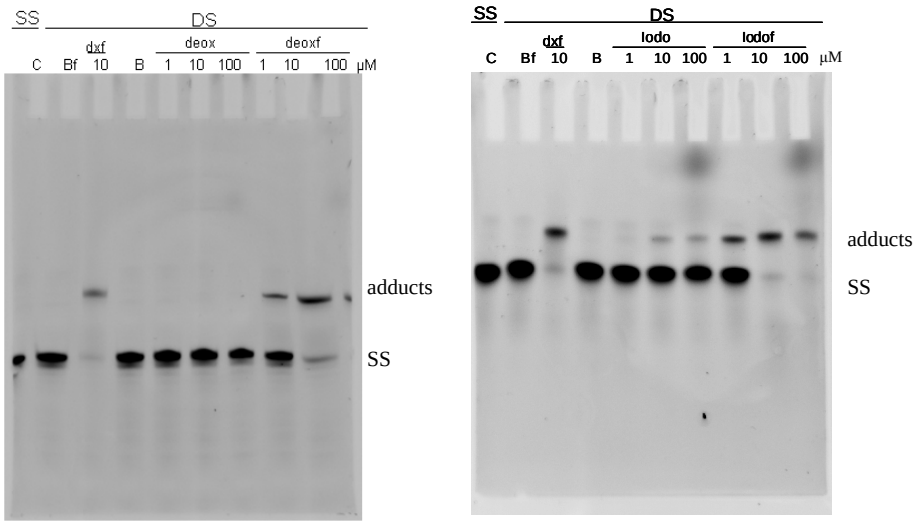

Fig. 60 - Oligonucleotide 1μM z1f-zag1r (FAM-5'-ACT-ATT-CCC-GGG-TAA-TGA-3' annealed with 5'-TCA-TTA-CCC-GGG-AAT-AGT-3') double stranded (DS), incubated with deoxydoxorubicin and iododoxorubicin without formaldehyde, (deox) (iodo), or in the presence of formaldehyde (deoxf), (iodof). Samples were incubated in TE buffer 1X pH 7.5 for 3 hours at 37 °C. C (control) corresponds to the single stranded (SS) z1, B corresponds to the double stranded z1-zag1r, Bf is z1-zag1r incubated in the presence of 2 mM of formaldehyde, and dxf is doxorubicin incubated with z1f-zag1r in the presence of formaldehyde 2 mM. Samples were loaded on polyacrylamide denaturing gel (6 M urea). These gels containing fluorescent-labelled DNA were directly photographed with a Perkin-Elmer Geliance 600.

In contradiction with the hypothesis of the formation of an oxazolidine intermediate, deoxydoxorubicin and iododoxorubicin formed cross-links with formaldehyde already at the lower concentration (1 μM) as doxorubicin, idarubicin, and daunorubicin. Thus the rule of the hydroxyl group must be revised based on this experimental evidence. Both compounds, in fact, lack the –OH in 4' position and the oxazolidine ring cannot form. In deoxydoxorubicin in 4', the –OH is replaced by hydrogen, while iododoxoxorubicin contains iodine instead of the hydroxyl group.

Iododoxorubicin, interestingly, seems to form adducts also in the absence of formaldehyde at higher concentrations (10 μM, 100 μM) (Fig. 60). This surprising behavior of the iododoxorubicin needs to be explored further. We tried to improve the denaturing condition of the gel electrophoresis by heating the samples before loading the gel at 50 °C (Fig 61) and increasing the quantity of urea in the gel (Fig. 62) to determine if these unexpected adducts had the same behavior as adducts obtained in the presence of formaldehyde.

Duplex oligo z1f-zag1r was incubated with iododoxorubicin at different concentrations in the presence and absence of formaldehyde 3 hours at 37 °C as in the preceding experiments and then incubated at 50 °C for 31 minutes before the electrophoretic run (Fig. 61).

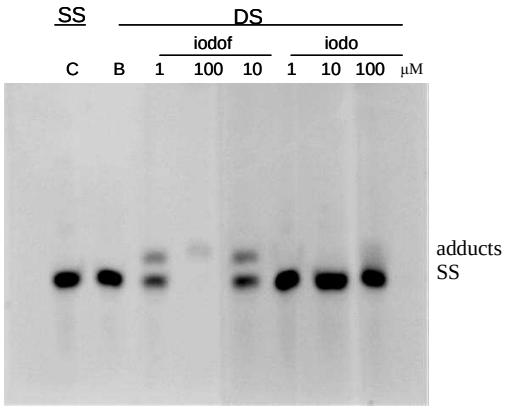

Fig. 61 - Oligonucleotide 1μM z1f-zag1r (FAM-5'-ACT-ATT-CCC-GGG-TAA-TGA-3' annealed with 5'-TCA-TTA-CCC-GGG-AAT-AGT-3') double stranded (DS), incubated with iododoxorubicin (iodo) without formaldehyde or in the presence of formaldehyde (iodof). Samples were incubated in TE buffer 1X pH 7.5 for 3 hours at 37 °C and successively for 31 min at 50 °C. C (control) corresponds to the single stranded (SS) z1f, and B corresponds to the double stranded z1f-zag1r. Samples were loaded on polyacrylamide denaturing gel (6 M urea). These gels containing fluorescent-labelled DNA were directly photographed with a Perkin-Elmer Geliance 600.

Incubation at 50 °C before the analysis causes the disappearance of the adducts that form in absence of formaldehyde, but does not influence the formation of adducts that are produced in the presence of formaldehyde.

We then conducted an experiment where the concentration of urea in the gel was increased to 8 M to improve the denaturing condition. The same duplex z1f-zag1r was incubated with doxorubicin and iododoxorubicin in the presence/absence of formaldehyde and the samples were loaded in the gel (Fig. 62).

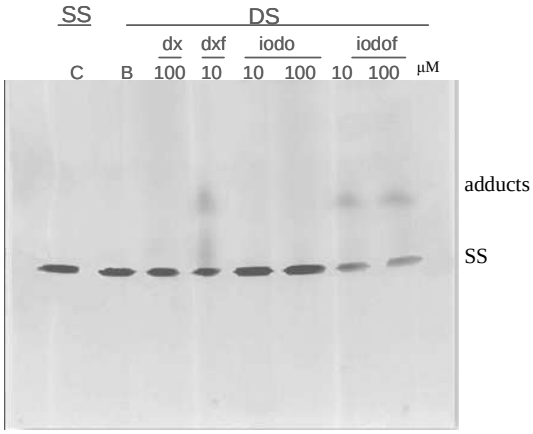

Fig. 62 - Oligonucleotide 1μM z1-zag1r (FAM-5'-ACT-ATT-CCC-GGG-TAA-TGA-3' annealed with 5'-TCA-TTA-CCC-GGG-AAT-AGT-3') double stranded (ds), incubated with doxorubicin (dx) and iododoxorubicin (iodo) without formaldehyde or in the presence of formaldehyde (dxf), (iodof). Samples were incubated in TE buffer 1X pH 7.5 for 3 hours at 37 °C. C (control) corresponds to the single stranded (SS) z1, and B corresponds to the double stranded z1-zag1r. Samples were loaded on polyacrylamide denaturing gel (8 M urea). These gels containing fluorescent-labelled DNA were directly photographed with a Perkin-Elmer Geliance 600.

Even in these conditions, iododoxorubicin does not stabilize the duplex in the absence of formaldehyde, while the adducts formed in the samples with formaldehyde were still detected. Likely iododoxorubicin has a different interaction with the duplex than the other anthracyclines that avoid complete denaturation even in the absence of conditions that promote the formation of cross-links (i.e., presence of formaldehyde). With improved denaturing conditions, instead, non covalent complexes completely denature and no adducts are detected.

The third group contains the compounds doxorubicinon and daunomicinon (Fig. 63). These compounds are the aglycones of doxorubicin and daunorubicin, (i.e., the anthracyclines without the daunosamine). We tested these compounds as a negative control. Theoretically aglycones do not form cross-link, and the absence of an amino group in the structure prevents the reaction with H_2CO and the successive formation of the link to the DNA.

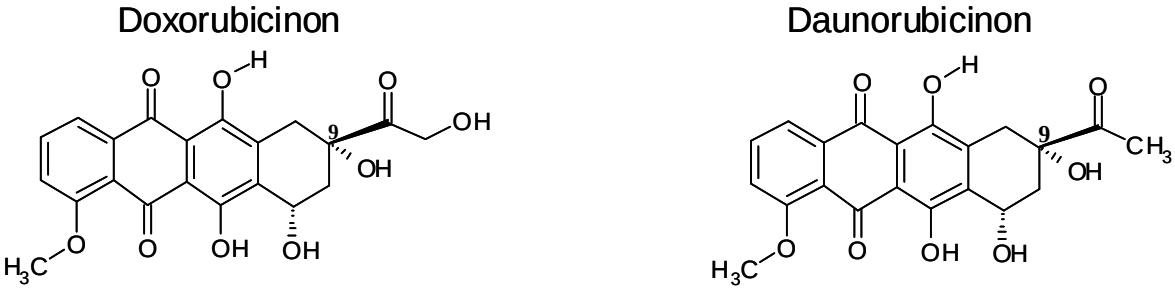

Fig. 63 – Structure of anthracyclines of second group

We then incubate the negative controls, - i.e., the aglycons of daunorubicin (daunorubicinon) and doxorubicin (doxorubicinon) - in the presence and in the absence of formaldehyde.

Daunorubicinon and doxorubicinon were incubated for 3 hours at 37 °C with oligonucleotides double strand z1f-zag1r in TE 1X pH 7.5 in the presence/absence of formaldehyde. Then the samples were loaded on denaturing DPAGE 6 M urea in the following sequence: we loaded in DPAGE oligo z1f single stranded (C), oligo duplex z1f-zag1r (B), oligo duplex z1f-zag1r incubated with 2 mM of formaldehyde (Bf), oligo duplex z1f-zag1r incubated with the anthracyclines daunorubicinon (dau) and doxorubicinon (dxr), and oligo z1f-zag1r incubated with the preceding anthracyclines in the presence of 2 mM of formaldehyde (dauf and dxrf). For both anthracyclines we tested 3 concentrations: 1 μM, 10 μM, and 100 μM.

These compounds, lacking the amino sugar, are confirmed not to form cross-links even if they present weak reactivity at the higher concentration 100 μM in presence of formaldehyde. This weak reactivity, more evident in the doxorubicinon, probably involves the side chain in the

position 9. We also observed two spots with low mobility (LM) at 100 μM, likely due to low solubility of aglycon (Fig. 64).

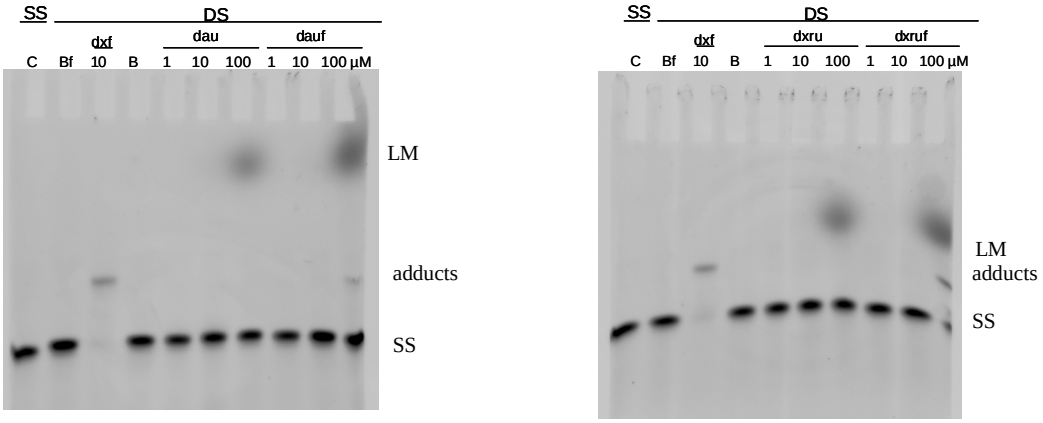

Fig. 64 - Oligonucleotide 1μM z1f-zag1r (FAM-5'-ACT-ATT-CCC-GGG-TAA-TGA-3' annealed with 5'-TCA-TTA-CCC-GGG-AAT-AGT-3') double stranded (DS), incubated with daunomycinon (dau) and doxorubicinon (dxru) without formaldehyde or in the presence of formaldehyde (dauf), (dxruf). Samples were incubated in TE buffer pH 7.5 for 3 hours at 37 °C. C (control) corresponds to the single stranded (SS) z1f, B corresponds to the double stranded z1f-zag1r, and Bf is z1-zag1r incubated in presence of 2 mM of formaldehyde. Dxf is doxorubicin incubated with duplex z1f-zag1r in the presence of 2 mM of formaldehyde. The samples were loaded on polyacrylamide denaturing gel (6 M urea). The gel was photographed with a Perkin-Elmer Geliance 600.

The daunosamine remains necessary for the formaldehyde-mediated cross-link activity and for the formation of a formaldehyde-mediated methylene bridge between the amino group of the daunosamine and the aminogroup of the guanine in the DNA.

Doxorubicin preferentially intercalates in the 5'-GC-3' sequences. We then used a different duplex, (the duplex z2f-zag2r) that has two 5'-GC-3' sites, in order to clarify if our anthracyclines would exhibit higher specificity in the formation of the cross-link with this duplex than z1f-zag1r not having 5'-GC-3'sites.

Duplex z1f-zag1r: z1 forward: FAM-5'-ACT-ATT-CCC-GGG-TAA-TGA-3'
zag1 reverse: 3'-TGA-TAA-GGG-CCC-ATT-ACT-**5'**

Duplex z2f-zag2r: z2 forward: FAM-5'-ACT-ATT- GGC-GCC -TAA-TGA-3'
zag2 reverse: 3'-TGA-TAA-CCG-CGG-ATT-ACT-**5'**

The duplexes (1 μM) were incubated 3 hours at 37 °C in TE 1X with doxorubicin at the concentrations of 1 μM, 10 μM and 100 μM in the presence of formaldehyde. Samples were then loaded in DPAGE 6 M urea. We loaded the single strand control z1f (SS) and the double strand control z1f-zag1r (DS).

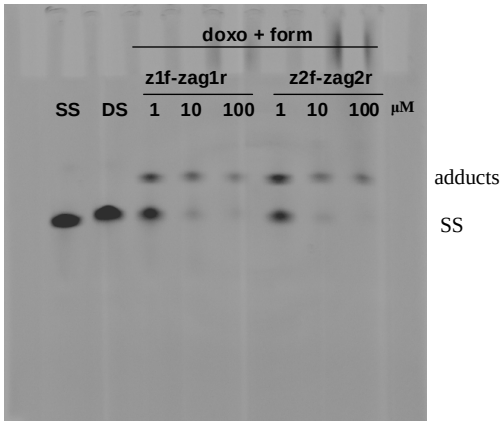

Fig. 65 – Doxorubicin 1, 10 and 100 μM incubated with oligonucleotide 1μM z1f-zag1r (FAM-5'-ACT-ATT-CCC-GGG-TAA-TGA-3' annealed with 5'-TCA-TTA-CCC-GGG-AAT-AGT-3') and z2f-zag2r (FAM-5'-ACT-ATT-GGC-GCC-TAA-TGA-3' annealed with 5'-TCA-TTA-GGC-GCC-AAT-AGT-3') double stranded, in the presence of formaldehyde. Samples were incubated in TE buffer pH 7.5 for 3 hours at 37 °C. SS correspond to the single stranded z1F, and DS correspond to the double stranded z1f-zag1r. The samples were loaded on polyacrylamide denaturing gel (6 M urea). The gel was photographed with a Perkin-Elmer Geliance 600.

Using this preferential binding sequence we did not observe an evident increment of cross-linking activity (Fig. 65). We performed the same comparative experiments for all the anthracyclines previously tested to quantify, using densitometric analysis, the formation of cross-links. We used the software Perkin Elmer GeneTools for the quantification. For every sample, we summed the intensities of the two bands (adducts + free oligos) and we considered this sum 100% in calculating the % formation of the adducts. In Tab. 9 and Tab. 10, we report the quantification of the adducts for doxorubicin and daunomycin.

		% cross-link
z1f-zag1r	Doxo 1 μM (H_2CO)	32
	Doxo 10 μM (H_2CO)	78
	Doxo 100 μM (H_2CO)	84
z2f-zag2r	Doxo 1 μM (H_2CO)	45
	Doxo 10 μM (H_2CO)	79
	Doxo 100 μM (H_2CO)	80

Tab. 9 - Densitometric analysis of adducts formation between doxorubicin and duplex oligos in the presence of H_2CO 2 mM.

		% cross-link
z1f-zag1r	Dauno 1 μM (H_2CO)	21
	Dauno 10 μM (H_2CO)	69
	Dauno 100 μM (H_2CO)	76
z2f-zag2r	Dauno 1 μM (H_2CO)	31
	Dauno 10 μM (H_2CO)	74
	Dauno 100 μM (H_2CO)	89

Tab. 10 -Densitometric analysis of adducts formation between daunomycin and duplex oligos in the presence of H_2CO 2 mM

We observe that z2 duplex is subject to a somewhat higher cross-linking, but the major activity is not substantial. The presence of two high affinity sites of intercalation does not increase cross-linking.

In Fig. 66 we summarize the quantification of adducts formed after incubation with duplexes zif-zag1r and z2f-zag2r for all anthracyclines at the concentration of 10 μM.

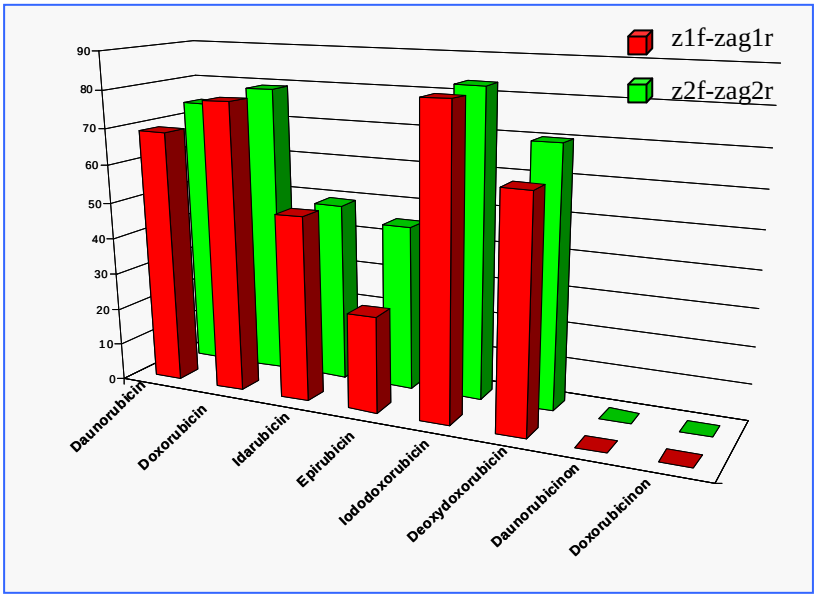

Fig. 66 - Duplexes (z1f-zag1r and z2f-zag2r) 1 μM incubated with the anthracyclines 10 μM in TE 1 X 3h at 37 °C. Adduct spots in DPAGE were quantified using densitometric analysis.

The anthracycline tested did not present particular specificity in the formation of the cross-links. Only epirubicin seemed more active with the duplex z2f-zag2r.

6.2 Formation of the "Virtual cross-link"

Cutts and colleagues extensively revised the interaction between doxorubicin and formaldehyde and the rule in the formation of DNA adducts [23]. Fenick and colleagues synthesized conjugates between doxorubicin and formaldehyde composed of two molecules of anthracycline as doxazolidine bound together with a third molecule of formaldehyde (Fig. 67) [28]. The original synthesis of the conjugate doxoform was performed by reaction of the drug with formaldehyde in an acetate buffer at pH 6. The buffer was removed using high vacuum and the product was dissolved in chloroform [28]. With this method, the presumed intermediate, doxazolidine, a monomeric doxorubicin oxazolidine, was not observed. In contrast, in a reaction of doxorubicin free base in chloroform-*d* solvent with paraformaldehyde, the polymer of formaldehyde, with monitoring by 1H NMR, showed formation of doxazolidine followed by formation of doxoform [29].

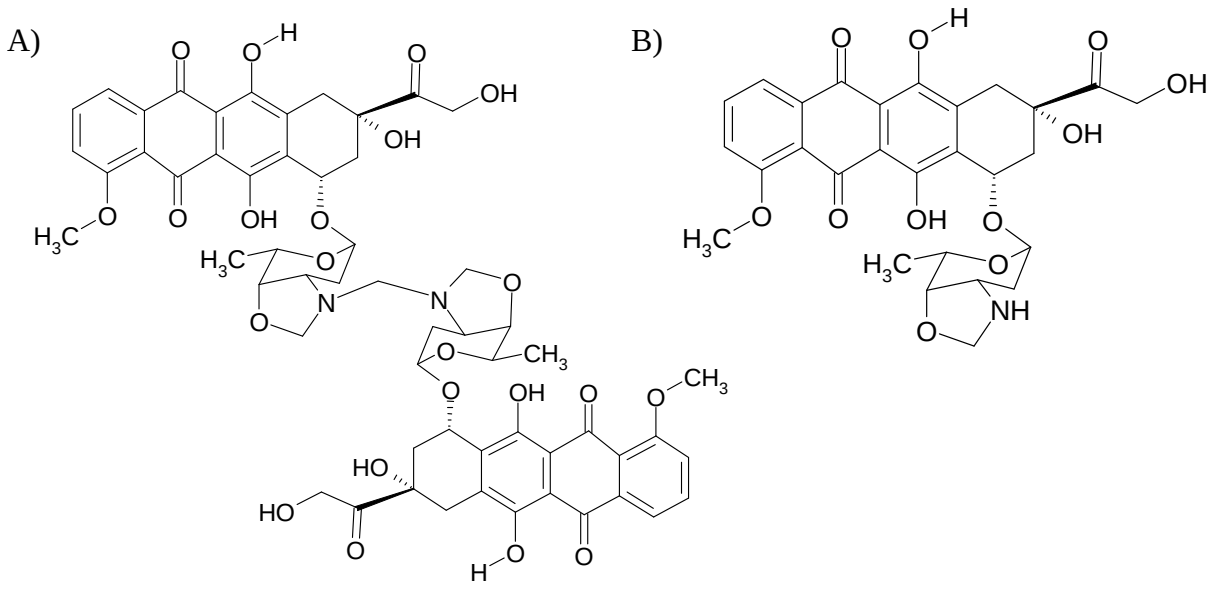

Fig. 67. – Structures of doxoform (A) ad doxazolidine (B).

Doxoform and doxazoline are reported to be instable in an aqueous medium. At pH 7.4 and 37 °C, doxoform rapidly hydrolyses to doxazolidine (half life 1 minute) and doxazolidine (half life 3 minutes) to doxorubicin [59]. An intermediate in the last hydrolysis is the acyclic doxorubicin-formaldehyde conjugate (aminol) [29] (Fig. 68).

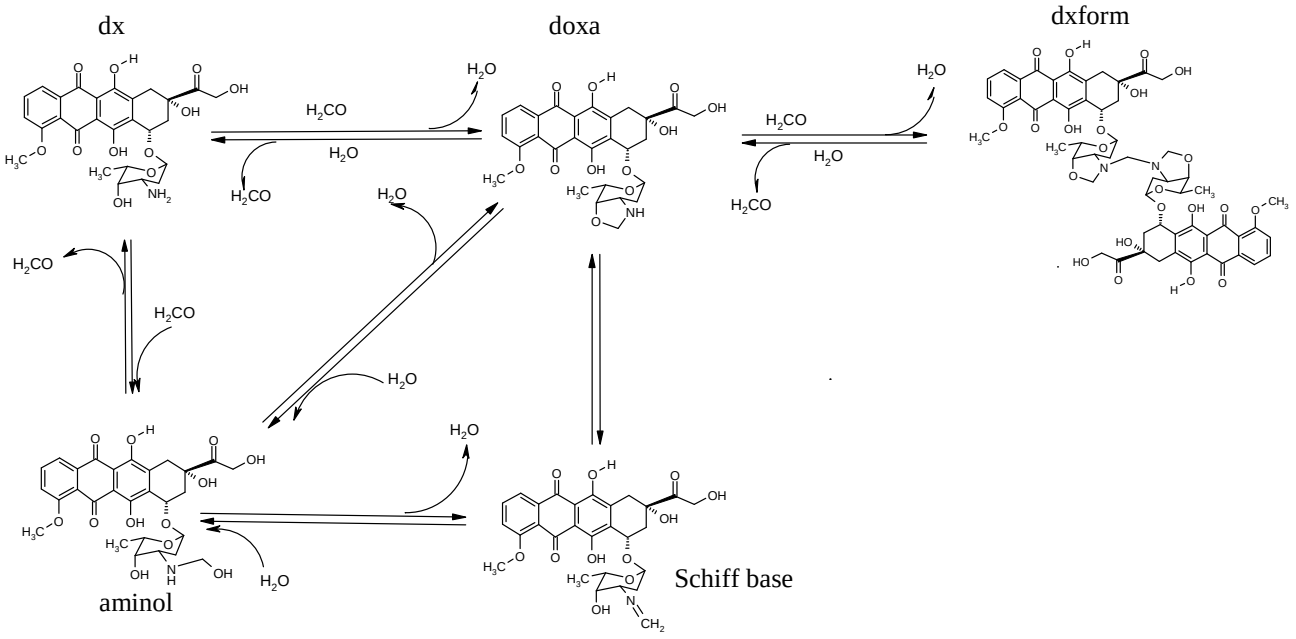

Fig. 68 – Synthesis of doxazolidine (doxa) and doxoform (dxform) from doxorubicin (dx) and their partial hydrolysis to doxazolidine and doxorubicin-formaldehyde conjugates (Schiff base or aminol), the presumed active cross-linking species [29].

Post suggests that the main active species that reacts with the DNA to form cross-links was expected to be the doxazolidine that is more cytotoxic than doxoform [29], even if the presence of reactivity in our experiment when the doxazolidine cannot form suggests that the aminol and the Schiff base are also involved in the reacting mechanism. We have in fact reported in the section “6.1 page 79” that iododoxorubicin and deoxydoxorubicin formed adducts detected by DPAGE, although the lack of 4'-OH should prevent the formation of the oxazolidinic ring. In order to clarify this mechanism, we further analyzed the reactivity of doxorubicin and doxorubicin activated by formaldehyde using IP RP-HPLC and mass spectrometry similarly to what we have done with PNU.

We incubated the annealed oligonucleotides (double stranded) z1f-zag1r 1 μM with doxorubicin 10 μM at different times (1 hour and 4 hours) at 37 °C in TE 1X pH 7.5. Samples were then analyzed by HPLC with instrument 1 and method C (see 4.4 section, pag 28). In these experimental conditions, we observed the signal of zag1r (t_R: 14.4 min), z1f (t_R: 16.1 min) and doxorubicin (t_R: 19.7 min), but did not observe the appearance of new signals (Fig. 69). No adducts of doxorubicin to DNA were detected in these experimental conditions, consistently with the lack of reactivity in the absence of formaldehyde.

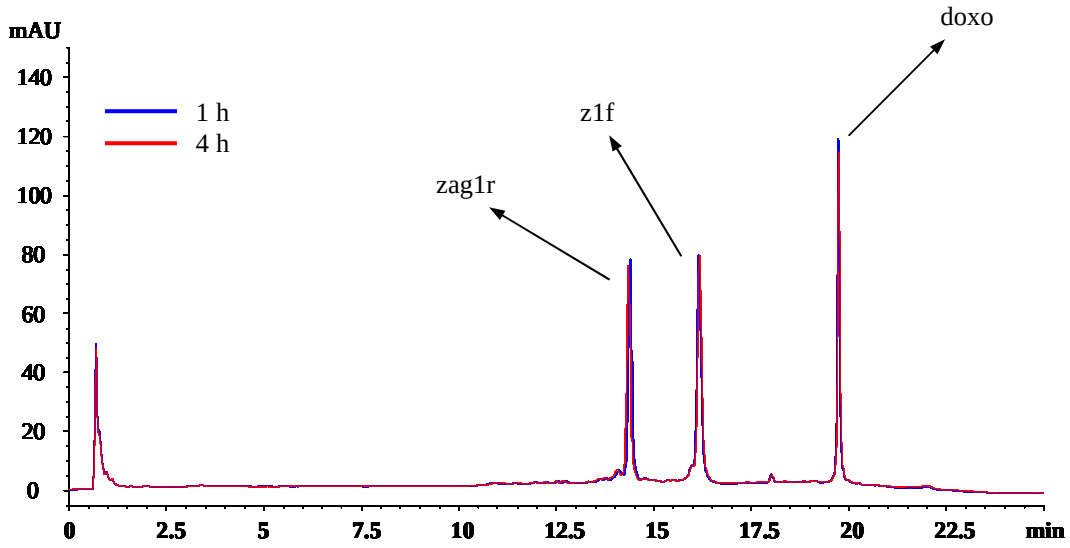

Fig. 69 – Chromatograms of the oligonucleotide z1f-zag1r DS 1 μM (FAM-5'-ACT-ATT-CCC-GGG-TAA-TGA-3' annealed with 5'-TCA-TTA-CCC-GGG-AAT-AGT-3') incubated in TE 1X pH 7.5 with doxorubicin 10 μM at 37 °C 1h (blue line) and 4h (red line). Spectrophotometric detector λ=260 nm. Instrument 1, method C.

We then repeated the experiment of oligonuclotides using doxorubicin activated with H_2CO. First doxorubicin (100 μM) in TE 1X was incubated with formaldehyde 2 mM 3 hours at 37 °C, lyophilised and resuspended in the same volume of purified water. Then we incubated the duplex DNA with this activated anthracycline. The oligo double stranded z1f-zag1r 1 μM and the activated doxorubicin (10 μM of nominal doxorubicin) were kept for different time (1hour and 4hours) at 37 °C in TE 1X pH 7.5. Analyzing the samples by HPLC (instrument 1, method C), we observed the formation of two new peaks (adducts) with the t_R of 17.0 min (adduct A) and 17.3 min (adduct B) (Fig. 70). The quantity of adducts formed between the oligo and the "doxoform" increased by increasing the incubation time. The quantity of adducts detected was low, consistent with the rapid hydrolysis of the doxoform that probably formed in this condition. As mentioned, doxoform is the putative species formed upon incubation of doxorubicin and formaldehyde.

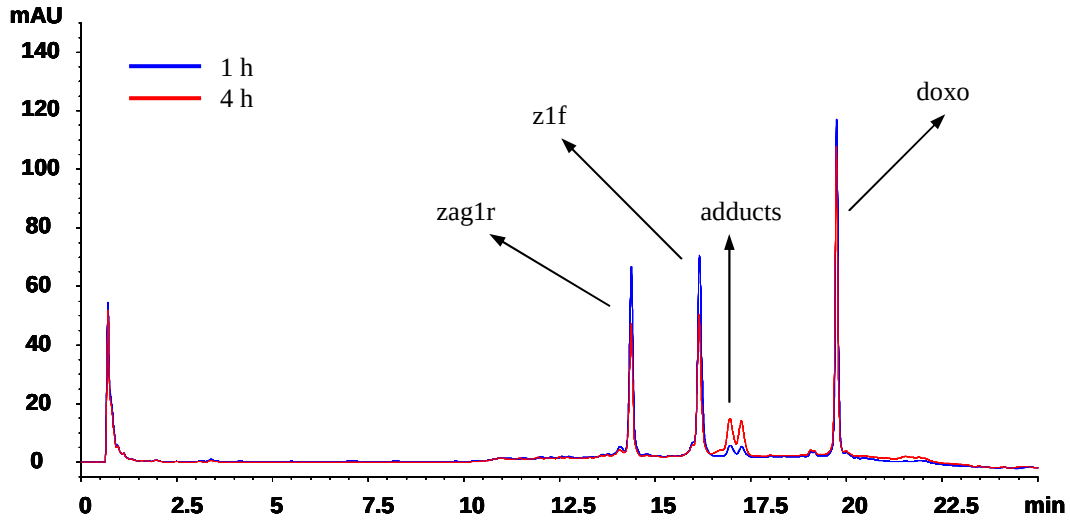

Fig. 70 – Chromatogram of the oligonucleotide z1f-zag1r DS 1 µM (FAM-5'-ACT-ATT-CCC-GGG-TAA-TGA-3' annealed with 5'-TCA-TTA-CCC-GGG-AAT-AGT-3') incubated at 37 °C in TE 1X pH 7.5 with doxo-H_2CO (doxorubicin 100 µM incubated 3 h with H_2CO 2mM at 37 °C in TE 1X, lyophilized ad resuspended in H_2O) 1h (blue line) and 4h (red line). Spectrophotometric detector λ=260 nm. Instrument 1, method C.

These preliminary results suggested the possibility of detecting and isolating by HPLC the adducts between DNA and the anthracyclines similarly to what we have experienced in the chapter of PNU-DNA adducts (chapter 5.4). Doxorubicin first reacted with formaldehyde and afterwards with the DNA. We proved the reaction between doxorubicin and formaldehyde by mass spectrometry. We incubated doxorubicin 100 µM 1 hour in water in the presence of formaldehyde 2 mM and we analyzed the mixture using mass spectroscopy (50% of methanol was added before analysis) obtaining the spectrum in Fig. 71. The instruments used for this spectrometric analysis was a Bruker ultrOTOF-Q™, an instrument endowed with a quadrupole filter and a TOF analyzer. We used ESI ionization system.

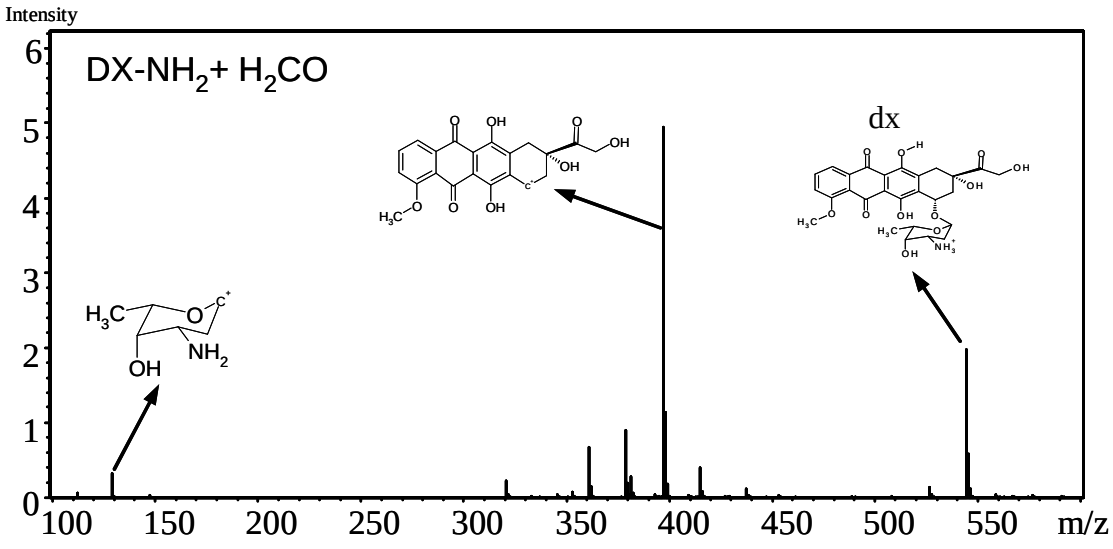

Fig. 71 – UltrOTOF-Q™ spectrum obtained after analysis of doxorubicin 100 µM incubated 1h with H_2CO 2 mM in water at 37 °C. 50 % methanol was added at the sample before analysis.

All the species detected in this condition are referable to the doxorubicin and its fragments, (daunosamine and aminosugar). The primary amine reacts with aldehyde to form instable Schiff-base, but in these conditions the Schiff-base formed between the doxorubicin and the formaldehyde was not detected. We conducted the same reaction and added sodium borohydride (200 μM) after the reaction between the doxorubicin and the formaldehyde to reduce the Schiff base and indeed detected this molecular species (Fig. 72).

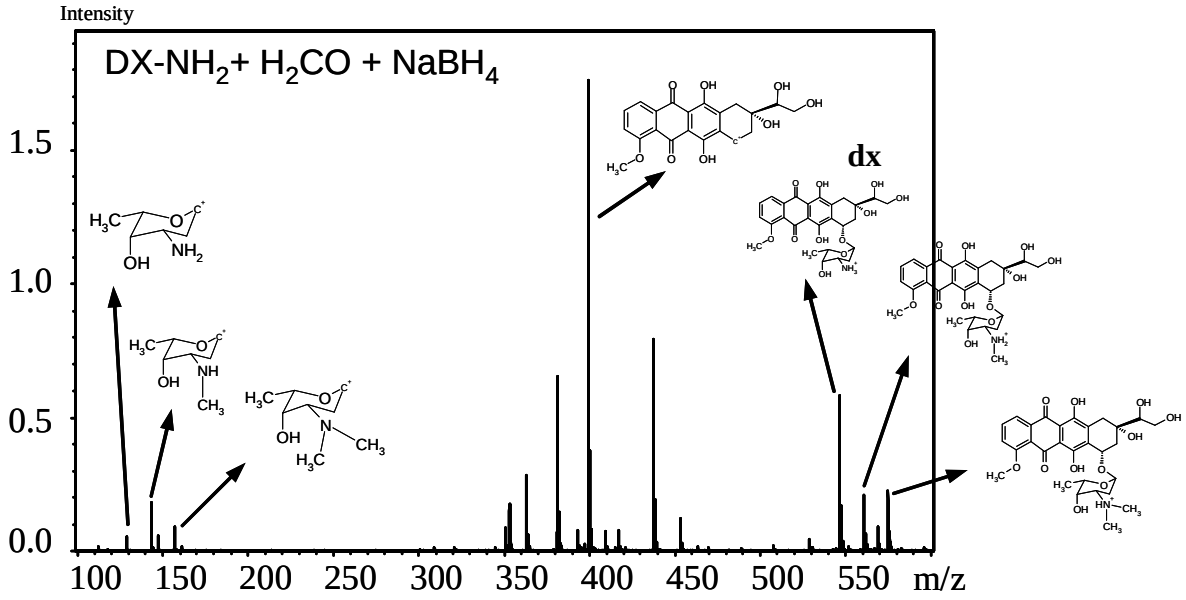

Fig. 72 – UltrOTOF-Q™ spectrum obtained after analysis of doxorubicin 100 μM incubated 1h with H_2CO 2 mM in water at 37 °C. At the mixture we added sodium borohydride (200 μM final concentration) and then we incubated for further 10 minutes. 50 % methanol was added at the sample before analysis.

Adding sodium borohydride, we detected ions with an incremental mass of 14 dalton and 28 dalton in comparison to the signal of doxorubicin and the sugar fragment. This is consistent with the additions of one or two methylene groups. This indicates that the Schiff base forms after the reaction between the doxorubicin and the formaldehyde and that it can be detected after the reduction to amine.

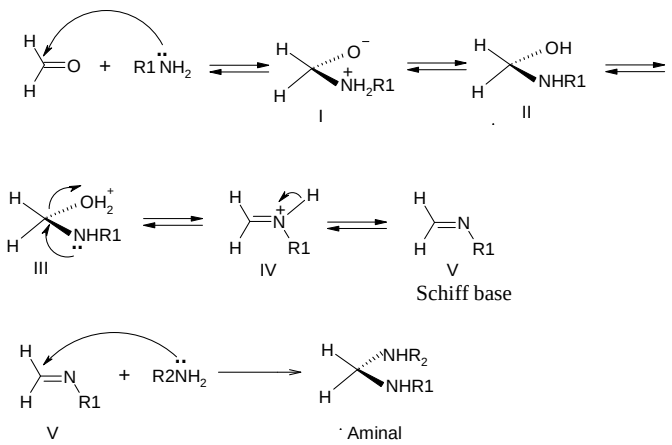

Fig. 73 – The mechanism proposed for the formation of aminal linkage between anthracyclines and DNA. R1 = dx and R2 = guanine of DNA [60].

Even if the doxazolidine is considered the main active metabolite in the formation of VXL, we suggest that the Schiff base plays an important role, as previously proposed by Leng [60] (Fig. 73). Probably both mechanisms (the formation of adducts via the Schiff base and via doxazolidine) are present in the formation of VXL, consistent with the adducts visualized in DPAGE after incubation of iododoxorubicin and deoxydoxorubicin that cannot form the doxazolidine-like intermediate.

The formation of formaldehyde-activated doxorubicin rationalized the formation of adducts, but the amount of the adducts was low. The adducts detected in the chromatogram in Fig. 70 were due to the presence of formaldehyde, but we did not know the quantity of activated doxorubicin that remain after lyophilisation. We decided then to directly analyze the mixture obtained after treatment in the same conditions of the previous DPAGE analysis, incubating the duplex directly with doxorubicin and formaldehyde. We used DS oligo with anthracycline plus formaldehyde so that our variable was the concentration of doxo, regardless of doxoform. Therefore in the experiments we analyzed the formation of adducts with the instrument 2 (chapter 4.4, page 34) equipped with a diode array. The diode array detector allowed us to determine if there were anthracyclines in the adducts measuring the absorbance at 485 nm. In this case, we did not use fluorescein-labelled oligo to avoid interference of the signal at 485 nm.

Briefly, the unlabelled oligonucleotide (zag1f-zag1r 1 μM) (Fig. 74) was incubated with doxorubicin 10 μM and formaldehyde 2 mM 3 hours in TE 1X pH 7.5 at 37 °C and the mixture of the reaction was directly analyzed by HPLC.

Duplex zag1f-zag1r:	zag1 forward: 5'-ACT-ATT-CCC-GGG-TAA-TGA-3'
	zag1 reverse: 3'-TGA-TAA-GGG-CCC-ATT-ACT-5'

Fig. 74 – Oligo zag1f and zag1r have the same molecular weight (i.e., the same bases); the different sequence is not sufficient to obtain a different retention time in IP RP HPLC analyses.

The two oligonucleotides forward and reverse (not labelled) had the same retention time (t_R: 13.9 min). When we incubated zag1r-zag1f with doxorubicin plus formaldehyde, we observed the formation of a new peak (t_R:14.8 min). Doxorubicin had a t_R of 20.9 min in these experimental conditions. The incubation with unlabelled oligonucleotides permitted us by diode array detector to demonstrate the presence of anthracycline in the new peak at 14.8 min (Fig. 75). The adduct was formed in high quantity; probably the copresence of formaldehyde

allowed the formation of a higher quantity of activated doxorubicin that reacted with the duplex DNA.

:

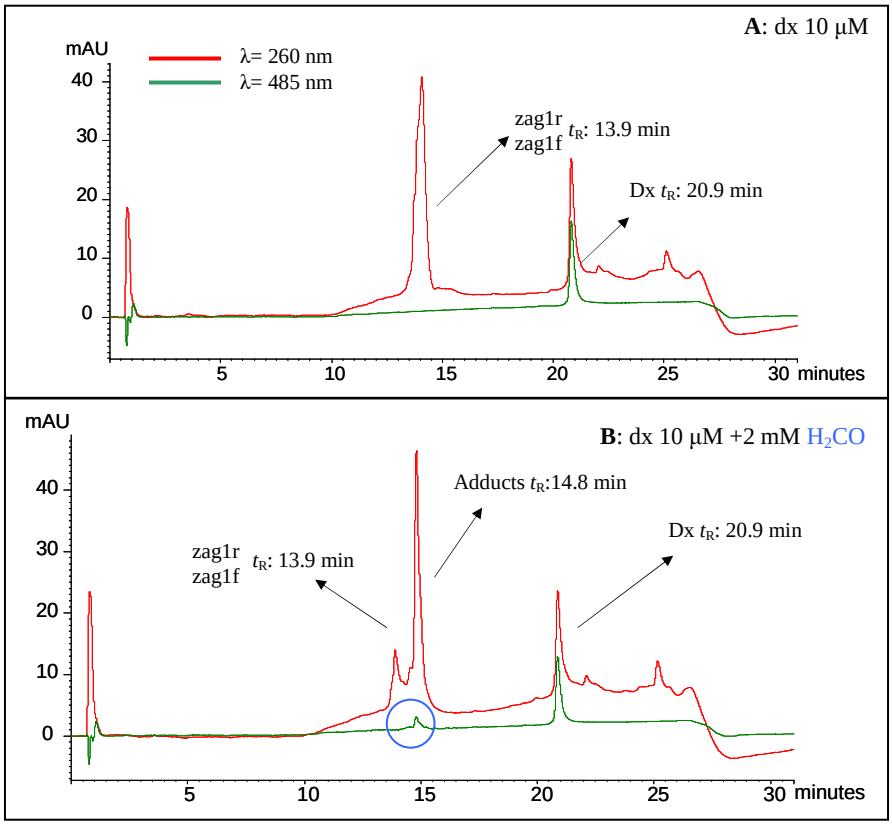

Fig. 75 – Chromatograms of the oligonucleotides DS zag1f-zag1r 1 µM (5'-ACT-ATT-CCC-GGG-TAA-TGA-3' annealed with 5'-TCA-TTA-CCC-GGG-AAT-AGT-3') incubated 3h at 37 °C in TE 1X with doxorubicin 10 µM (A) and with doxorubicin in presence of formaldehyde 2 mM (B). Spectrophotometric detector λ=260 nm and λ=485 nm. Instrument 2, method A.

Our analysis demonstrates unambiguously that the presence of formaldehyde fixes the anthracycline onto the DNA (i.e., resulting in the formation of VXL), forming adducts detected also at 485 nm (λ_{max} of doxorubicin), consistently with the gel electrophoresis experiments described in section 6.1, page 75.

We then concentrated our attention on iododoxorubicin that does not contain the 4'-OH and cannot form the oxazolidine ring. We continued our analysis using fluorescein labelled oligo z1f-zag1r, the same duplex that we used for the analysis of the PNU (chapter 5) and for the SAR (chapter 6.1). We prepared the samples for HPLC in the same conditions as the gel electrophoresis (chapter 6.1), incubating the duplex z1f-zag1r 3 hours at 37 °C in TE 1X pH 7.5 with iododoxorubicin.

When we analyzed oligonucleotides incubated with iododoxorubicin without formaldehyde, we did not observe the formation of adducts. These conditions were sufficiently denaturating

to eventually denature the non-covalent complexes that we detected in DPAGE (see section 6.1 page 79). In the chromatographic run, we observed three peaks with the same retention time (t_R) of zag1 reverse (zag1r) (t_R: 13.4 min), z1 forwardfam (z1f) (t_R:14.7 min) and iododoxorubicin (t_R: 26.8 min) (Fig. 76).

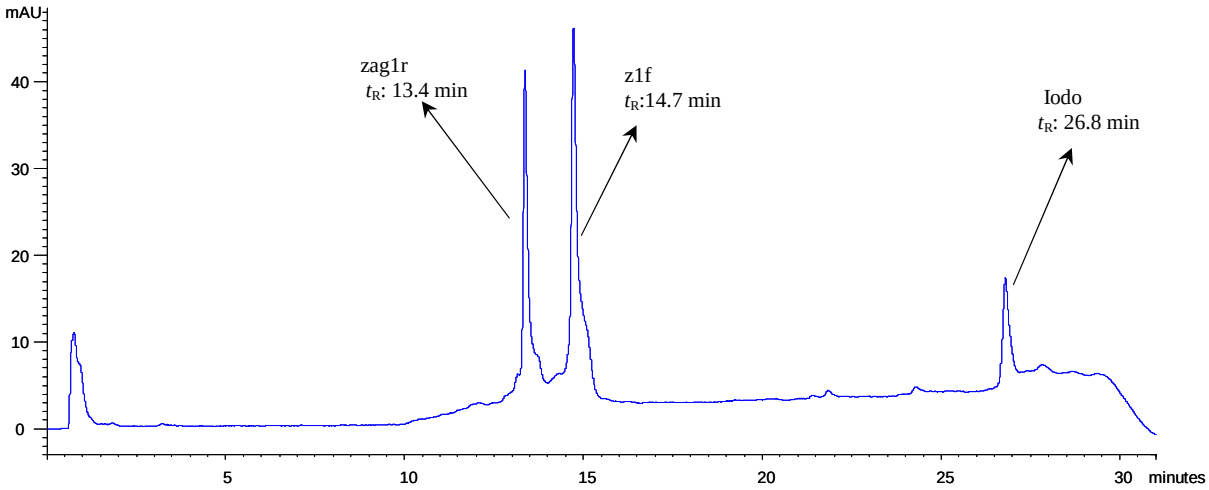

Fig. 76 – Chromatogram of the duplex z1f-zag1r 1 µM (FAM-5'-ACT-ATT-CCC-GGG-TAA-TGA-3' annealed with 5'-TCA-TTA-CCC-GGG-AAT-AGT-3') incubated 3h at 37 °C in TE 1X pH 7.5 with iododoxorubicin 10 µM without formaldehyde. Spectrophotometric detector λ=260 nm. Instrument 2, method B.

Instead, when we incubated the same duplex z1f-zag1r 1 µM with iododoxorubicin 10 µM in presence of formaldehyde 2 mM in TE 1X pH 7.5, we observed the formation of two new peaks, one higher peak with a t_R of 15.6 min that we named adduct B, and another smaller peak with a t_R of 15.3 min (adduct A) (Fig. 77). The appearance of the new peaks corresponds to a sharp decrease in the signals corresponding to zag1r and z1f, indicating that both of these two species are implicated in the formation of the new adducts. In the absence of formaldehyde, the signal of iododoxorubicin is higher than in its presence: this observation is consistent with the assumption that free iododoxorubicin is consumed when formaldehyde is present to allow formation of the adduct.

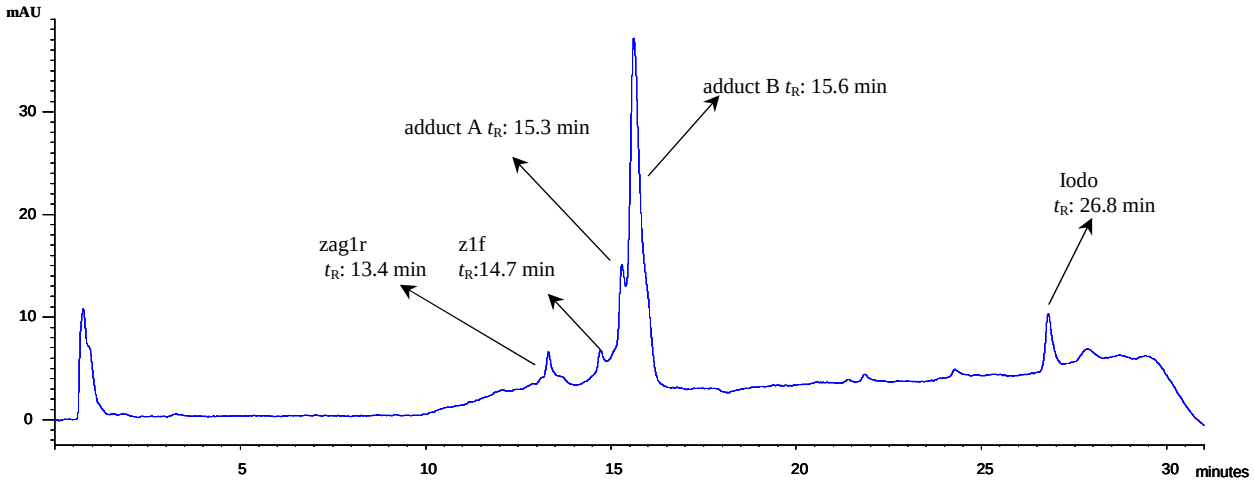

Fig. 77 – Chromatogram of the oligonucleotide DS z1f-zag1r 1 µM (FAM-5'-ACT-ATT-CCC-GGG-TAA-TGA-3' annealed with 5'-TCA-TTA-CCC-GGG-AAT-AGT-3') incubated 3h at 37 °C in TE 1 X pH 7.5 with iododoxorubicin 10 µM and formaldehyde 2 mM . Spectrophotometric detector λ=260 nm. Instrument 2, method B.

When we reduced the concentration of the anthracycline, we observed a different behavior: when we incubated the oligo DS z1f-zag1r 1 µM with iododoxorubicin 1 µM in the presence of formaldehyde 2 mM, we obtained the same new peaks, but the adduct A (t_R: 15.3 min) was now the major peak and the adduct B (t_R: 15.6 min) was smaller. The correlation between decrease in the oligos and the quantity of adducts formed was less stringent (Fig. 78).

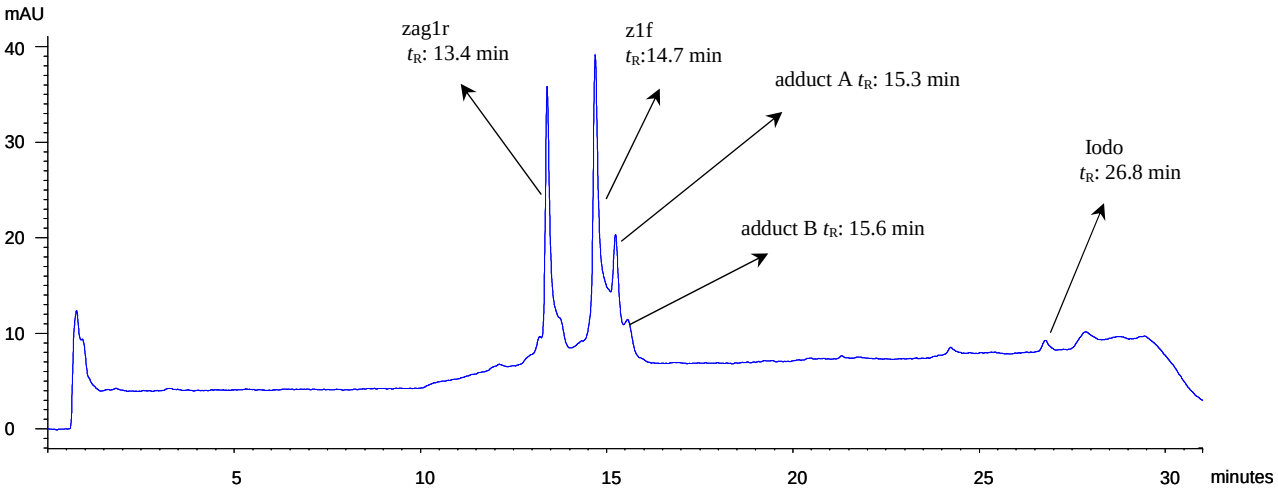

Fig. 78 – Chromatogram of the oligonucleotide DS z1f-zag1r 1 µM (FAM-5'-ACT-ATT-CCC-GGG-TAA-TGA-3' annealed with 5'-TCA-TTA-CCC-GGG-AAT-AGT-3') incubated 3h at 37 °C in TE 1 X pH 7.5 with iododoxorubicin 1 µM in presence of formaldehyde 2 mM . Spectrophotometric detector λ=260 nm. Instrument 2, method B.

The lack of the reactivity of the iododoxorubicin when incubated in absence of formaldehyde is consistent with the consideration in the chapter 6.1 when non covalent complexes detected in DPAGE were denatured improving the denaturing condition (page 80). Iododoxorubicin is quite different than the other anthracyclines, the basicity of the amino group and then the electrostatic binding is lower for the presence of iodine. Nevertheless this anthracycline

presents cooperative binding with isolated DNA [61], this behavior likely leads to accumulation of drugs in the same area of the duplex forming cluster. This is consistent with the presence of non-covalent adducts when DNA was incubated with iododoxorubicin in absence of formaldehyde, adducts that disappear improving the denaturing conditions or in HPLC conditions.

In the presence of formaldehyde, instead, we found two adducts, just as when we incubated in presence of activated doxorubicin. Different adducts (A and B) formed with iododoxorubicin in the presence of formaldehyde, depending on the different concentrations of anthracycline used, respectively 1 μM and 10 μM. They probably differ in the number of anthracyclines bound to the DNA; we obtained two different adducts A and B in the analysis of the PNU with the same duplex (chapter 5). Probably adducts detected after the reaction of anthracyclines in presence of formaldehyde are similar to adducts formed by PNU even if PNU does not need formaldehyde activation.

6.3 Structure of the "Virtual Cross-Link"

To better clarify the nature of the cross-link through anthracyclines and DNA we focused our attention on doxorubicin as it represents an important reference drug. We investigated its reactivity using native polyacrylamide gel electrophoresis (PAGE) and fully denaturing polyacrylamide gel electrophoresis (DPAGE). The following electrophoretic analyses were performed with some differences from the experiments described before. We used Sigma Stains-All to make visible the DNA in the polyacrylamide gels; this compound is suitable to stain both double stranded and single stranded DNA. Stain-All allowed us to use unlabelled oligonucleotides, even if this meant that we had to load the gel with a higher quantity of DNA. We performed PAGE and DPAGE of doxorubicin incubated with three different oligo-sequences in double and single stranded form. In all of the following gel electrophoresis experiments, we first loaded the two singles stranded and the double stranded oligos, the same in the presence of doxorubicin and the same in the presence of doxorubicin and formaldehyde. The last sample was duplex with formaldehyde without doxorubicin.

Samples with oligos zag (single stranded and duplex) were incubated for 3 hours at 37 °C in TE 1X. Then, to 10 μl of each sample was added 5 μl of GLB (50% glycerol in water for PAGE samples' and 50% glycerol in 8 M urea for DPAGE samples'). To the last sample in both gels (PAGE and DPAGE) we added 0.2% bromophenol blue (BB) to the GLB. Then the samples

were run in native polyacrylamide gel for 40 minutes at 160 volts and in denaturing gel for 140 min at 160 volts.

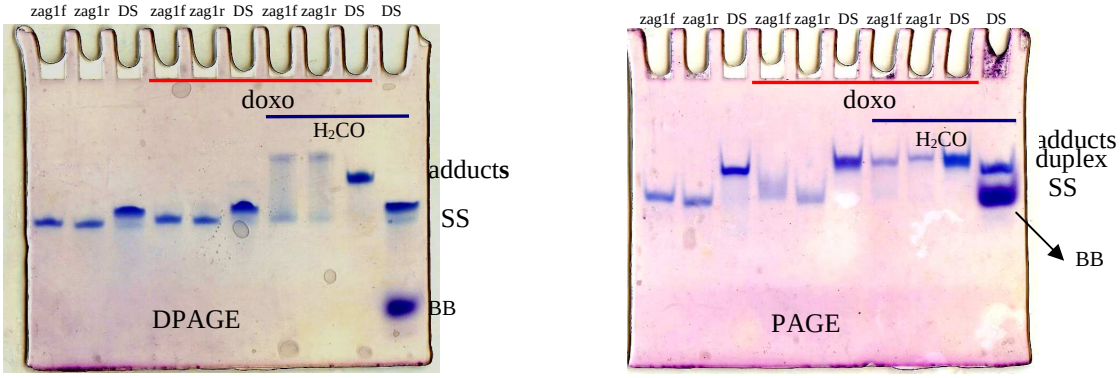

Fig. 79 - Oligonucleotides 10µM (single stranded (zag1f and zag1r) and duplex (DS)) were incubated in presence and absence of H_2CO 2 mM and in presence and absence of doxorubicin 100 µM for 3h in TE buffer pH 7.5 at 37 °C. Samples were loaded in polyacrylamide native (29:1) and denaturing gel (19:1) 7.5 M urea. Electrophoretic run was conducted at 160 V for 40 min (native) and 160 volts for 140 min (denaturing) in TBE 1X. Gels were coloured with Sigma Stains-All and the images were captured with an HP 7400 scanner.

Oligos incubated with doxorubicin did not show particular differences in electrophoretic mobility compared to oligos without the drug. When we added doxorubicin, we observed a smear with single stranded oligos and a little delay for the double strand in PAGE due to the interaction between anthracycline and DNA. But when we added H_2CO to the mixture, we observed in PAGE a duplex-like electrophoretic mobility also for the single stranded oligos (Fig. 79).

Our goal was to investigate the characteristics of the bond between the oligos and the doxorubicin using high resolution mass spectrometry. The first problem deals with the buffer. In fact TE is incompatible with the ESI mass spectrometry. We then analyzed the interaction between our oligos and the doxorubicin in the presence and absence of formaldehyde; conducting the incubation in water rather than in TE 1X to see if the reactivity remained.

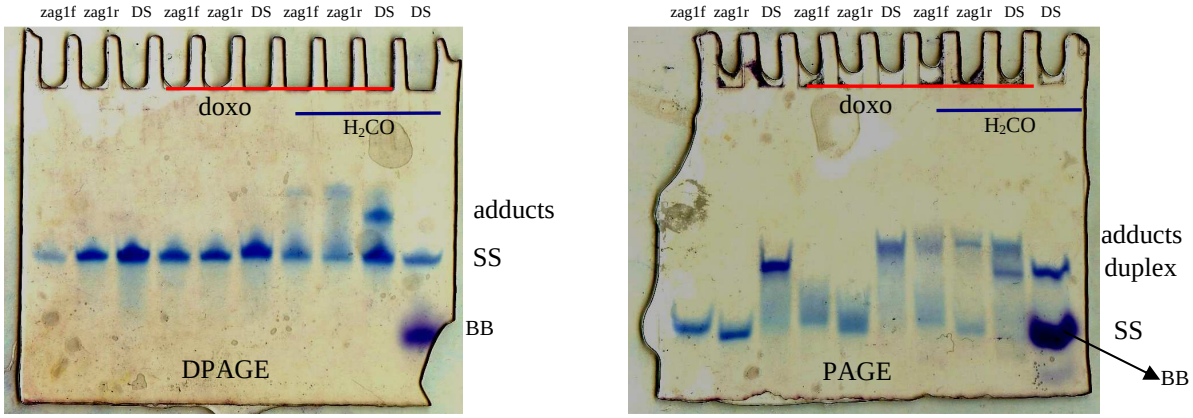

Fig. 80 - Oligonucleotides 10µM (single stranded (zag1f and zag1r) and duplex (DS)) was incubated in the presence and absence of H_2CO 2 mM and in the presence and absence of doxorubicin 100 µM for 3h in purified water at 37 °C. Samples were loaded in polyacrylamide native and denaturing gel (19:1) 7.5 M urea. Electrophoretic run was conducted at 150 V for 120 min in TBE 1X. Gels were coloured with Sigma Stains-All and the images were captured with an HP 7400 scanner.

The reactivity of doxorubicin in water was the same as the reactivity in TE 1X pH 7.5, even if the stabilization of the duplex was lower. The delay of the duplex in native gel when we added doxorubicin was more evident in this case. If we observe in detail the PAGE in Fig. 80, the first 3 bands correspond to the single stranded zag1f and the zag1r that have similar electrophoretic mobility, and the duplex (DS) with lower mobility. The native conditions do not change the structure of the DNA, and the electrophoretic mobility is consistent with the single stranded and duplex structure. In the next wells we loaded the same DNA, but incubated with doxorubicin. This caused a smear of the single stranded DNA and a delay of the duplex due to interaction with doxorubicin. The situation drastically changed when we added formaldehyde. The single stranded oligos split into two bands, one with the mobility of the single stranded and one with the mobility of the duplex delayed by doxorubicin. The duplex in presence of doxorubicin and formaldehyde split into two bands one with the mobility of the duplex and one with the mobility of the duplex delayed by doxorubicin. The last well contained the duplex incubated with formaldehyde; this duplex kept the same mobility as of the duplex alone. The extra bands in the last well of every gel corresponded to the bromophenol blue added only in the last sample. The bands delayed by doxorubicin were called adducts; these are complexes with doxorubicin and DNA with lower mobility. Observation of the denaturing gel gave us further information; only the copresence of doxorubicin and formaldehyde led to the formation of stable adducts in the denaturing gel, consistent with the formation of covalent complexes, while noncovalent complexes formed by doxorubicin were not detected. Adducts at a single stranded oligo were characterized by a different electrophoretic mobility as compared to the adducts at a duplex. Probably in this condition the single stranded system was partially associated, as we can see also in the PAGE, but it can have a different structure in the DPAGE where the single stranded adducts have a shorter electrophoretic run. One further aspect revealed in these experiments was that single stranded DNA interacted with doxorubicin to form a “virtual covalent” adduct, even if the main interaction reported in the literature is the intercalation of anthracyclines into the duplex DNA. Clearly, electrostatic and stacking interactions can explain the affinity of the drug for a single-stranded nucleic acid, rendering the covalent process feasible also in the absence of a canonical helical arrangement. Before mass analysis we wanted to clarify this behavior by testing different oligos: complementary oligos kt3 and kt4, and complementary oligos zemen1 (zm1) and zemen2 (zm2) (Fig. 81).

zag1r: 5'-TCA-TTA-CCC-GGG-AAT-AGT-3'
zag1f: 5'-ACT-ATT-CCC-GGG-TAA-TGA-3'

kt1: 5'-TCT-CGC-TCT-T-3'
kt2: 5'-AAG-AGC-GAG-A-3'

kt 3: 5'-TCT-CTC-GCT-CTT-CT-3'
kt 4: 5'-AGA-AGA-GCG-AGA-GA-3'

zemen1: 5'-AAT-TAT-GCT-TAA-AA-3'
zemen2: 5'-TTT-TAA-GCA-TAA-TT-3

Fig. 81 – Sequences of complementary oligos zag, kt and zemen.

Complementary oligos kt3 and kt4 single and double stranded were incubated with doxorubicin in the presence and absence of formaldehyde in purified water overnight at 4 °C. (The duplex kt1-kt2 has a lower melting temperature than the duplex zag, and the low incubation temperature is necessary to keep the duplex form.)

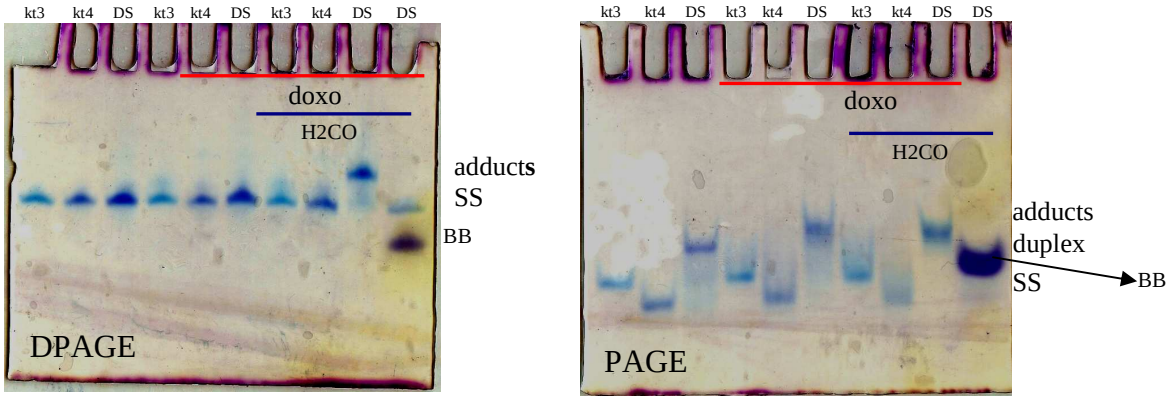

Fig. 82 - Oligonucleotides 10μM (single stranded (kt3 and kt4) and duplex (DS)) was incubated in the presence and absence of H_2CO 2 mM and in the presence and absence of doxorubicin 100 μM overnight in purified water at 4 °C. Samples were loaded in polyacrylamide native and denaturing gel (19:1) 7.5 M urea. Electrophoretic run was conducted at 105 V for 120 min for both gels in TBE 1X. Gels were colored with Sigma Stain-All and the images were captured with an HP 7400 scanner.

The scheme of loading was the same: first we loaded the single stranded kt3 and kt4 and the duplex, then the same samples incubated with doxorubicin in the absence and in the presence of formaldehyde. The last sample was the duplex incubated with formaldehyde (Fig. 82). In these conditions, only the duplex formed adducts in the presence of doxorubicin and formaldehyde as detected by DPAGE. The single stranded kt3 and kt4 did not lead to the formation of detectable adducts.

Finally, we tested the oligos zemen (zm) with only one GC in the sequence. The oligo zm single and double stranded was incubated in water with doxorubicin in the absence and the presence of formaldehyde at room temperature overnight. In this experiment, we used less doxorubicin (50

μM). We conducted the electrophoresis by surrounding the apparatus with ice to cool the buffer in order to avoid partial denaturation of the duplex in the PAGE (Fig. 83). The duplex zemen was in fact partially denatured if we conduced the electrophoretic run at room temperature.

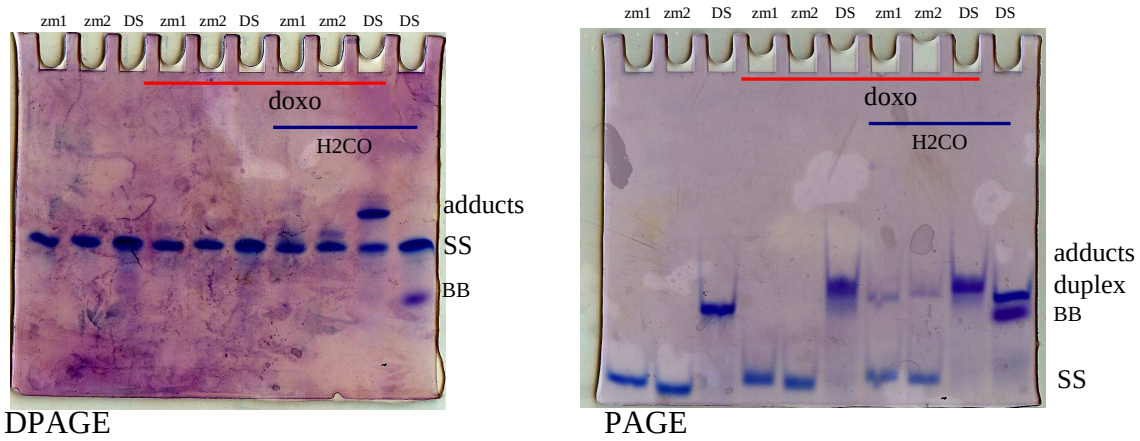

Fig. 83 - Oligonucleotides 10μM (single stranded (zm1 and zm2) and duplex (DS)) were incubated in the presence and absence of H_2CO 2 mM and in presence and absence of doxorubicin 50 μM overnight in purified water at room temperature. Samples were loaded in polyacrylamide native and denaturing gel (19:1) 7.5 M urea. Electrophoretic run was conducted at 140 V for 240 min for both the gels in TBE 1X cooled on ice. Gels were coloured with Sigma Stain-All and the images were captured with an HP 7400 scanner.

The samples obtained using the oligo zemen had the same behavior as oligos zag when incubated with doxorubicin and formaldehyde and analyzed in PAGE, single stranded zm oligos formed complexes when incubated with doxorubicin and formaldehyde. In DPAGE we observed only the complexes that formed when the DNA was incubated with both doxorubicin and formaldehyde. The extra bands observed in the denaturing gel of the samples obtained by incubating the single stranded oligos with doxorubicin and formaldehyde were close to the bands of oligos alone.

Only oligos zag and zm had the capability to form covalent complexes in the single strand form with doxorubicin when activated with formaldehyde, even if the anthracyclines are known to interact with the duplex. This was probably due to the possibility that this oligos can be partially self-complementary (Fig. 84).

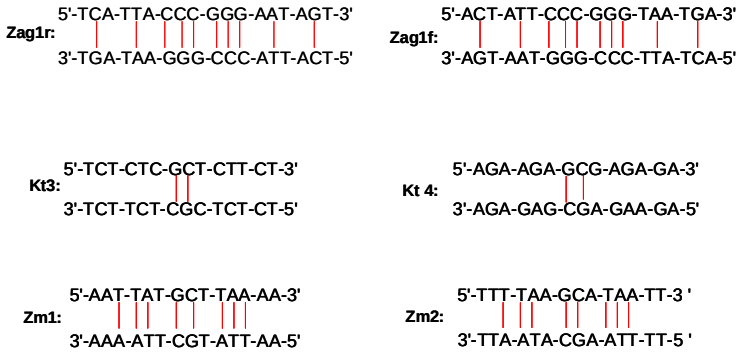

Fig. 84 - Possible partial annealing of oligos single stranded.

In fact, oligos zag and zemen theoretically can partially anneal and then the doxorubicin can intercalate. This process can be promoted by the presence of doxorubicin that stabilizes this unusual duplex. This stabilization increases in the presence of formaldehyde by the formation of VXL, and then as a result we can detect the adducts even with the single stranded structures.
Oligos kt3 and kt4, which have less possibility of self-annealing, do not form cross-linking in single stranded form, evidence that supports this hypothesis.

The reactivity of doxorubicin in water in the presence of formaldehyde was maintained and we could perform our analysis using mass spectrometry to investigate the characteristics of the aminal linkage in doxorubicin-DNA covalent complexes. The ability to transfer weak non-covalent complexes intact to the gas phase has moved electrospray ionization mass spectrometry (ESI-MS) to the forefront of new technologies developed for investigating the interactions between biomolecules and cognate species. ESI-MS in particular has been used extensively to study the interactions of DNA and RNA with many different classes of ligands [57]. This technique can unambiguously determine the identity and abundance of different complexes from direct observation, since the mass of every component serves as an intrinsic detection “label.” For this reason, we have applied ESI-MS to the characterization of doxorubicin-DNA complexes formed in vitro under accepted experimental conditions. These mass spectrometry experiments were obtained with a Bruker Daltonics (Billerica, MA) Apex IV FTICR equipped with a 12T superconductive magnet.
Samples containing 10μM duplex oligos were incubated overnight at room temperature in water with doxorubicin 50 μM in the presence and the absence of formaldehyde 2 mM.
Then the samples were purified and concentrated by ultracentrifugation after the addition of ammonium citrate 100 mM (1° step) and ammonium acetate 10 mM (2° step) to reduce

unwanted aspecific gas phase interactions. Ammonium acetate 10 mM was added to dilute the samples before ESI-FTICR analyses.

When duplex DNA (zm1-zm2) was incubated with doxorubicin, non-covalent adducts were detected for the duplex and for the single stranded components of the system (Fig. 85).

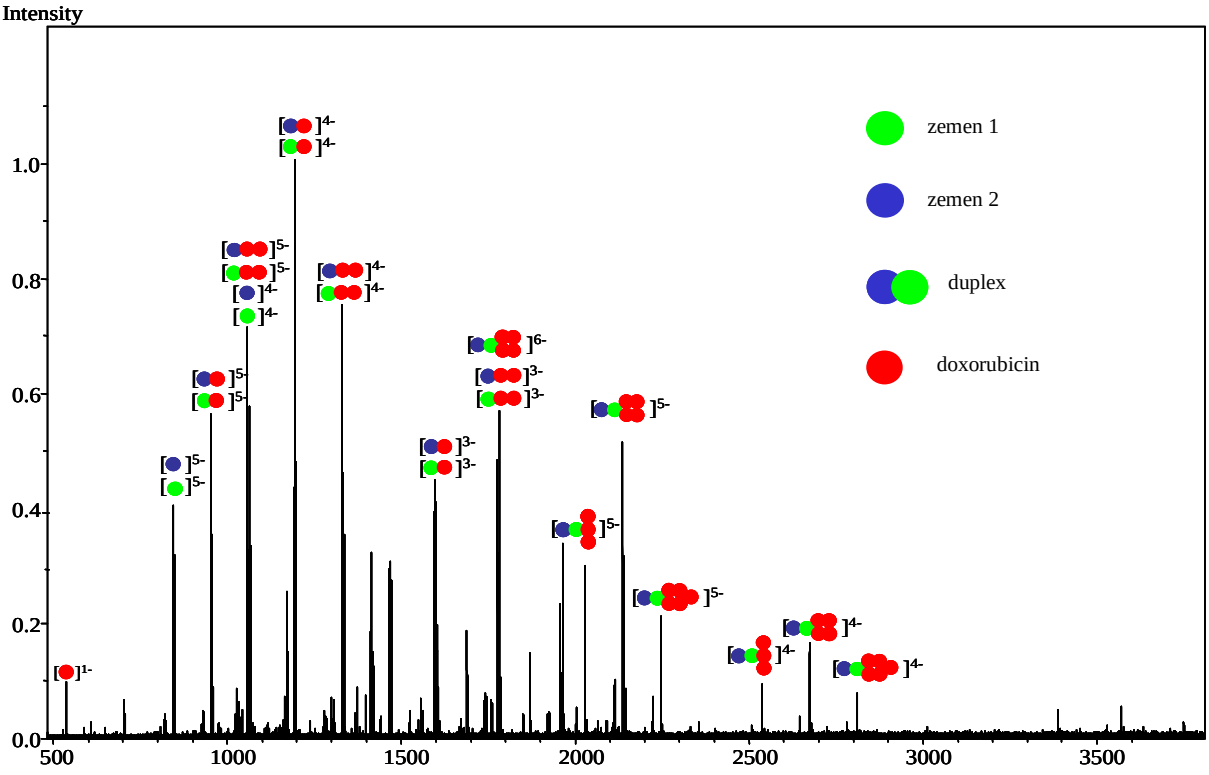

Fig. 85 - Mass spectrum of duplex zemen 10 µM incubated overnight in water at room temperature with doxorubicin 50 µM. Samples were purified and concentrated using ultracentrifugation, and diluted again in ammonium acetate 10 mM before mass spectrometry analysis.

In the spectrum of Fig 85 the species detected are labelled with little coloured circles that correspond to the species reported on the right of the picture or a complex with different species when the label contains combined circles. In this way we can observe adducts of single stranded and duplex oligos containing several doxorubicin molecules.

In the presence of formaldehyde, new adducts with an incremental mass of 12 Da were detected, in addition to those observed in picture 85 (black circles) (Fig. 86).

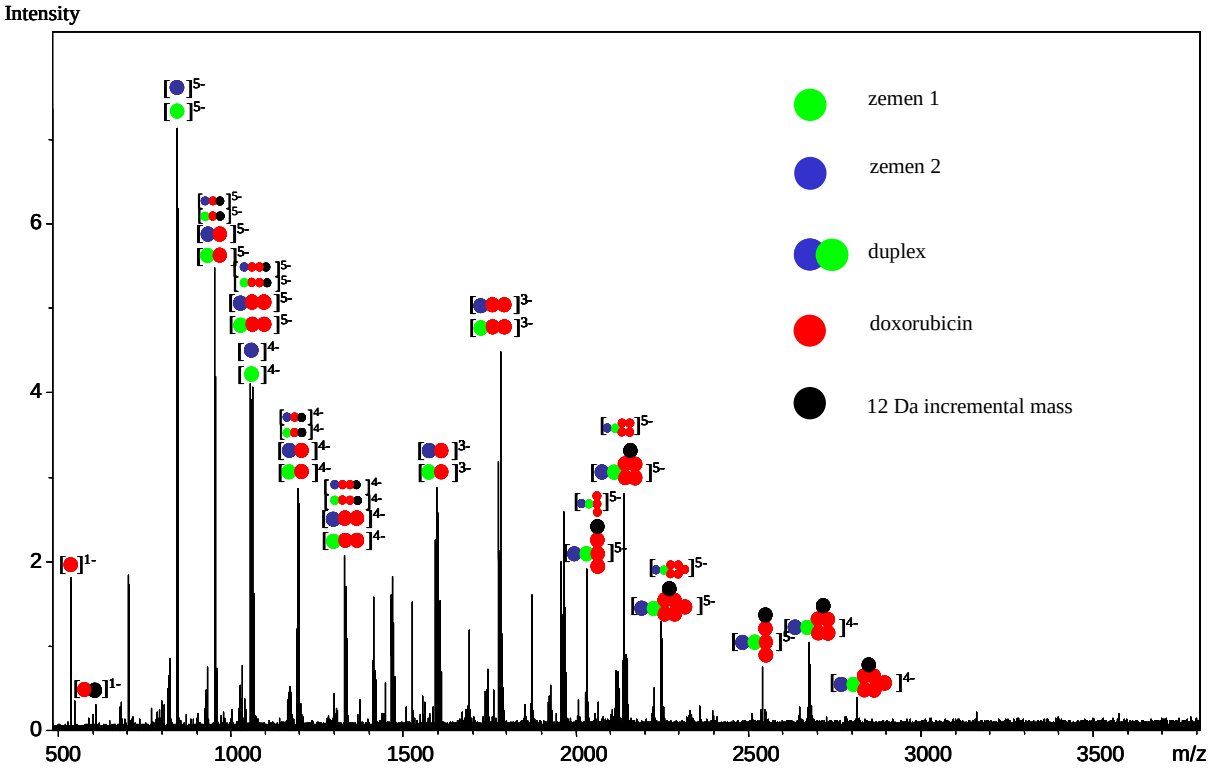

Fig. 86 - Mass spectrum of duplex zemen 10 µM incubated overnight in water at room temperature with doxorubicin 50 µM in the presence of H_2CO 2 mM. Samples were purified and concentrated using ultracentrifugation and diluted again in ammonium acetate 10 mM before mass spectrometry analysis.

Single stranded oligos and their doxorubicin complexes are abundant in these spectra, but the same samples analyzed by gel electrophoresis (Fig. 83) do not show single stranded bands. This is consistent with the observation that the single stranded oligos and their complexes detected in mass spectrometry form during ESI ionization rather than being present in solution. Only the sample incubated with formaldehyde led to the formation of DNA-doxorubicin adducts with 12 dalton incremental mass consistent with the formation of formaldehyde-mediated VXL.

Single stranded oligos incubated in the same conditions in the presence of doxorubicin led to the formation of complexes of single strand-doxorubicin and the 12 dalton incremental mass when we incubated in the presence of formaldehyde. The conditions of the ESI do not permit detection of self-complementary duplex complexes visible in native gel electrophoresis. Duplex zemen that contained only one GC in the sequence promoted the formation of only one 12 dalton-incremented mass, even if the complexes contained more than one anthracycline (Fig. 87B). When we conducted the same experiment using the duplex kt1-kt2 with more Gs in the sequence, we obtained adducts with more than one 12 dalton incremented mass. We obtained three new adducts in decreasing amounts respectively with one, two, and three more carbons (Fig. 87 A).

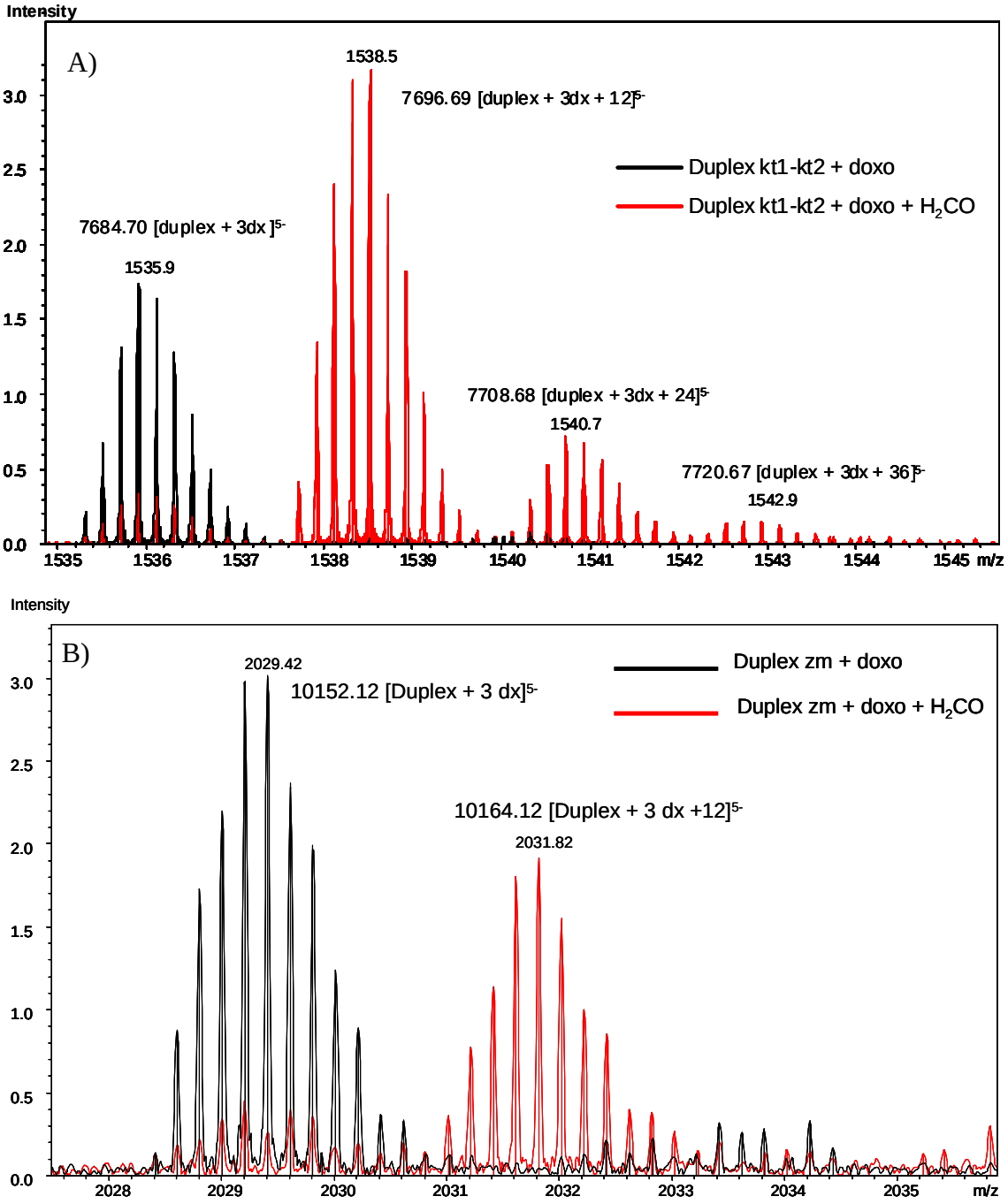

Fig. 87 - A) Mass spectra of duplex kt1-kt2 10µM incubated overnight in water at 4°C with doxorubicin 50 µM in the presence of H_2CO 2 mM (red spectrum) and the absence of H_2CO (black spectrum). B) Mass spectra of duplex zemen 10µM incubated overnight at room temperature with doxorubicin 50 µM in the presence of H_2CO 2 mM (red spectrum) and the absence of H_2CO (black spectrum). All samples were purified and concentrated by ultracentrifugation, and diluted again in ammonium acetate 10 mM before mass spectrometry analysis.

This incremental mass of 12 dalton is consistent with the anthracycline-DNA-formaldehyde structure proposed by Phillips and colleagues [23]. There is also a relationship between the number of incremental masses (+12) and the number of guanines present in the sequence.

We used tandem mass spectrometry (MS/MS) to obtain more information about the structure of these adducts. We isolated the adducts of interest in the quadrupole present in the first part of the

instrument and we activated the precursor ions directly in the ICR (ion cyclotron resonance) cell by SORI-CID or IRMPD.

Sustained Off-Resonance Irradiation Collision-Induced Dissociation (SORI-CID) is a CID technique used in Fourier Transform Ion Cyclotron Resonance Mass Spectrometry (FT-ICR-MS) which involves accelerating the ions in cyclotron motion (in a circle inside of the ICR cell) and then increasing the pressure, resulting in collisions that produce fragments. After the SORI-CID process is complete, the pressure is reduced back to high vacuum and the analysis of the fragment ions is performed.

InfraRed MultiPhoton Dissociation (IRMPD) is a mechanism of fragmentation that involves the absorption of infrared photons. The ions in gas phase become excited into more energetic vibrational states until the bonds are broken, leading to the formation of fragments.

We used both techniques to investigate the covalent complexes formed when the duplexes were incubated with doxorubicin in the presence of formaldehyde.

We analyzed adducts between the zemen duplex and doxorubicin with a 12 (one C) incremental mass, obtained by incubating the duplex under the previously described conditions, (zemen duplex 10μM incubated overnight in water at room temperature with doxorubicin 50 μM in the presence of H_2CO 2 mM and purified by ultracentrifugation).

.

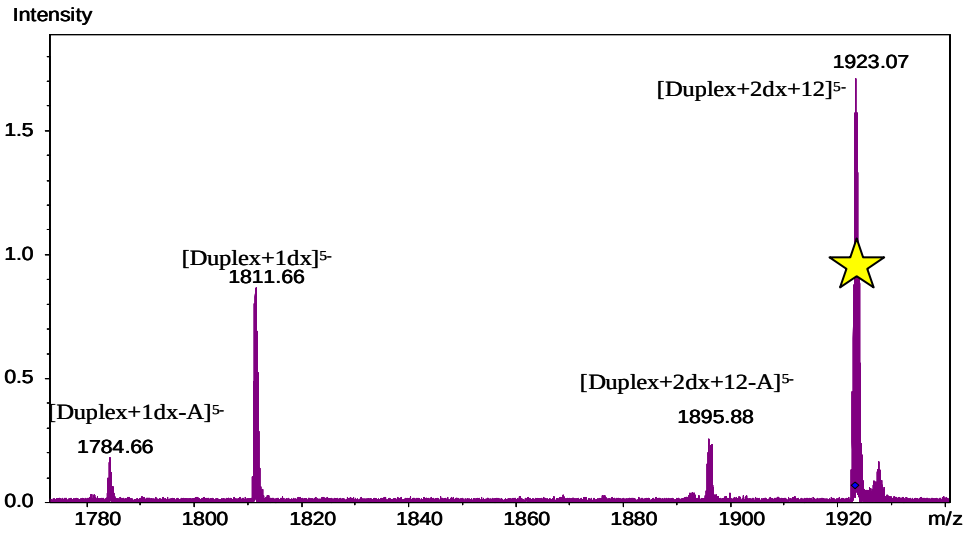

Fig. 88 - Tandem mass spectrometry of the zemen duplex adduct $[Duplex + 2dx +12]^{5-}$ m/z 1923.07 obtained with SORI-CID. The precursor ion was isolated in the quadrupole and fragmented in the cell.

In figure 88 we show the spectrum obtained by fragmenting the adduct corresponding to the duplex zemen binding to two doxorubicin molecules and with 1 C incremental mass with SORI-CID. This adduct dissociates losing adenine, or losing one doxorubicin and the C. This was an unexpected result, as evidence shows that when more than one anthracycline binds to the DNA, the adduct first loses the anthracycline carrying the 12 dalton incremental mass.

We conducted tandem mass spectrometry even with the complexes obtained by incubating the duplex kt1-kt2 10 μM with doxorubicin 20 μM overnight at 4 °C in presence of H_2CO 2 mM and purified by ultracentrifugation (Fig. 89).

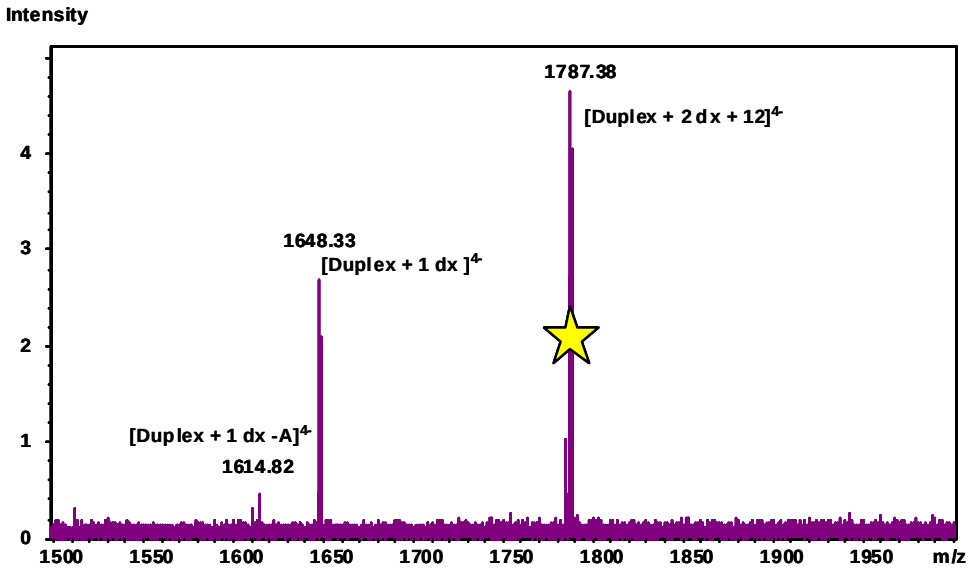

Fig. 89 - Tandem mass spectrometry of the kt1-kt2 duplex adduct $[Duplex + 2dx + 12]^{4-}$ m/z 1787.38 obtained with IRMPD. The precursor ion was isolated in the quadrupole and fragmented in the cell.

Also this complex dissociates losing first the doxorubicin carrying the 12 Dalton incremental mass at variance with the formation of the VXL.

A possible explanation of this apparent contradiction is that in gas phase and under high vacuum condition in ICR cell the electrostatic interaction between the protonated amino group of doxorubicin and the negative charged DNA backbone is stronger than in solution. In the covalent bound anthracyclines, the amino group, instead, is blocked and the ionic interaction is likely less efficient. Probably this finding combined with the intrinsic instability of the aminal linkage can explain the unusual fragmentation of these adducts that first lost the anthracycline carrying the 12 dalton incremental mass.

7. CONCLUSION

Several anthracyclines, such as cyanomorpholinyl-doxorubicin and barminomycin or doxorubicin-activated species, can react covalently with nucleic acids. All of these compounds have an electrophilic carbon near the nitrogen of the daunosamine that can react with an amino group of the DNA (Fig. 90).

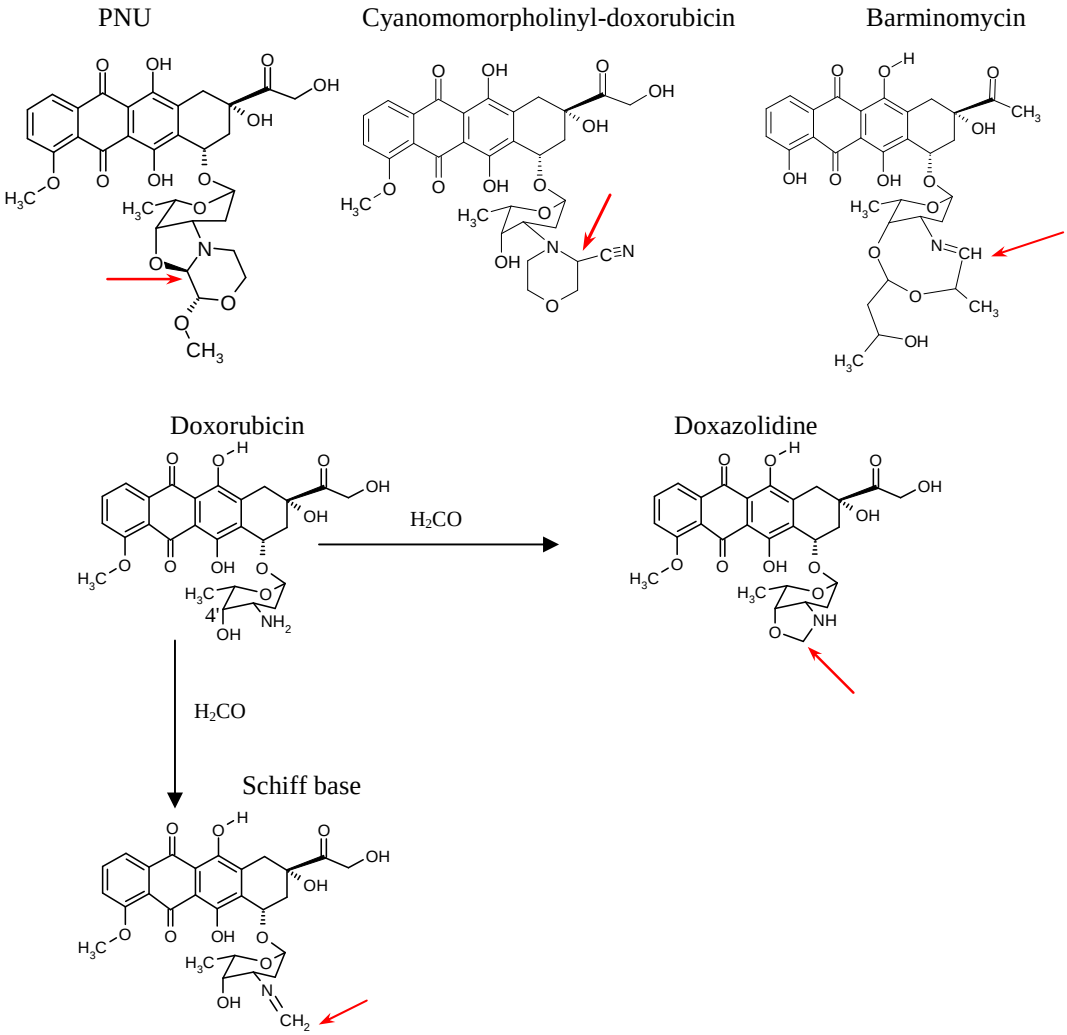

Fig. 90 – Structure of PNU, cyanomomorpholinyl-doxorubicin, barminomycin and the formaldehyde-doxorubicin active species doxazolidine and doxorubicin-H_2CO Schiff base.

The daunosamine nitrogen close to an electrophilic carbon is necessary for the cross-linking activity. What remains controversial is the function of the 4' position. Post asserts that 4' hydroxyl group is important to form the reactive oxazolidine ring and proposed a mechanism of formation of VXL according to which doxazolidine is the species that reacts with the DNA (Fig 91) [29]. In our analysis, we also found that anthracyclines lacking this hydroxyl group maintain their virtual cross-linking potential, suggesting that the anthracycline Schiff bases',

which we confirmed to be present in solution, play an important role in the formation of the cross-link. Probably both mechanisms are involved in doxorubicin VXL formation which does not seem to be sequence-specific in vitro, even if the behavior can be different in vivo. It is instead base-specific; there is a good correlation between the number of cross-links formed and the number of guanines present in the sequence, confirming the involvement of the 2-amino substituent in the process.

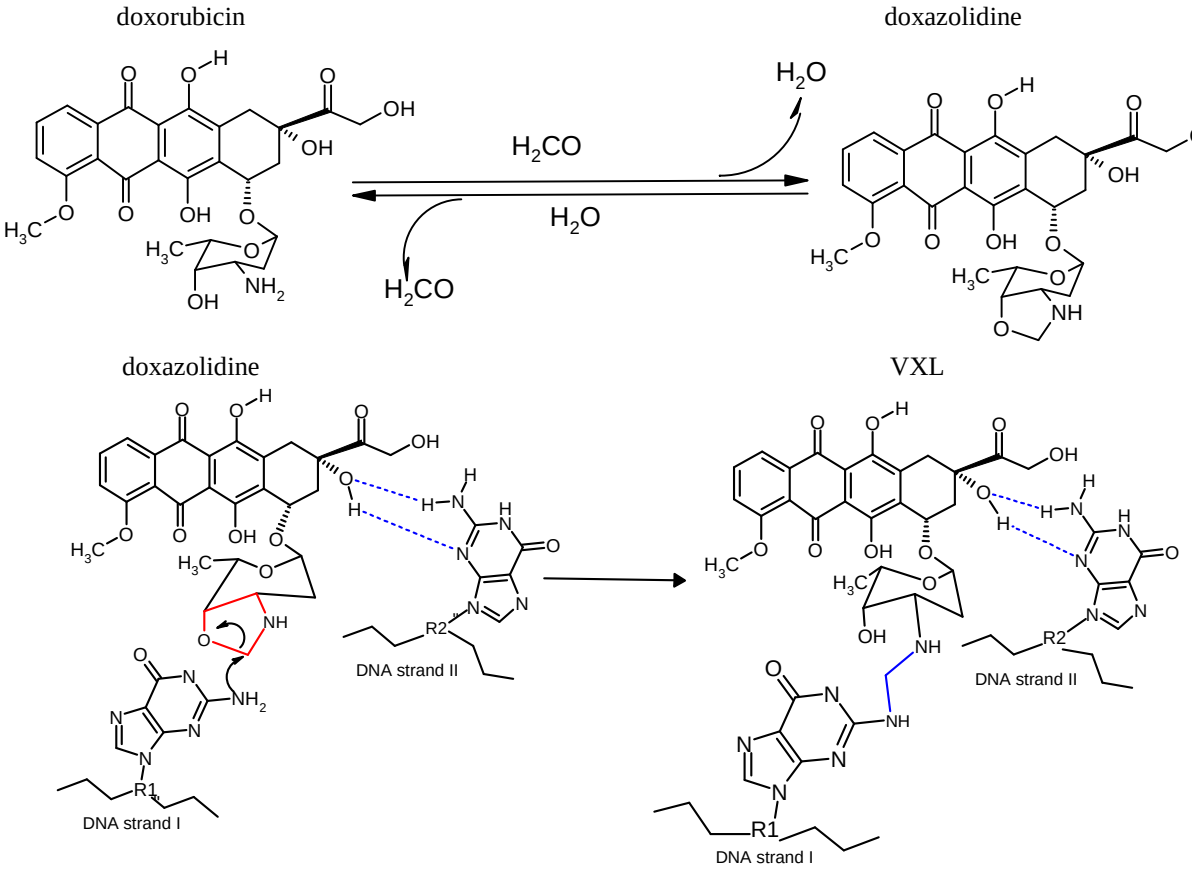

Fig. 91 – Mechanism of formation of VXL between doxorubicin-formaldehyde conjugate doxazolidine and DNA [29].

Nemorubicin (MMDX), the precursor of our metabolite PNU, is a topoisomerase I and II inhibitor when tested in vitro [47], but can overcome atypical (i.e., topoisomerase II-mediated) multidrug resistance [44]. However, PNU does not inhibit the catalytic activity of the enzyme topoisomerase II at the tested concentration. The high cytotoxicity of PNU must be explained by other processes. Particularly relevant is the strong interaction with DNA, ability evidenced even in the first experiment of topo II inhibition. Highly cytotoxic anthracyclines, cyanomorpholinyl-doxorubicin, barminomycin, or activated doxorubicin-formaldehyde form covalent monoadducts with the DNA. Doxorubicin, which intercalates in the nucleic acid, changes its reactivity when activated by formaldehyde forming covalently monoadducts called VXL. Our hypothesis that

PNU would have been able to form the same VXLs with DNA was confirmed by the following experimental evidence:

- PNU interacts with DNA to form adducts that exhibit different behaviors than the non-covalent intercalation-complex between doxorubicin and DNA. The intercalation complex presents a dynamic equilibrium according to which the anthracyclines are bound to DNA depending upon the binding constant. The intercalative process equally affects the melting and the annealing temperatures, which are close to each other in the presence of intercalative drugs. When we introduced formaldehyde, however, the formation of VXLs between DNA and doxorubicin affected the equilibrium and we saw a substantial difference between the melting and the annealing temperatures. This difference was a direct consequence of the new methylene bridge between the guanine amino group and the doxorubicin amino group. DNA incubated with PNU shows a substantial difference between melting and annealing temperatures indicating that PNU behaved essentially as a virtual cross-linker rather than as an intercalator.
- PNU reacted with the duplex DNA to produce adducts isolable by RP-HPLC. Formation of the different adducts was correlated to the oligo/PNU ratio and to the incubation time. The observation that doxorubicin did not form isolable adducts, even if the doxorubicin was intercalated in DNA with a good affinity (or, better, formed adducts when in the presence of formaldehyde), provides further strong evidence that PNU forms cross-links to the DNA. The isolation of one adduct after the reaction between the same oligos and the established alkylating agent cyanomorpholinyl-doxorubicin confirms this hypothesis.
- PNU did not react with single stranded DNA, suggesting the need of the duplex to form monoadducts. The first step in this reaction is likely intercalation in the duplex, and once it has reached the correct position within the complex, PNU can react with the DNA.
-The observations that these adducts show a melting temperature remarkably higher than that of the original duplex (the duplex-PNU complexes denature between 70 and 80 °C, depending on the quantity of PNU present in the solution) and that these isolated adducts release oligos with time suggest that PNU, similarly to the formaldehyde-treated complexes of doxorubicin, forms a VXL rather than a classical cross-link. Moreover, during MS/MS experiments adducts fragment easily, losing the PNU bound differently than we expected in the presence of a classical cross-link.

It is important to observe that PNU contains the same oxazolidinic ring as doxorubicin-formaldehyde conjugate doxazolidine (Fig. 92).

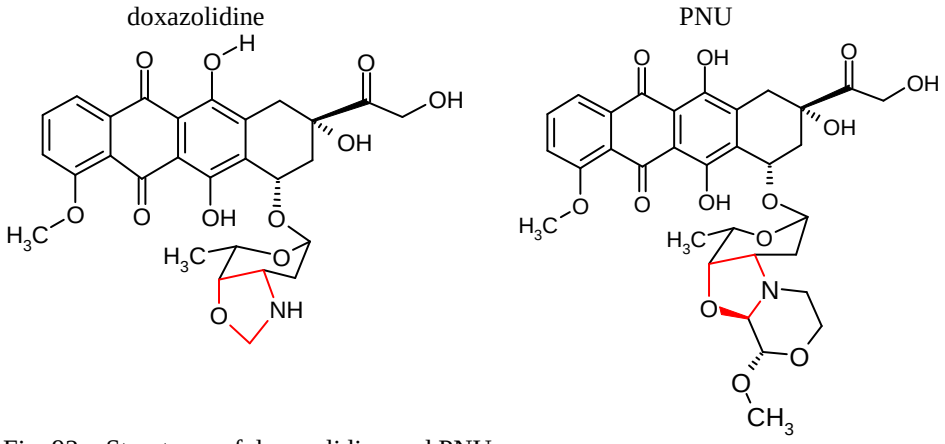

Fig. 92 – Structures of doxazolidine and PNU.

This structural analogy combined to the similar characteristic between the cross-links formed by PNU and by doxorubicin in presence of formaldehyde lead us to propose an analogous mechanism of formation of the adduct between PNU and DNA (Fig 93).

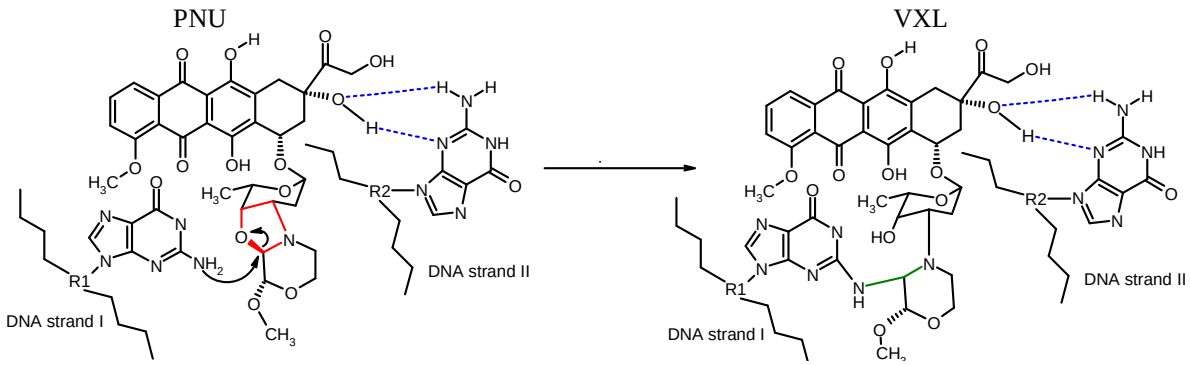

Fig. 93 – Mechanism of formation of VXL proposed between PNU and DNA

The VXL, a combination of intercalation, covalent bonding and hydrogen bonding, leads to the formation of more stable complexes between the anthracycline and the DNA, improving the drugs'cell killing ability. As has become apparent during our studies these complexes are characterized by an intrinsic instability that makes structural investigation difficult. Nevertheless, the conclusions we were able to shed more light into the molecular mechanisms of drug action, which is crucial for a full understanding of anthracycline pharmacological properties. In addition, the information thus far obtained will help us in rationally designing novel, more effective, and more tolerable anticancer agents.

8. ACRONYM AND ABBREVIAIONS

- ✓ A: adenine
- ✓ BB: Bromophenol blue
- ✓ C: carbon
- ✓ CID: Collision Induced Dissociation
- ✓ Da: Dalton
- ✓ DAB: Dabcyl
- ✓ DPAGE: denaturing polyacrylamide gel electrophoresis
- ✓ DS: double stranded DNA
- ✓ e.g.: exempli gratia
- ✓ ESI: ElectroSpray Ionization
- ✓ FAM: 6-carboxy-fluorescein
- ✓ FID: Free Induction Decay
- ✓ FQA: Fluorescence-Quenching Assay
- ✓ FRET: Fluorescence Resonance Energy Transfer
- ✓ FT-ICR-MS: Fourier Transform-Ion Cyclotron Resonance-Mass Spectrometry
- ✓ G: guanine
- ✓ GLB: Gel Loading Buffer
- ✓ h: hours
- ✓ HPLC: High Pressure Liquid Chromatography
- ✓ i.e. : id est
- ✓ IP RP HPLC: Ion-Pair Reverse-Phase High Pressure Liquid Chromatography
- ✓ IRMPD: InfraRed MultiPhoton Dissociation
- ✓ m/z: mass/charge ratio
- ✓ MALDI-TOF: Matrix Assisted Laser Desorption Ionization-Time of Flight
- ✓ min: minutes
- ✓ PAGE: native polyacrylamide gel electrophoresis
- ✓ RET: Resonance Energy Transfer
- ✓ SORI-CID: Sustained Off-Resonance Irradiation Collision-Induced Dissociation
- ✓ SS: single stranded DNA
- ✓ TIC: Total Ion Current.
- ✓ t_R: retention time
- ✓ VXL: Virtual cross-link
- ✓ µHPLC-MS: micro-HPLC-mass spectrometry

9. REFERENCE

1. Quintieri, L., et al., *Formation and antitumor activity of PNU-159682, a major metabolite of nemorubicin in human liver microsomes.* Clin Cancer Res, 2005. **11**(4): p. 1608-17.
2. Minotti, G., et al., *Anthracyclines: molecular advances and pharmacologic developments in antitumor activity and cardiotoxicity.* Pharmacol Rev, 2004. **56**(2): p. 185-229.
3. *UK cancer incidence statistics by age.* Cancer Research UK January 2007.
4. *WHO World Health Organization* 2011.
5. Anand, P., et al., *Cancer is a preventable disease that requires major lifestyle changes.* Pharm Res, 2008. **25**(9): p. 2097-116.
6. Croce, C.M., *Oncogenes and cancer.* N Engl J Med, 2008. **358**(5): p. 502-11.
7. Knudson, A.G., *Two genetic hits (more or less) to cancer.* Nat Rev Cancer, 2001. **1**(2): p. 157-62.
8. Merlo, L.M., et al., *Cancer as an evolutionary and ecological process.* Nat Rev Cancer, 2006. **6**(12): p. 924-35.
9. Grandi, M., et al., *Novel anthracycline analogs.* Cancer Treat Rev, 1990. **17**(2-3): p. 133-8.
10. Weiss, R.B., *The anthracyclines: will we ever find a better doxorubicin?* Semin Oncol, 1992. **19**(6): p. 670-86.
11. Danesi, R., et al., *3'-Deamino-3'-(2-methoxy-4-morpholinyl)-doxorubicin (FCE 23762): a new anthracycline derivative with enhanced cytotoxicity and reduced cardiotoxicity.* Eur J Cancer, 1993. **29A**(11): p. 1560-5.
12. Simunek, T., et al., *Anthracycline-induced cardiotoxicity: overview of studies examining the roles of oxidative stress and free cellular iron.* Pharmacol Rep, 2009. **61**(1): p. 154-71.
13. Zambetti, M., et al., *Long-term cardiac sequelae in operable breast cancer patients given adjuvant chemotherapy with or without doxorubicin and breast irradiation.* J Clin Oncol, 2001. **19**(1): p. 37-43.
14. Doroshow, J.H., G.Y. Locker, and C.E. Myers, *Enzymatic defenses of the mouse heart against reactive oxygen metabolites: alterations produced by doxorubicin.* J Clin Invest, 1980. **65**(1): p. 128-35.
15. Gewirtz, D.A., *A critical evaluation of the mechanisms of action proposed for the antitumor effects of the anthracycline antibiotics adriamycin and daunorubicin.* Biochem Pharmacol, 1999. **57**(7): p. 727-41.
16. Binaschi, M., et al., *Anthracyclines: selected new developments.* Curr Med Chem Anticancer Agents, 2001. **1**(2): p. 113-30.
17. Binaschi, M., et al., *In vivo site specificity and human isoenzyme selectivity of two topoisomerase II-poisoning anthracyclines.* Cancer Res, 2000. **60**(14): p. 3770-6.
18. Tewey, K.M., et al., *Adriamycin-induced DNA damage mediated by mammalian DNA topoisomerase II.* Science, 1984. **226**(4673): p. 466-8.
19. Gigli, M., et al., *Quantitative study of doxorubicin in living cell nuclei by microspectrofluorometry.* Biochim Biophys Acta, 1988. **950**(1): p. 13-20.
20. Cummings, J. and C.S. McArdle, *Studies on the in vivo disposition of adriamycin in human tumours which exhibit different responses to the drug.* Br J Cancer, 1986. **53**(6): p. 835-8.
21. Terasaki, T., et al., *Nuclear binding as a determinant of tissue distribution of adriamycin, daunomycin, adriamycinol, daunorubicinol and actinomycin D.* J Pharmacobiodyn, 1984. **7**(5): p. 269-77.

22. Sinha, B.K. and C.F. Chignell, *Binding mode of chemically activated semiquinone free radicals from quinone anticancer agents to DNA.* Chem Biol Interact, 1979. **28**(2-3): p. 301-8.
23. Cutts, S.M., et al., *The power and potential of doxorubicin-DNA adducts.* IUBMB Life, 2005. **57**(2): p. 73-81.
24. Kato, S., et al., *Formaldehyde in human cancer cells: detection by preconcentration-chemical ionization mass spectrometry.* Anal Chem, 2001. **73**(13): p. 2992-7.
25. Sinha, B.K. and E.G. Mimnaugh, *Free radicals and anticancer drug resistance: oxygen free radicals in the mechanisms of drug cytotoxicity and resistance by certain tumors.* Free Radic Biol Med, 1990. **8**(6): p. 567-81.
26. Kato, S., et al., *Mass spectrometric measurement of formaldehyde generated in breast cancer cells upon treatment with anthracycline antitumor drugs.* Chem Res Toxicol, 2000. **13**(6): p. 509-16.
27. Cutts, S.M., et al., *Formaldehyde-releasing prodrugs in combination with adriamycin can overcome cellular drug resistance.* Oncol Res, 2005. **15**(4): p. 199-213.
28. Fenick, D.J., D.J. Taatjes, and T.H. Koch, *Doxoform and Daunoform: anthracycline-formaldehyde conjugates toxic to resistant tumor cells.* J Med Chem, 1997. **40**(16): p. 2452-61.
29. Post, G.C., et al., *Doxazolidine, a proposed active metabolite of doxorubicin that cross-links DNA.* J Med Chem, 2005. **48**(24): p. 7648-57.
30. Kalet, B.T., et al., *Doxazolidine induction of apoptosis by a topoisomerase II independent mechanism.* J Med Chem, 2007. **50**(18): p. 4493-500.
31. Taatjes, D.J., et al., *Redox pathway leading to the alkylation of DNA by the anthracycline, antitumor drugs adriamycin and daunomycin.* J Med Chem, 1997. **40**(8): p. 1276-86.
32. Taatjes, D.J. and T.H. Koch, *Nuclear targeting and retention of anthracycline antitumor drugs in sensitive and resistant tumor cells.* Curr Med Chem, 2001. **8**(1): p. 15-29.
33. Cutts, S.M., et al., *Activation of clinically used anthracyclines by the formaldehyde-releasing prodrug pivaloyloxymethyl butyrate.* Mol Cancer Ther, 2007. **6**(4): p. 1450-9.
34. Coldwell, K.E., et al., *Detection of Adriamycin-DNA adducts by accelerator mass spectrometry at clinically relevant Adriamycin concentrations.* Nucleic Acids Res, 2008. **36**(16): p. e100.
35. Cutts, S.M., et al., *Recent advances in understanding and exploiting the activation of anthracyclines by formaldehyde.* Curr Med Chem Anticancer Agents, 2005. **5**(5): p. 431-47.
36. Zeman, S.M., D.R. Phillips, and D.M. Crothers, *Characterization of covalent adriamycin-DNA adducts.* Proc Natl Acad Sci U S A, 1998. **95**(20): p. 11561-5.
37. Taatjes, D.J., et al., *Alkylation of DNA by the anthracycline, antitumor drugs adriamycin and daunomycin.* J Med Chem, 1996. **39**(21): p. 4135-8.
38. Wang, A.H., et al., *Formaldehyde cross-links daunorubicin and DNA efficiently: HPLC and X-ray diffraction studies.* Biochemistry, 1991. **30**(16): p. 3812-5.
39. Moufarij, M.A., et al., *Barminomycin functions as a potent pre-activated analogue of Adriamycin.* Chem Biol Interact, 2001. **138**(2): p. 137-53.
40. Jesson, M.I., et al., *Characterization of the DNA-DNA cross-linking activity of 3'-(3-cyano-4-morpholinyl)-3'-deaminoadriamycin.* Cancer Res, 1989. **49**(24 Pt 1): p. 7031-6.
41. Ripamonti, M., et al., *In vivo anti-tumour activity of FCE 23762, a methoxymorpholinyl derivative of doxorubicin active on doxorubicin-resistant tumour cells.* Br J Cancer, 1992. **65**(5): p. 703-7.

42. Mariani, M., et al., *Growth-inhibitory properties of novel anthracyclines in human leukemic cell lines expressing either Pgp-MDR or at-MDR.* Invest New Drugs, 1994. **12**(2): p. 93-7.
43. Bakker, M., et al., *Mechanisms for high methoxymorpholino doxorubicin cytotoxicity in doxorubicin-resistant tumor cell lines.* Int J Cancer, 1997. **73**(3): p. 362-6.
44. Capranico, G., et al., *Influence of structural modifications at the 3' and 4' positions of doxorubicin on the drug ability to trap topoisomerase II and to overcome multidrug resistance.* Mol Pharmacol, 1994. **45**(5): p. 908-15.
45. Ghielmini, M., et al., *Hematotoxicity on human bone marrow- and umbilical cord blood-derived progenitor cells and in vitro therapeutic index of methoxymorpholinyldoxorubicin and its metabolites.* Cancer Chemother Pharmacol, 1998. **42**(3): p. 235-40.
46. Quintieri, L., et al., *In vivo antitumor activity and host toxicity of methoxymorpholinyl doxorubicin: role of cytochrome P450 3A.* Cancer Res, 2000. **60**(12): p. 3232-8.
47. Lau, D.H., et al., *Metabolic conversion of methoxymorpholinyl doxorubicin: from a DNA strand breaker to a DNA cross-linker.* Br J Cancer, 1994. **70**(1): p. 79-84.
48. Baldwin, A., et al., *Identification of novel enzyme-prodrug combinations for use in cytochrome P450-based gene therapy for cancer.* Arch Biochem Biophys, 2003. **409**(1): p. 197-206.
49. Lu, H. and D.J. Waxman, *Antitumor activity of methoxymorpholinyl doxorubicin: potentiation by cytochrome P450 3A metabolism.* Mol Pharmacol, 2005. **67**(1): p. 212-9.
50. Förster, T., *Intermolecular energy migration and fluorescence. .* Annalen der Physik, 1948(2): p. 55-75.
51. Lakowicz, J.R., *Principles of fluorescence spectroscopy*. Third ed. 2006, Baltimore: Springer
52. Tyagi, S., D.P. Bratu, and F.R. Kramer, *Multicolor molecular beacons for allele discrimination.* Nat Biotechnol, 1998. **16**(1): p. 49-53.
53. Marras, S.A., F.R. Kramer, and S. Tyagi, *Efficiencies of fluorescence resonance energy transfer and contact-mediated quenching in oligonucleotide probes.* Nucleic Acids Res, 2002. **30**(21): p. e122.
54. Luce, R.A. and P.B. Hopkins, *Chemical cross-linking of drugs to DNA.* Methods Enzymol, 2001. **340**: p. 396-412.
55. Smith, R.D., et al., *New developments in microscale separations and mass spectrometry for biomonitoring: capillary electrophoresis and electrospray ionization mass spectrometry.* J Toxicol Environ Health, 1993. **40**(2-3): p. 147-58.
56. Mirza, U.A., S.L. Cohen, and B.T. Chait, *Heat-induced conformational changes in proteins studied by electrospray ionization mass spectrometry.* Anal Chem, 1993. **65**(1): p. 1-6.
57. Hofstadler, S.A. and R.H. Griffey, *Analysis of noncovalent complexes of DNA and RNA by mass spectrometry.* Chem Rev, 2001. **101**(2): p. 377-90.
58. Ni, J., et al., *Interpretation of oligonucleotide mass spectra for determination of sequence using electrospray ionization and tandem mass spectrometry.* Anal Chem, 1996. **68**(13): p. 1989-99.
59. Koch, T., et al., *Anthracycline–Formaldehyde Conjugates and Their Targeted Prodrugs.* Topics in Current Chemistry, 2008. **283**: p. 141-170.
60. Leng, F., et al., *Base Specific and Regioselective Chemical Cross-Linking of Daunorubicin to DNA.* Journal of the American Chemical Society, 1996. **118**(20): p. 4731-4738.

61. Cera, C. and M. Palumbo, *The peculiar binding properties of 4'-deoxy,4'-iododoxorubicin to isolated DNA and 175 bp nucleosomes.* Nucleic Acids Res, 1991. **19**(20): p. 5707-11.